INFORMATION TO USERS

This manuscript has been reproduced from the microfilm master. UMI films the text directly from the original or copy submitted. Thus, some thesis and dissertation copies are in typewriter face, while others may be from any type of computer printer.

The quality of this reproduction is dependent upon the quality of the copy submitted. Broken or indistinct print, colored or poor quality illustrations and photographs, print bleedthrough, substandard margins, and improper alignment can adversely affect reproduction.

In the unlikely event that the author did not send UMI a complete manuscript and there are missing pages, these will be noted. Also, if unauthorized copyright material had to be removed, a note will indicate the deletion.

Oversize materials (e.g., maps, drawings, charts) are reproduced by sectioning the original, beginning at the upper left-hand corner and continuing from left to right in equal sections with small overlaps.

Photographs included in the original manuscript have been reproduced xerographically in this copy. Higher quality 6" x 9" black and white photographic prints are available for any photographs or illustrations appearing in this copy for an additional charge. Contact UMI directly to order.

Bell & Howell Information and Learning
300 North Zeeb Road, Ann Arbor, MI 48106-1346 USA
800-521-0600

Université d'Ottawa · University of Ottawa

Elucidation of the Biochemical Significance of GM_1 Ganglioside in Model Membranes of Perdeuterated 1,2-Dimyristoyl-L-α-Phosphatidylcholine; A Fourier Transform Infrared Spectroscopic Investigation

Maroun Bou Khalil

Thesis Submitted to the Department of Biochemistry, Microbiology and Immunology in Partial Fulfilment of the Requirements for the Degree of Master of Science.

University of Ottawa
Ottawa, Ontario, Canada

This Thesis is Dedicated to my Parents

ACKNOWLEDGEMENTS

Through my research experience in the Biochemistry field, the scientific abilities acquired were very valuable because I have had direct input from fellow student colleagues, professors (Dr. Kates, Dr. Proulx, Dr. Baenziger, Dr. Mezl, Dr. Berubé, Dr. Tanphaichitr, etc.) and especially my direct supervisor Dr. Danielle Carrier.

First of all, I would like to thank my advisor, Dr. Danielle Carrier for her excellent supervision. Dr. Carrier had made use of her extraordinary skills as scientist, professor, proofreader, and logician, requiring perfection of me as she supervised my undergraduate research project and as she continued to supervise my ambitious graduate work.

Prior to embarking in the Biochemistry Research field under the supervision of Dr. Carrier, I had modest knowledge of infrared spectroscopy and physical Biochemistry techniques; this was rapidly rectified due to my supervisor's wealth of knowledge, her unlimited patience, and her talent of transforming intricate concepts into easily comprehensive ideas. I will always be grateful to her because her high expectations of me have helped me realize what I am truly capable of. For all of this, Many Thanks.

ABSTRACT

The monosialoganglioside GM_1 is an anionic glycosphingolipid found ubiquitously in the plasma membrane of mammalian cells. Although its exact normal biological function(s) and physical properties are unknown, it is speculated that GM_1 may play a role in calcium transport and synaptic transmission in neural tissues. Fourier Transform Infrared (FTIR) spectroscopy was employed to test the model of bovine brain GM_1 ganglioside incorporated into perdeuterated dimyristoylphosphatidylcholine ($DMPC_{d54}$) multilamellar dispersions. The interaction of Ca^{2+} ions with the mixed $DMPC_{d54}/GM_1$ bilayers and its effect on the hydrogen bonding at the interfacial region was also investigated. No thermal phase transition was displayed by the GM_1 micellar suspensions over the temperature range from 5 to 60 °C, even at concentrations of 110 mg/ml. On the other hand, in the mixed $DMPC_{d54}/GM_1$ multilamellar bilayers, both the acyl chains of GM_1 and the perdeuterated hydrocarbon chains of $DMPC_{d54}$ exhibited a single, cooperative gel to liquid crystalline phase transition, occurring at a higher temperature than in pure $DMPC_{d54}$ dispersions. This suggests that the ceramide moiety of the glycolipid inserts into the hydrophobic core of the phospholipid bilayer and that the mixed liposomes consisted of a homogeneous mixture of GM_1 and $DMPC_{d54}$ molecules. GM_1 had an ordering effect on the mixed bilayers that was further enhanced by the divalent cation Ca^{2+}. Spectral changes of the amide I and ester carbonyl bands at the interfacial zone indicated a reduced hydrogen bonding of these groups in the mixed liposomal bilayers. Our results also suggested that the ceramide moiety of GM_1 inserts into the lipid bilayer of shorter chain symmetric phospholipids and terminates at the bilayer center (i.e., no interdigitation), forcing the carbohydrate headgroup to protrude farther

out of the bilayer surface to allow a better binding to Ca^{2+} ions than $DMPC_{d54}$. The divalent cation increased the probability of hydrogen bonding at the interfacial region. It is strongly believed that GM_1 is involved in the translocation of extracellular signals across the plasma membrane and that the glycolipid affects interfacial hydrogen bonding and local hydrophobicity of the cell surface, which might modulate various surface events such as cell/cell and cell/surface protein interactions.

RÉSUMÉ

Le monosialoganglioside GM_1 est un glycosphingolipide anionique retrouvé dans la membrane plasmique des cellules animales. Même si ses fonctions biologiques et ses propriétés physiques exactes sont inconnues, il est présumé que GM_1 joue un rôle dans le transport des ions Ca^{2+} et la transmission synaptique des tissus neuronaux. La spectroscopie infrarouge par transformée de Fourier (FTIR) a été utilisée pour étudier le comportement thermotropique des dispersions de 1,2-dimyristoyl-L-α-phosphatidylcholine perdeutérée ($DMPC_{d54}$) et du monosialoganglioside GM_1. L'interaction du Ca^{2+} avec les liposomes de $DMPC_{d54}/GM_1$ ainsi que l'effet de cette interaction sur la formation des liens hydrogène à la surface des bicouches ont été étudiés. Les micelles de GM_1 n'ont pas démontré de transition de phase entre 5 et 60 °C, même à des concentrations de 1 10 mg/ml. Cependant, dans les bicouches multilamellaires de $DMPC_{d54}/GM_1$, les chaînes acyles du glycolipide et les chaînes hydrocarbonées perdeutérées du phospholipide ont démontré une transition de phase coopérative centrée à une température plus élevée que celle des dispersions de $DMPC_{d54}$. Ces résultats suggèrent que la portion céramide du glycolipide est insérée dans la partie hydrophobe des bicouches. GM_1 a stabilisé les bicouches et les ions Ca^{2+} ont augmenté l'ordre des chaînes acyles de $DMPC_{d54}$. Les changements spectroscopiques des bandes amide I et C=O ester à l'interface indiquent une diminution de la formation des liens hydrogène dans les bicouches de $DMPC_{d54}/GM_1$. Nos résultats indiquent que la portion céramide du GM_1 s'insère dans les bicouches lipidiques et se termine au centre de ces derniers (pas d'interdigitation), ce qui contribue à une position spéciale de la tête polaire du glycolipide à la surface, permettant au glycolipide d'interagir plus efficacement que $DMPC_{d54}$ avec les

ions Ca^{2+}. Donc, le monosialoganglioside GM_1 affecte la conformation des proteines et des lipides membranaires en altérant la formation des liens hydrogène et l'hydrophobicité à l'interface et il peut agir comme un récepteur membranaire pour la translocation des signaux externes à travers la membrane plasmique.

CONTENTS

CHAPTER THREE

RESULTS

CHAPTER FOUR

DISCUSSION

APPENDIX ONE

THEORY OF INFRARED SPECTROSCOPY

APPENDIX TWO

THEORY OF MASS SPECTROMETRY

LIST OF FIGURES

LIST OF TABLES

LIST OF ABBREVIATIONS

ADP	Adenosine Diphosphate
Ag	Antigen
AIDS	Acquired Immunodeficiency Syndrome
ATP	Adenosine Triphosphate
cAMP	cyclic Adenosine Monophosphate
CD_x	T-lymphocyte Surface Markers
CNS	Central Nervous System
DMPC	Dimyristoyl ($C_{14:0}$) L-α Phosphatidyl-DL-Choline
$DMPC_{d54}$	Perdeuterated Dimyristoyl ($C_{14:0}$) L-α Phosphatidyl-DL-Choline
DPPC	Dipalmitoyl ($C_{16:0}$) L-α Phosphatidyl-DL-Choline
ESR	Electron Spin Resonance
FAB MS	Fast Atom Bombardment Mass Spectrometry
FTIR	Fourier Transform Infrared Spectroscopy
GD_y	Disialoganglioside GD_y (y = 1a, 1b, 2, & 3)
GM_x	Monosialoganglioside GM_x (x = 1, 2, 3, & 4)
GQ_{1b}	Tetrasialoganglioside GQ_{1b}
GT_z	Trisialoganglioside GT_z (z = 1a & 1b)
GTP	Guanidine Triphosphate
HHV-7	Human Herpes Virus 7
HIV	Human Immunodeficiency Virus

MCT	Mercury-Cadmium-Telluride Detector
MS	Mass Spectrometry
NeuAc	N-Acetylneuraminic Acid or Sialic Acid
NMR	Nuclear Magnetic Resonance Spectroscopy
PC	Phosphatidylcholine
POPC	Dioleoyl ($C_{18:1}$) L-α Phosphatidyl-DL-Choline
T-cell	T-lymphocytes
TLC	Thin Layer Chromatography
T_m	Phase Transition Temperature

CHAPTER ONE

INTRODUCTION

1.1 Gangliosides

The gangliosides were first discovered by Klenk in 1930 during an investigation of some peculiar lipidoses which specifically affect the brain. They were also recognized as the major storage material in the brains of children with Tay Sachs disease and found in minute amounts in normal brain. As the name implies, this class of lipids is mainly found in the ganglion rich fraction and upon further fractionation of the normal brain, the largest amounts are found in plasma membranes from the synaptosomal fraction (Hill & Lester, 1972; Walkley *et al.*, 1995, Ledeen *et al.*, 1998). Gangliosides (Figure 1.1) are a large family of acidic glycosphingolipids with a common neutral tetrasaccharide moiety to which are bound one to five sialic acids, which provide a corresponding number of carboxylic acid groups. Brain tissue (grey and white matter) contains the largest concentrations (Table I) with ganglioside GM_1 and GD_{1a} being the major species (Table II), but they also occur outside the nervous system and have been chromatographically identified in all organs studied. Their concentration in grey matter is about 6% of the total lipid, whereas the white matter contains only 0.6% and a trace or nil has been found in myelin. In neurons, gangliosides account for 10 mol% of the total lipid in the plasma membrane and since this class of lipids is located almost exclusively in the outer surface of this structure, the concentration there is about 20 mol% (Felgner *et al.*, 1983, and references therein).

Figure 1.1 Chemical structure of the four major gangliosides (GM_1, GD_{1a}, GD_{1b} and GT_{1b}) of mammalian brain, with the nomenclature of Svennerholm (1963). The gangliosides have a ceramide moiety and a common neutral tetrasaccharide portion (I, II, III, IV) to which are bound one to three sialic acids (A, B, C). The monosialoganglioside GM_1 has one sialic acid (A). The disialoganglioside GD_{1a} has two sialic acid residues (A, B) and GD_{1b} has A and C. The trisialoganglioside GT_{1b} has three sialic acids (A, B, C). *Abbreviations:* I, glucose; II & IV, galactose; III, N-acetylgalactosamine; A, B & C, N-acetylneuraminic acid (Ledeen and Yu, 1982).

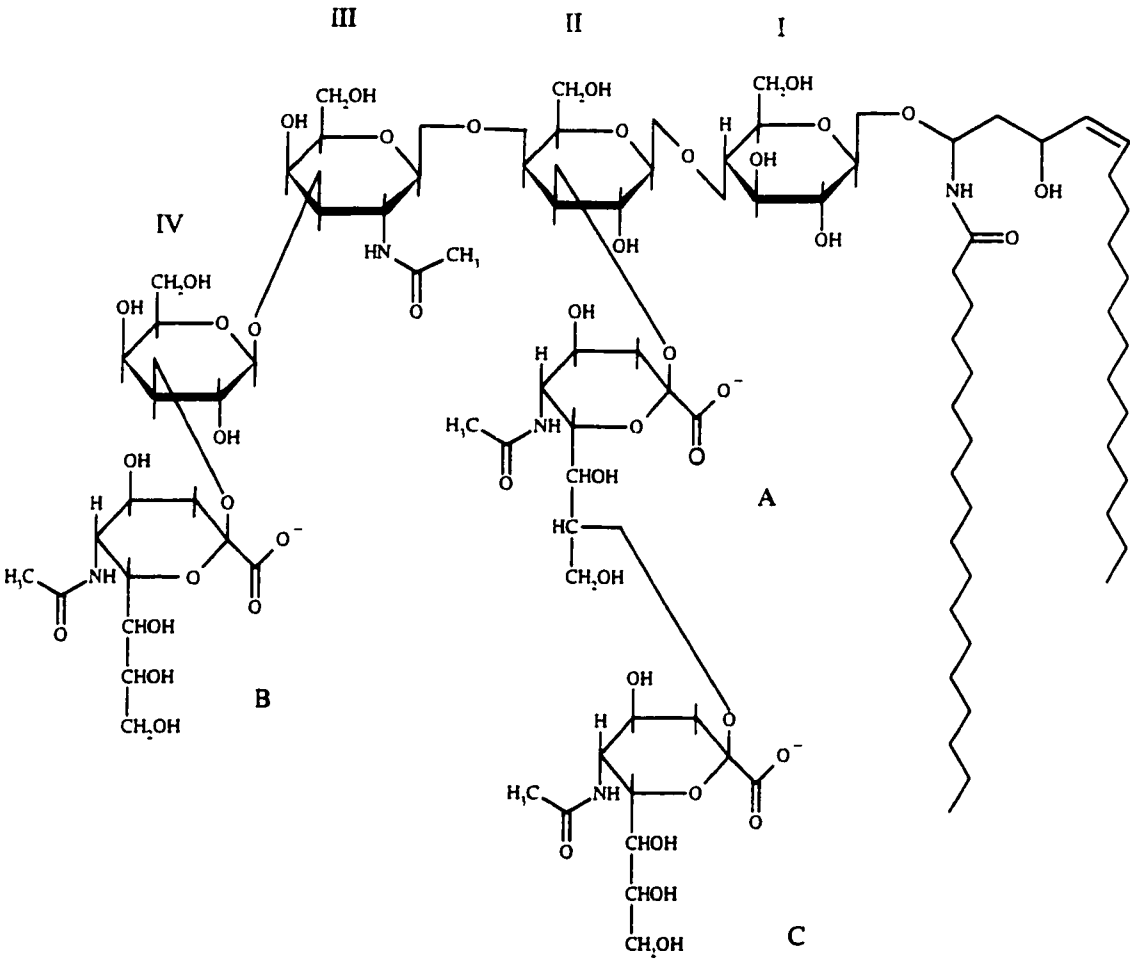
III
II
I
IV
A
B
C

Table I

Ganglioside Content of Human and Bovine Brain Tissues[a]

Tissue	Concentration (μg of lipid-bound sialic acid/g wet weight)
Human grey matter[¶]	880
Human white matter[¶]	275
Bovine white matter[§]	326

[a] These assays were carried out by gas-liquid chromatography ([¶]Ledeen & Yu, 1982) and thin layer chromatography ([§]Urban *et al.*, 1979) in the authors' laboratories.

Table II

Ganglioside Distribution in Nervous Tissue

	Bovine White matter	Human White Matter	Human Grey Matter
Lipid-bound sialic acid (µg / g wet weight)	326	275[1]	880[1]
		Sialic acid distribution [a] (%)	
GM_4	-	8.4	0.7
GM_3	2.6	4.1	3.8
GM_2	2.3	1.7	2.6
GM_1	***31.0***	***19.5***	***19.3***
GD_{1a}	***24.1***	***16.0***	***24.8***
GT1a	2.6	2.5	3.7
GD_3	-	7.6	10.0
GD_{1b}	***10.5***	***17.2***	***17.0***
GT_{1b}	***9.1***	***20.0***	***16.7***
GQ_1	1.2	3.0	1.4

[a] Results are expressed as the percentage of total ganglioside-NeuAc recovered form a total lipid extract. Gangliosides were named according to Svennerholm's nomenclature (1963). These assays were carried out by thin layer chromatography (Urban *et al.*, 1979; [1]Ledeen & Yu, 1982).

The gangliosides of various sources differ in the patterns of fatty acids and sphingosines, and in the number of units in the carbohydrate chain. Pure gangliosides so far prepared have only been uniform as regards to their sugar moiety (Svennerholm, 1972). Gangliosides are predominantly localized on the surface of animal cells (including human lymphocytes) with their oligosaccharide chains exposed on the cell surface (Gazzotti *et al.*, 1985; Kawaguchi *et al.*, 1989).

As components of the plasma membrane, they contribute to the carbohydrate rich glycocalyx that determines surface properties of cells (Ledeen & Yu, 1982). Gangliosides have attracted particular attention in the field of brain research, since they were found not only to be abundant in neural tissue but also to have intricate structures in synaptic membranes. Therefore, it was postulated that gangliosides in cellular membranes play two major functional roles: mediators of cell-cell or cell-substratum interaction and modulators of transmembrane signalling (Hakomori, 1996; Tsuji *et al.*, 1996).

The possible signal mechanisms and physiological role of gangliosides, outlined in Table III, have been suggested and reviewed by R. Ledeen and his group (1998), but many general questions still remain unanswered. Briefly summarizing, we can point out the following important mechanisms: 1. membranotropic effects of gangliosides (alteration of membrane fluidity, bilayer reorganizations, etc.); 2. specific modulation of membrane proteins activity *in vivo* and *in vitro* (CD_4, Ca^{2+} channels, etc.); 3. binding of some physiologically active substances (hormones, toxins, mediators); 4. binding of calcium (regulation of calcium homeostasis); 5. interaction with growth factors and effects of gangliosides on cellular development and differentiation (Kalueff, 1996).

Table III

Physiological properties of individual gangliosides potentially involved in signalling mechanisms in the CNS (Kalueff, 1996)

Physiological Effects (gangliosides)
Alteration of lipid environment
interaction with other membrane lipids (GM_1, GM_3)
creation of lipid domains (GM_1, GM_3, GD_{1a}, GD_{1b}, GD_3)
lipid-lipid recognition in synaptic areas (GM_1, GT_{1b})
short- and long-term ganglioside membrane memory
effects on receptor's surrounding (GD_{1b}, GT_1, GD_3)
Regulation of Ca^{2+} homeostasis
direct binding of Ca^{2+} and activation of Ca^{2+} L-type channels (GM_1)
regulation of synaptic transmission (GM_1, GT_{1b})
alteration of Ca^{2+} dependent kinases (GM_1)
Specific recognition by:
some bacteria and bacterial toxins (GM_1, GD_{1b}, GT_{1b}, GQ_{1b})
some viruses (GM_1, GT_{1a}, GT_{1b}, GQ_{1b})
Specific binding to:
hormones (GM_1, GT_{1b}, GD_{1b}, GD_3) and hormonal receptors (GD_3)
some mediators (GM_1, GD_3)
membrane, structural and cytoskeleton proteins (GM_1, GM_4)
Interaction with growth factors
role in reception of growth factors (GM_1, GM_2)
interaction with neurotrophic factors (GM_1, GM_2)
Regulation of neuronal growth and activity
induction of neuritogenesis (GM_1), synaptogenesis (GD_1) and axonal growth (GM_1)
induction of nerve regeneration and reanimation of synaptic terminals (GM_1)
enhancement of repairs or the CNS damage (GM_1)
Effects on different cellular proteins
activation of Na/K and Mg/Ca ATPases
activation of adenilylcyclases and phosphodiesterases
modulation of protein kinases (GM_1) and direct regulation of some receptors
Effects of antibodies against individual gangliosides
specific ganglioside binding by antibodies
AB-activation of some neuronal processes as behavior, memory and learning

In addition, exogenously added gangliosides have a variety of biological activities in cell growth and differentiation (Kawaguchi *et al.*, 1989).

1.2 Tay Sachs Disease

In the diseases associated with an accumulation of gangliosides, the concentrations are increased many folds and give rise to a gross disruption of neurological function including both demyelination and a failure to myelinate.

Tay Sachs disease is an inherited genetic disorder of the central nervous system (CNS) and is transmitted as an autosomal recessive gene. The disease becomes clinically evident in the fourth to sixth month of life, is characterized by progressive neurological impairment and leads to death usually before the age of four. The development of pathological changes in the brain is associated with the accumulation of excess GM_2 monosialoganglioside which is present in only minute quantities in normal brain. The concentration of ganglioside GM_2 is abnormally high because the enzyme normally responsible for removal of the terminal N-acetylgalactosamine of GM_2, β-N-galactosaminidase or hexosaminidase A, is absent. The absence of the critical enzyme can be detected during pregnancy by amnioscentesis and assaying for β-N-acetylhexosaminidase activity. A morphological characteristic of Tay Sachs disease is the presence of *membranous cytoplasmic bodies*, which are aggregates of phospholipids, cholesterol and gangliosides together with a small fraction of protein (Hill & Lester, 1972).

In normal cells, gangliosides are continuously synthesized and degraded by the lysosomes, cell organelles containing digestive enzymes. If the pathways for degradation of

these lipids are inhibited, gangliosides accumulate in the nervous system and the body "drowns in its own lipids." In diseases arising from imbalances of ganglioside metabolism, death usually occurs at an early age. In Tay Sachs disease death is usually preceded by blindness and slow physical development (Fürst & Sandhoff, 1992; Hill & Lester, 1972; Lester *et al.*, 1972).

1.3 Human Immunodeficiency Virus (HIV)

The human immunodeficiency virus (HIV), the aetiologic agent of AIDS, selectively infects cells expressing the CD_4 molecule. The HIV genome is much more complex than other retroviruses and encodes at least seven regulatory proteins whose functions have not been clearly defined yet. A decline in T cell populations marks the onset of progressive immunological disease in individuals infected with the HIV. Because CD_4^+ cells help to coordinate efficient immune responses, some of the defects in the immune function in advanced cases of AIDS may be explained by the disappearance of these cells (Garcia & Miller, 1991).

The CD_4 antigen, an integral membrane glycoprotein of 55 kDa, is present on MHC class II restricted immunocytes and serves as a marker of helper and suppressor-inducer T cells. CD_4 is also the binding site of the envelope glycoprotein gp 120 of the HIV. The expression of CD_4 on cell membranes can be modulated by anti-CD_4 antibodies, phorbol esters and gangliosides. CD_4 down modulation by phorbol esters is induced by the phosphorylation of all three serine residues in the cytoplasmic tail of CD_4 (Repke *et al.*, 1992). Garcia & Miller (1991), Repke *et al.* (1992), Sorio *et al.* (1993) and other researchers

have demonstrated that the ganglioside induced CD_4 internalization and degradation occurs independently of serine phosphorylation in the cytoplasmic tail of CD_4 molecule. Exogenously added gangliosides induced a selective and complete modulation of CD_4 on human T cells but did not modulate other T cell-surface markers (CD_2, CD_8, CD_{25}) (Kawaguchi *et al.*, 1989).

The monosialoganglioside GM_1 causes a down modulation of CD_4 on T-lymphocytes and their endocytosis. HIV is also known to modulate CD_4 receptors (Kawaguchi *et al.*, 1989; Garcia & Miller, 1991; Repke *et al.*, 1992; Sorio *et al.*, 1993; Saggioro *et al.*, 1993; Clancy *et al.*, 1994). Recently, data demonstrating that CD_4 is an essential component of the receptor for human herpes virus 7 (HHV-7) have been accumulating. Since gangliosides and phorbol esters are known to induce selective down modulation of cell surface CD_4 expression, it might be expected that treatment with these agents would interfere with HHV-7 or HIV infection of CD_4^+ T-cells. Yasukawa *et al.* (1995) have demonstrated that the addition of GM_1 or 12-O-tetradecanoylphorbol-13-acetate effectively induced disappearance of CD_4 from the cell surface and also reduced HHV-7 infectivity. Sorio *et al.* (1993) and others have demonstrated that the induced down modulation of CD_4 by GM_1 is accompanied by inhibition of HIV infectivity (Kawaguchi *et al.*, 1989; Garcia & Miller, 1991; Repke *et al.*, 1992; Saggioro *et al.*, 1993).

1.4 Choleragen

Gangliosides can also act as receptors for several bacterial toxins. Of the various bacterial toxins (e.g., enterotoxin of *E. coli*, tetanus toxin, etc.) that have been reported to

interact with gangliosides, choleragen (cholera toxin) has been the most extensively studied, understood and reviewed. The heat-labile enterotoxin of *E. coli* is very similar to cholera toxin both conformationally and functionally, and can use GM_1 as a cell surface receptor, whereas the potent neurotoxin tetanus toxin has a high affinity for gangliosides GD_{1b} and GT_{1b} and binds to neurons containing these gangliosides (Brady & Fishman, 1979; Fishman, 1982).

The cholera toxin is produced by *Vibrio Cholerae* and elicits the characteristic watery diarrhea associated with cholera. It is a globular protein of 84 kDa comprising two structurally and functionally distinct non toxic components. The B component consists of five identical polypeptides and binds with high affinity to cell surface receptors. On the other hand, the A component consists of two dissimilar polypeptides linked by a disulfide bond and does not bind to cells. The pathological effects are mediated by binding of choleragen to specific receptors on the intestinal mucosal cell and activating adenylate cyclase, causing a subsequent rise in cAMP and resulting in chloride and water secretion by the cells (Fishman, 1982; Myers *et al.*, 1984).

Cholera toxin binds with high affinity and specificity to GM_1. Fishman (1982) have found that exogenously incorporated GM_1 was functionally equivalent to endogenously induced GM_1 as a receptor for choleragen. Although cholera toxin binds to GM_1 on the external side of the plasma membrane, it activates adenylate cyclase on the cytoplasmic side, which inhibits GTP hydrolysis and maintains the cyclase in an activated state. GM_1 appears to facilitate the transmembrane movement of the toxin. Binding of the toxin causes a perturbation of the lipid bilayer (Holmgren *et al.*, 1979; Myers *et al.*, 1984).

1.5 Properties of Gangliosides, Phospholipids and Phospholipid/Ganglioside Bilayers in Aqueous Dispersions

The properties of the gangliosides in aqueous dispersions have been measured by Gammack (1963) and other researchers. They showed that these glycosphingolipids exist in micellar solution above a critical micelle concentration of about 0.02 g/100 ml. Their sedimentation analysis and viscosity measurements revealed that the ganglioside micelles assumed a spheroidal shape, owing to the large polar moiety of the molecules and the small non polar end which gives them a wedge shape. The size of the ganglioside micelle depended on the length of the fatty acid chains in the ceramide backbone. Contrasted to this are the normal membrane lipids such as phosphatidylcholine (PC) which characteristically form a smectic mesophase or lamellar structure (liposomes) in aqueous dispersions (Hill & Lester, 1972).

The insertion of gangliosides into phospholipid membranes induces changes of their physicochemical properties, such as phase behavior and morphology (Müller & Blume, 1993; Kalueff, 1996; Müller *et al.*, 1996). Kojima *et al.* (1988) have showed by electron microscopy that ganglioside/DPPC (dipalmitoylphosphatidylcholine) mixtures formed multilamellar structures at lower concentrations of the gangliosides, and the structures changed to cylindrical and spherical micelles as the ganglioside concentration was increased. Felgner *et al.* (1981) presented ^{31}P NMR results which demonstrate that purified gangliosides spontaneously incorporated into the outer surface of preformed unilamellar PC vesicles, without appreciably altering the character of the phospholipid bilayer. Sillerud *et al.* (1979) and Hinz *et al.* (1981) suggested that, at low ganglioside concentrations ($x_g \leq$

0.25), GM_1, GD_{1a} and GT_{1b} were molecularly dispersed in DPPC bilayers. This conclusion was supported by fluorescence polarization studies using diphenylhexatriene (Uchida *et al.*, 1981). However, other studies support the notion of ganglioside clusters formation in both gel and fluid regions of the matrix phospholipid DPPC (Delmelle *et al.*, 1980; Baret *et al.*, 1982; Gershfeld, 1982; Probst *et al.*, 1984; Thompson *et al.*, 1985, and references therein; Dixon *et al.*, 1987; Cheresh *et al.*, 1987; Seybold *et al.*, 1989; Rahmann *et al.*, 1994, 1998).

1.6 Properties of Membrane Lipids

Phospholipids are the major components of biological membranes and exhibit a strong tendency to spontaneously aggregate in water to form bilayers. Bilayers of controlled composition are extensively used as model systems to gain insight into the structure and function of complex biological membranes. The application of novel spectroscopic techniques to phospholipids in bilayers continues to be essential to elucidate the physicochemical interactions which give rise to the unique and diverse properties to biological membranes.

One of the most important properties of lipids, other than their amphiphilic nature, is their ability to interact with each other and with proteins via intermolecular hydrogen bonds. Since the interfacial regions of membrane lipids are well endowed with proton accepting groups, such as the ester and the amide I C=O groups of glycerolipids and glycolipids, it is natural to assume that molecules with proton donating groups, such as the OH group of cholesterol, are anchored in biomembranes by hydrogen bonding at the interfacial region. Hydrogen bonding between phospholipids and other biological

membranes constituents (notably cholesterol, glycolipids, membrane proteins and interfacial water) have been presented and is believed to play a decisive role in establishing the stability of the membrane (Sharom & Grant, 1977, 1978; Seimiya *et al.*, 1978b; Uchida *et al.*, 1981; Bach *et al.*, 1982; Probst *et al.*, 1984; Boggs, 1986; Mushayakarara *et al.*, 1986; Choma & Wong, 1992; Müller & Blume, 1993). However, the unequivocal detection of such hydrogen bonding, even in model systems, is not a straightforward task.

1.7 Conformational Features of Gangliosides and Their Interactions with Membrane Components

Pascher (1976), Harris and Thornton (1978) and Pascher *et al.* (1992) have shed some light on the conformational features of the ganglioside molecules. The ceramide portion of gangliosides adopts a rigid conformation, with the two hydrocarbon chains packed closely together and oriented parallelly. The oligosaccharide moiety conformation of gangliosides is dependent on the high stability and the number of sialic acid residues and the type of sugars vicinal to sialic acid (Czarniecki & Thornton, 1977). In GM_1, the plane of the inner sialic acid is perpendicular to that of the N-acetylgalactosamine (Sillerud *et al.*, 1982; Müller *et al.*, 1996) and the region of the sialic acid and the tetrasaccharide defines an oxygen rich surface suitable for interaction with cations (Koerner *et al.*, 1983). Abrahamsson *et al.* (1977) suggested that the intramolecular hydrogen bond between the NH group of the ceramide backbone and the glycosidic oxygen tends to impose a shovel position. However, data from the laboratories of McDaniel *et al.* (1984) and Wynn and Robson (1986) questioned this shovel position and suggested that the forces arising from the ganglioside

interactions with the other membrane components may prevent this bend, providing a projected conformation.

Many papers ascertained the capability of gangliosides to affect the activity of a number of functional proteins (Quinet *et al.*, 1984; Masserini *et al.*, 1985; Venerando *et al.*, 1985, 1987; Beitinger *et al.*, 1987; Yasuda *et al.*, 1988; Igarashi *et al.*, 1989; Ledeen, 1989; Yates *et al.*, 1989; Fueshko & Schengrund, 1990; Tiemeyer *et al.*, 1990; Schifferer *et al.*, 1998, 1991; Higashi & Yamagata, 1992; Higashi *et al.*, 1992; Sonnino *et al.*, 1992). Both the plasma membrane linked pumps and channels of Na^+ and Ca^{2+} appear to be modulated by gangliosides, particularly GM_1 (Leon *et al.*, 1981; Spiegel *et al.*, 1986; Nagata *et al.*, 1987; Spiegel, 1988; Varon *et al.*, 1988; Cuello, 1990; Slenzka *et al.*, 1990; Hilbush & Levine, 1992; Nagai 1995), suggesting an important role of gangliosides in the regulation of cation fluxes through the membrane. The Ca^{2+}/ganglioside interactions were the object of accurate investigations (Thomas & Brewer, 1990; Rahmann, 1992; Rahmann *et al.*, 1998) and it was concluded that gangliosides act as modulators of neuronal function, particularly synaptic transmission. The implication of gangliosides in receptor function has a large experimental support. GM_1 acts as the receptor of the cholera toxin (Holmgren *et al.*, 1979) and this glycolipid is essential to the penetration of the toxin into the cell membrane (Brady & Fishman, 1979; Fishman, 1982). Krifuks *et al.* (1998) showed that GM_1 preferentially elicited the down modulation of CD_4 molecules that are associated with $CD_{45}RA$. They concluded that cell surface expression of CD_4 is regulated by the $CD_{45}RA$, a potent activator of the protein kinase $p56^{lck}$.

Under established conditions, gangliosides undergo lateral phase separation with formation of enriched "clusters" (Myers *et al.*, 1984; Masserini & Freire, 1986; Masserini *et al.*, 1988; Palestini *et al.*, 1991), indicating that, besides chemical diversity, aggregation diversity may play a role in governing ganglioside/ligand or ganglioside/protein interactions. Complexes were described to occur between micellar gangliosides and enzymes such as the neural cytosolic sialidase, α-L-fucosidase (Masserini *et al.*, 1985; Venerando *et al.*, 1985, 1987) and bovine serum albumin (Tomasi *et al.*, 1980).

1.8 Spectroscopic Studies

Harris and Thornton (1978) used ^{13}C-NMR and ^{1}H NMR to study the dynamic properties of ganglioside micelles. This study demonstrated a gradient in mobility along the apolar chains and no mobility gradient along the length of the glycosyl headgroup. T_1 relaxation time measurements indicated that the acyl chain methylene groups in ganglioside micelles were less mobile than the egg yolk PC acyl chain methylenes in sonicated vesicles.

In a different vein, McDaniel and McIntosh (1986) used X-ray diffraction to study the orientation of the glycosyl headgroup of GM_1 in 7:3 POPC/GM_1 multilamellar bilayers. This work demonstrated that the glycosyl headgroup is fully extended, and is approximately perpendicular to the plane of the bilayer.

Sharom and Grant (1978) used ESR to study the behavior of bovine brain gangliosides which were spin labeled in the glycosyl headgroup. Reduction of the nitroxide spin label with ascorbate was used to assay for transbilayer ganglioside movement in sonicated egg PC vesicles containing 2 mol% ganglioside. Over a 5 h period, no transbilayer

movement of ganglioside was observed. Plots of correlation time as a function of ganglioside content for egg PC/ganglioside vesicles were sigmoidal, indicating a glycosyl headgroup interaction resulting in decreased mobility. However, in general, the nitroxide-labeled glycosyl headgroups are not highly immobilized.

Lee *et al.* (1980) studied the behavior of spin-labeled gangliosides (1 mol%) in unsonicated dispersions of DMPC (dimyristoylphosphatidylcholine) or DPPC. In each case, a sharp increase in mobility was observed upon heating to a temperature 6-9 °C lower than the phase transition temperature (T_m) of the PC matrix. This was interpreted as an indication that ganglioside molecules were segregated into regions of concentration greater than 1 mol%, which were capable of undergoing the acyl chain order/disorder over a lower, broader temperature range.

Bertoli *et al.* (1981) used a nitroxide-labeled fatty acid probe to study the effects of ganglioside incorporation into small unilamellar egg PC vesicles. With increasing ganglioside content, the fluidity of the apolar bilayer interior decreased. The effect of the monosialo-ganglioside GM_1 was slightly greater than that of the di and trisialoganglioside GD_{1a} and GT_{1b}, respectively.

Recent FTIR-ATR (attenuated total reflection) work by Müller and Blume (1993) indicated that the phosphate asymmetric stretching band of DMPC was affected by Ca^{2+} ions more than the COO^- vibrational band of the monosialoganglioside GM_1 in the mixed DMPC/GM_1 model membranes (5:1, mol/mol), leading the authors to conclude that the binding of the divalent cation to gangliosides is weak.

Müller *et al.* (1996) studied the phase behavior and molecular order of mixed bilayers of DMPC/ganglioside (GM_1, lyso-GM_1, deacetyl-GM_1, deacetyllyso-GM_1, GM_3) by FTIR-ATR spectroscopy. They concluded that (*a*) the insertion of double chain gangliosides into the DMPC matrix had a greater effect on the phase transition temperature of the mixed bilayers than the single chain gangliosides, (*b*) the amide I groups of gangliosides were involved in intermolecular hydrogen bonds, (*c*) the conformation of the headgroup region of gangliosides in the DMPC matrix is crucial for their ability to bind Ca^{2+} ions and (*d*) this conformation is determined by the chemical nature of the oligosaccharide region and the number of hydrocarbon chains in the ceramide backbone of the gangliosides.

1.9 Research Objectives

Enzyme assays are used for the pre and postnatal diagnosis of inherited metabolic glycolipid disorders caused by lysosomal enzyme deficiencies (e.g., Tay Sachs disease). However, the detection of an enzyme deficiency does not necessarily allow prediction of the clinical course of the disorder since further supportive biochemical information on the accumulated gangliosides and their effects on biological membranes is also required.

Although gangliosides have been recognized as important constituents of cell surfaces for quite some time, very little is known concerning their normal biological functions and physical properties, partly because of their cost and difficulty to synthesize. Therefore, an easy, simple extraction and purification method had to be found or developed to isolate this interesting class of glycosphingolipids and to investigate its conformational and dynamical properties. To address this issue, the methods of Folch *et al.* (1951 & 1957),

Svennerholm (1957, 1963 & 1972) and Fredman (1980), Hakomori and Siddiqui (1974), Iwamori and Nagai (1978), Fredman *et al.* (1980), Ledeen and Yu (1973 & 1982), Myers *et al.* (1984) and Reed *et al.* (1987) were carefully studied and combined, and an isolation/purification procedure, with a few modifications, was adopted for this study.

FTIR was employed to examine the thermotropic profile of $DMPC_{d54}/GM_1$ bilayer membrane systems in a 10:0.66 molar ratio which mimic the semi-fluid nature of plasma membranes and the low overall glycosphingolipid biomembrane concentrations. The content of GM_1 in the mixed $DMPC_{d54}/GM_1$ bilayers was increased to mimic the physiological conditions associated with the accumulation of gangliosides (neurological disorders such as GM_1 gangliosidosis and Tay Sachs disease). Synthetic perdeuterated $DMPC_{d54}$ was used as a host phospholipid. In perdeuterated acyl chains, bands at 2195 and 2090 cm^{-1} are due to the CD_2 asymmetric and symmetric stretching vibrations. The use of deuterated acyl chains provides a useful means to circumvent problems associated with interferences from the CH_2 asymmetric (2929 cm^{-1}) and symmetric (2850 cm^{-1}) stretching vibrations by GM_1. Since gangliosides are involved in the regulation of Ca^{2+} homeostasis and synaptic transmission, we have also been interested in determining whether this divalent cation interacts with the negatively charged sialic acid moiety of GM_1 and whether this interaction affects the hydrogen bonding of the interfacial region, the dynamics of the lipid hydrocarbon chains and the phase transition behavior of $DMPC_{d54}/GM_1$ mixed model membranes. Both the OH and the ester and amide I C=O stretching vibrations are infrared active. Therefore, carbonyl and hydroxyl associations can be examined conveniently and non invasively by FTIR to assess the extent of hydrogen bonding formation at the interfacial zone of multilamellar bilayers.

CHAPTER TWO

MATERIALS & METHODS

2.1 Reagents & Tissue Material

The following chemical products were all obtained from VWR Canada: methanol, chloroform, isobutanol, propanol, potassium chloride, potassium hydrogen carbonate, resorcinol reagent, sodium acetate trihydrate, calcium chloride dihydrate, potassium acetate, EDTA, sodium hydroxyde, α-naphthol, sodium molybdate dihydrate, hydrazine sulfate, hydrochloric acid (density 1.19, 36.5 % HCl, and Fe^{3+} not more than 0.0001 %), sulfuric acid, cupric sulfate pentahydrate, Spectra/Pro CE (Cellulose Ester) dialysis membrane (20 mm diameter) MWCO 500, precoated thin layer plates Diamond K6F silica gel 60 Å, 2.5 x 7.5 cm, 250 µm layer thickness and K6 silica gel 60 Å, 5.0 x10 cm, 250 µm layer thickness, silica gel (Kieselgel G, 230-400 mesh). DEAE-Sepharose CL-6B, a macroporous bead formed weak anion exchanger based on a traditional cross-linked agarose gel with a mean particle size of 90 µm, particle size range 45-165 µm in wet form, was obtained from Pharmacia. Synthetic perdeuterated $DMPC_{d54}$ was purchased from Avanti Polar Lipids and used without further purification. Gangliosides GM_1 and GT_{1b} were purchased from Sigma Chemical Co. and used without further purification for TLC analysis. Deuterated water was purchased from MSD Isotopes (Montréal, Québec, Canada). Bovine brains (grey and white matter) were obtained from a local slaughter house.

2.2 Extraction of Gangliosides from Bovine Brain Tissue

Cerebral tissue (0.480 kg) was homogenized with 1.5 l of distilled water in a waring blender at a medium speed for 4 min at 4 °C. The brain homogenate was poured into 5.4 l of CH_3OH at room temperature under constant stirring and afterwards 2.7 l of $CHCl_3$ was added. The mixture was stirred for 30 min at room temperature and was then centrifuged at 3200 rpm for 30 min. The supernatant was cleared by filtration through a Büchner funnel with a Whatman filter paper, filtration being stopped before the insoluble residue became dry. The brain residue was reextracted once by homogenization in 1.0 l of water in the waring blender and poured into 4.0 l of $CHCl_3$:CH_3OH (1:2, v/v). Centrifugation and filtration were done as before (Svennerholm & Fredman, 1980).

2.2.1 Isolation of Crude Gangliosides by Solvent Partition

The two extracts were combined in a large funnel and 2.6 l of water was added to give a final $CHCl_3$:CH_3OH:water (+ tissue) ratio of 1.0:2.0:1.4. The solvents were carefully mixed by turning the funnel up and down several times but shaking was omitted to prevent emulsification. When the 2 phases were distinctly separated (generally within 6 hr), the lower phase was removed and the upper phase set aside. To the lower phase (ca. 3 l), 1.5 l of CH_3OH was added. After thorough shaking of the funnel, 1.0 l of 0.01 M KCl in water was added slowly and carefully mixed with the extract. The funnel was left overnight at 4 °C. The 2 upper phases were combined and evaporated to dryness in a rotating evaporator operated at 40-50 °C after the addition of isobutanol to prevent foaming (Svennerholm & Fredman, 1980).

2.2.2 Purification of the crude ganglioside fraction

The residue of the upper phases was dissolved in 0.5 l of $CHCl_3$:CH_3OH:water (60:30:4.5) and left for 24 h at room temperature. The precipitate was removed by centrifugation. The ganglioside extract was evaporated and the residue dissolved in 0.2 l of water. It was dialyzed against running tap water for 48 h and then against 2 volumes of distilled water for 24 h each. The dialyzed gangliosides were evaporated and then redissolved in 0.2 l of $CHCl_3$:CH_3OH:water (60:30:4.5) (Svennerholm & Fredman, 1980).

2.3 Separation of Gangliosides on "DEAE-Sepharose" Anion Exchange Resin

2.3.1 Preparation of DEAE-Sepharose

Sepharose CL-6B (500 ml), preswollen in 20% ethanol, was washed exhaustively with distilled water. It was then converted to the acetate form as follows: the resin was washed with $CHCl_3$:CH_3OH: 1.0 M sodium acetate (30:60:8, v/v) and left for 2 days in the same solution. The gel suspension was packed into two glass columns (3.0 cm inner diameter x 40 cm, 250 ml) with a stopcock to a bed volume of 200 ml each. It was then washed exhaustively with $CHCl_3$:CH_3OH:water (30:60:8, v/v) to remove sodium acetate and packed in the same solvent to avoid floating of the resin (Svennerholm & Fredman, 1980; Iwamori & Nagai, 1978; Hakomori & Siddiqui, 1974; Ledeen & Yu, 1973 & 1982; Myers *et al.*, 1984 and Reed *et al.*, 1987).

2.3.2 Separation of Gangliosides on DEAE-Sepharose

Dialyzed brain gangliosides, corresponding to 1 mmol of NeuAc, dissolved in 200 ml of $CHCl_3$:CH_3OH:water (60:30:4.5, v/v) were placed on the columns. *For complete retention of gangliosides on the exchanger, the crude ganglioside extract had to be free from salts, for even small amounts would cause a leakage of monosialogangliosides in the neutral fraction.* The extract was passed through the column, the effluent rate did not exceed 0.5 ml/min *(leakage of gangliosides occurred when the extract was placed on the column with a flow rate higher than 0.5 ml/min).* Each column was then rinsed with 200 ml of $CHCl_3$:CH_3OH:water (60:30:8, v/v) and 200 ml of CH_3OH. All the effluents were collected in one batch. The gangliosides were eluted at a rate of 1-2 ml/min and separated according to the following scheme:

Fraction I: 1.6 l (8 volumes) of 0.02 M potassium acetate in CH_3OH

Fraction II: 2.0 l (10 volumes) of 0.10 M potassium acetate in CH_3OH

Fraction III: 1.6 l (8 volumes) of 0.20 M potassium acetate in CH_3OH

The eluates were collected in batches and evaporated to dryness. The dried lipids were dissolved in 200 ml of water, dialyzed against running tap water for 48 hr and then against 2 changes of distilled water for 24 hr each. After evaporation of the contents of the dialysis bags, the ganglioside fractions I, II and III were dissolved in 100 ml of $CHCl_3$:CH_3OH:water (60:30:4.5, v/v). A small portion (2 mg) of solid $KHCO_3$ was added to the extracts (Svennerholm & Fredman, 1980; Fredman *et al.*, 1980).

2.4 Final Purification of the Individual Gangliosides

The three ganglioside fractions from the DEAE-Sepharose column consisted of mono, di and trisialogangliosides, respectively. They were subsequently separated and purified by silica gel column chromatography (Fredman *et al.*, 1980; Hakomori & Siddiqui, 1974; Ledeen & Yu, 1973 & 1982; Myers *et al.*, 1984 and Reed *et al.*, 1987).

2.4.1 Silica Gel Column Chromatography

Column chromatography was performed on silica gel Merck 230-400 mesh, used without any pretreatment, equilibrated with either $CHCl_3$:CH_3OH (4:1, v/v) or $CHCl_3$: CH_3OH:2.5 M aqueous NH_3 (60:32:7, v/v). Fractions of 20 ml were collected when the column consisted of 100 g of silica gel or more (Fredman *et al.*, 1980). Each of the 3 fractions contained a large number of minor gangliosides, but the following description was adopted for the elution of the major gangliosides.

Fraction I: Optimal loading was 250 µmol NeuAc/100 g of gel. The column was packed in $CHCl_3$:CH_3OH (4:1, v/v) and gangliosides were placed on the column dissolved in $CHCl_3$: CH_3OH:water (65:25:4, v/v). The column was then eluted with the same solvent and fractions of 20 ml were collected on a fraction collector. The elution of the gangliosides was monitored by TLC in $CHCl_3$:CH_3OH:0.20 % $CaCl_2$ (60:40:9, v/v) and spraying of the plates with the resorcinol and α-naphthol reagents. The monosialogangliosides GM_3, GM_2 and GM_1 were eluted in this order with a small overlap. When ganglioside GM_1 appeared in the effluent, the eluant was changed to $CHCl_3$:CH_3OH:water (60:32:7, v/v).

Fraction II: The disialogangliosides, dissolved in $CHCl_3$:CH_3OH:water (65:25:4, v/v), were separated on a silica gel column packed in $CHCl_3$:CH_3OH (4:1, v/v). Ganglioside GD_3 was eluted with 25 gel volumes of $CHCl_3$:CH_3OH:water (65:25:4, v/v) and then the solvent was changed to $CHCl_3$:CH_3OH:2.5 M aqueous NH_3 (60:32:7, v/v). In this system, gangliosides GD_{1a} and GD_2 were eluted with a broad overlap but well separated from the ganglioside GD_{1b}.

Fraction III: The silica gel column was packed in $CHCl_3$:CH_3OH:2.5 M aqueous NH_3 (60:32:7, v/v) and the gangliosides were dissolved in the same solvent and placed on the column. Elution was performed with the same solvent. The ganglioside GT_{1a} was eluted before GT_{1b} with some overlap.

2.5 Base Treatment of Contaminating Acidic Lipids

This step was introduced into the gangliosides' purification procedure for the hydrolysis (or methanolysis) of contaminating lipids and fatty acids containing O-acyl esters. The residue from evaporation of the crude ganglioside fraction, containing acidic lipids (e.g. sulfatides, free fatty acids, etc.), was solubilized with mild sonication in 0.1 *N* methanolic sodium hydroxyde. This was conveniently carried out in the same round bottom flask (250 or 500 ml) in which the crude fraction was evaporated. After heating at 35-40 °C for 2-3 hr, the mixture was quickly evaporated under reduced pressure to remove the methanol. The remaining mixture was transferred to prewashed dialysis tubing and the container was rinsed a number of times with a total of about 20 ml of water. One milliliter of 0.5 M EDTA

(tetrasodium salt) was added to eliminate divalent cations. Dialysis was carried out for 2 days in the cold (T = 4 °C) against distilled water and the dialysis tubing contents were lyophilized to dryness. However, an additional silicic acid column chromatography step was needed to remove the acidic lipids that survived the base treatment (Ledeen and Yu, 1982).

2.6 Purity Verification of Gangliosides

2.6.1 Thin Layer Chromatography (One-Dimensional)

Thin layer chromatography (TLC) was the standard tool for resolution of ganglioside mixtures for analytical pattern determination and for preparative purposes as well. It was carried out on precoated thin layer plates Diamond K6F silica gel 60 Å, 2.5 x 7.5 cm, 250 µm layer thickness and K6 silica gel 60 Å, 5.0 x 10 cm, 250 µm layer thickness. The plates were freshly activated by heating at 85-100 °C for 30-60 min, cooled in a dessicator and placed in a chamber containing ca. 100 ml of developing solvent ($CHCl_3$:CH_3OH:0.20% $CaCl_2$, 60:40:9, v/v). The closed chamber was allowed to equilibrate for at least 2 hours with fresh solvent before plate insertion. The solvent was allowed to ascend to within 1 cm or so of the top of the plate. Two consecutive ascending runs were carried out with the developing solvent, the plates being thoroughly dried in a vacuum dessicator between runs. Resorcinol-HCl and α-naphthol reagents were employed to detect gangliosides and they were applied as a fine, even spray. After spraying, the plates were placed horizontally in a closed jar for 30 min at 110 °C until maximum color developed (Svennerholm, 1957; Svennerholm, 1963; Ledeen *et al.*, 1973; Ledeen & Yu, 1982).

2.6.2 Preparation of Resorcinol Reagent

Two grams of resorcinol were dissolved in 100 ml of distilled water (resorcinol stock solution). Ten milliliters of this solution was added to 80 ml of concentrated HCl containing 0.25 ml of 0.1 M copper sulfate pentahydrate. The volume of the reagent was made up to 100 ml with distilled water. The reagent was prepared at least 4 hours before use. The aqueous stock solution remained stable for several months at 4 °C and was usable until the yellow color changed to green. Gangliosides produced red/violet spots, which changed to a brownish hue when overheated; other glycolipids produced yellow spots (Svennerholm, 1957; Svennerholm, 1963; Ledeen *et al.*, 1973; Ledeen & Yu, 1982).

2.6.3 α-Naphthol Stain for Glycolipids

The α-naphthol solution (0.5%) was prepared by dissolving 0.5 g of α-naphthol in 100 ml of CH_3OH:water (1:1, v/v). The TLC plates, developed in $CHCl_3$:CH_3OH:0.20% $CaCl_2$ (60:40:9, v/v), were sprayed until damp. They were allowed to dry in air, sprayed lightly with a concentrated sulfuric acid solution (H_2SO_4:water, 95:5, v/v), placed in a closed jar and heated at 120 °C until maximum color developed. Glycolipids (cerebrosides, sulfatides, gangliosides, glycosyl diglycerides, etc.) gave blue-purple spots while other polar lipids and cholesterol produced yellow spots and grey-red spots, respectively (Kates, 1986).

2.6.4 Procedure of Beiss (1964) for Phosphorus Analysis

The method of Beiss (1964) as described in detail by Kates (19886) was followed. The Zinzade's reagent was prepared by dissolving 6.85 g of sodium molybdate dihydrate and

400 mg of hydrazine sulfate in 100 ml water. Concentrated H_2SO_4 (250ml) and 600 ml water were added to the reagent. The dried chromatogram was immersed in Zinzade's reagent for several minutes until maximum blue color of phosphatides developed (Kates, 1986).

2.7 Preparation of Multilamellar Bilayers

Infrared spectroscopy was employed to study pure micellar suspensions of bovine brain GM_1 and multilamellar dispersions of pure $DMPC_{d54}$ and mixed $DMPC_{d54}/GM_1$ with a molar ratio of 10:0.66, 8:0.66, 6:0.66, 4:0.66, 2.64:0.66, 2:0.66 and 1:0.66.

For the $DMPC_{d54}$/ganglioside mixtures, each lipid was dissolved in $CHCl_3$:CH_3OH (2:1, v/v) and then mixed. The chloroform was evaporated under a stream of nitrogen and then the lipid mixtures were left overnight under vacuum. The lipidic dispersions (10% w/v) were prepared by hydrating the dry lipid mixture with the appropriate amount of D_2O or H_2O buffer, at p^2H 7.5 or pH 7.5, respectively, without Ca^{2+} or with 10 mM $CaCl_2$. At least four freeze (liquid nitrogen, -80 °C)/thaw (water bath, 80 °C) cycles were performed to ensure a homogeneous organization of the liposomes. This preparation led to the formation of multilamellar bilayers in which the gangliosides were incorporated. GM_1 micellar suspensions (10% w/v) and $DMPC_{d54}$ dispersions (10% w/v) were prepared in the same manner. In D_2O, the amide II band of the ganglioside GM_1 shifts to wavenumbers below 1500 cm^{-1} due to the H/D exchange at the amide groups (Müller & Blume, 1993). Therefore, the use of D_2O for this study can be justified by the fact that the amide I and ester C=O functional groups are the only vibrational modes that absorb in the range 1500-1700 cm^{-1}, without interference from the amide II stretching mode.

2.8 Spectroscopic Analysis

To study the thermotropic behavior of GM_1, $DMPC_{d54}$ and mixtures of $DMPC_{d54}/GM_1$, the samples were placed between two calcium fluoride windows separated by a 6 μm spacer. The temperature-dependent FTIR measurements were carried out by recording a spectrum between 5 °C and 60 °C. A thermostat-equipped cell mount and a variable temperature water bath were used to heat the sample. Infrared spectra were measured at room temperature using a Digilab FTS-40A spectrometer equipped with a liquid nitrogen cooled mercury-cadmium-telluride detector (MCT). For each spectrum, 256 interferograms were accumulated with a spectral resolution of 2 cm^{-1}. The instrument was purged continuously with dry air to eliminate spectral contributions from atmospheric water vapor. Fourier self-deconvolution of overlapping IR bands was performed using the resolution enhancement procedure described by Kauppinen *et al.* (1981). Frequencies were determined with the aid of Fourier derivation (Cameron & Moffatt, 1987).

CHAPTER THREE

RESULTS

3.1 Characterization of the Monosialoganglioside GM_1

The monosialoganglioside GM_1 was purified from bovine brain. The final purity of GM_1 was greater than 99 %, as judged by thin layer chromatography (TLC). Purity of the GM_1 samples was verified by TLC using the solvent system $CHCl_3$:CH_3OH: 0.20 % $CaCl_2$ (60:40:9, v/v) (Ledeen and Yu, 1982) and the glycolipid staining was performed either with the resorcinol-HCl reagent (Svennerholm, 1957) (Figure 3.1) or the α-naphthol/H_2SO_4 reagent (Kates, 1986) (Figure 3.2) followed by charring. All the samples showed positive staining, verifying that they were glycolipids. The GM_1 sample gave a single band with its relative R_f value of 0.49 (Table IV).

The negative ion FAB mass spectra of underivatized bovine brain monosialoganglioside GM_1 is shown in Figure 3.3. The ion observed at m/z 1544 on the negative ion FAB mass spectrum was assigned to the molecular ion $(M-H)^-$. This m/z value was used to deduce the size of the carbohydrate chain [three hexoses (3 x 162), one *N*-acetylgalactosamine (1 x 203), one *N*-acetylneuraminic acid (1 x 291) added to 565 (ceramide) totals 1545]. Random fragmentation at glycosidic bonds with negative charge retention on the oligoglycosyl ceramide residue gives a series of fragment ions at m/z 1382, 1179, 888 and 282, used to deduce the sequence of the carbohydrate units in the glycosphingolipid.

Figure 3.1 Thin layer chromatograms of gangliosides from bovine brain (BB) white and grey matter. Precoated thin layer plates, Diamond K6F silica gel 60 Å, 2.5 x 7.5 cm, 250 µm layer thickness were used. The solvent system $CHCl_3$:CH_3OH: 0.20 % $CaCl_2$ (60:40:9, v/v) was used. Ganglioside bands were revealed with the resorcinol-HCl reagent after charring. Std denotes standards; GM, GD and GT denote the mono, di and trisialoganglioside molecular species; GANG denotes the crude gangliosides fraction composed of different ganglioside molecular species

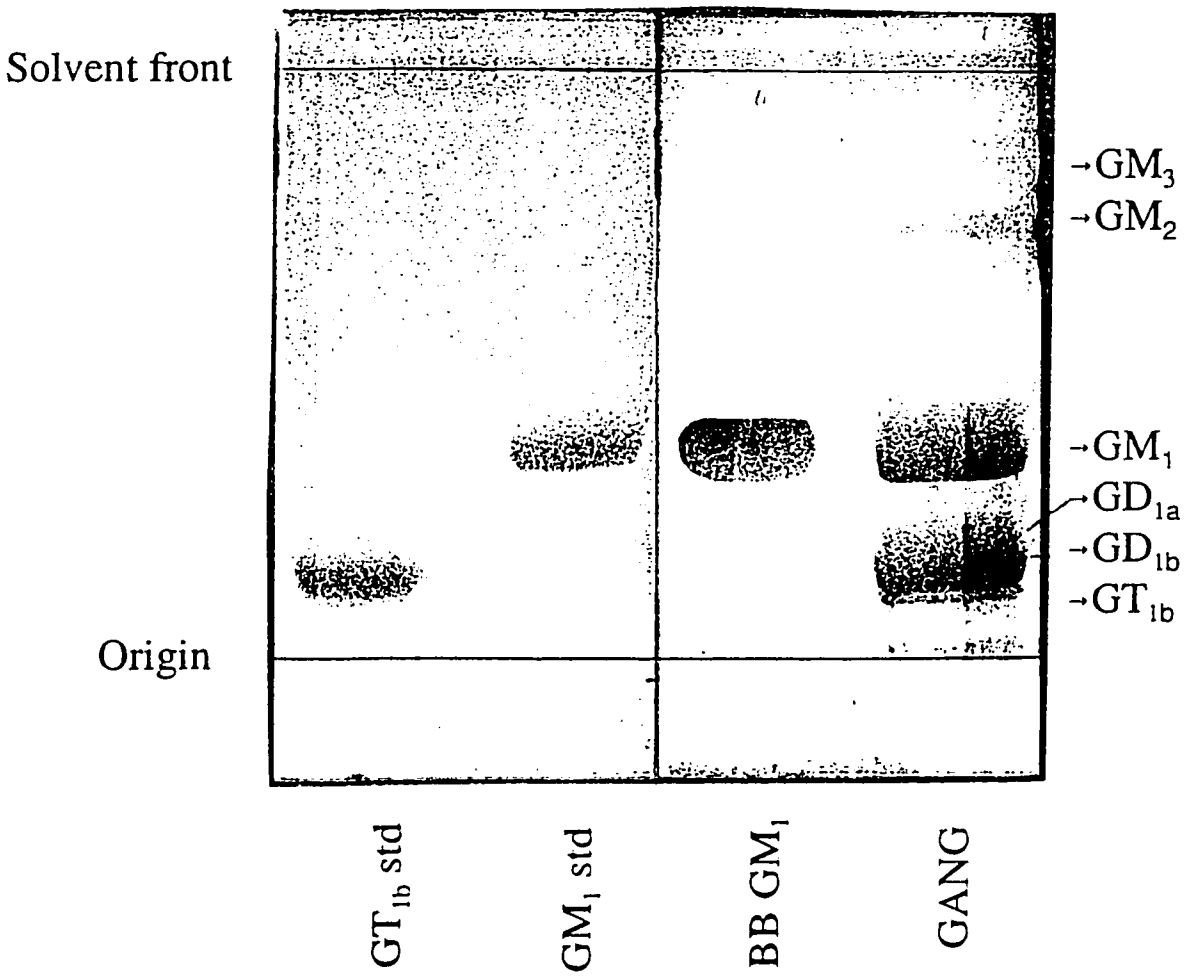
Solvent front
Origin
→GM3
→GM2
→GM1
→GD1a
→GD1b
→GT1b
GT1b std
GM1 std
BB GM1
GANG

Figure 3.2 Thin layer chromatograms of gangliosides from bovine brain (BB) white and grey matter. Precoated thin layer plates, Diamond K6F silica gel 60 Å, 2.5 x 7.5 cm, 250 µm layer thickness were used. The solvent system $CHCl_3$:CH_3OH: 0.20 % $CaCl_2$ (60:40:9, v/v) was used. Ganglioside bands were revealed with the α-naphthol reagent after charring. Std denotes standards; GM, GD and GT denote the mono, di and trisialogangliosides molecular species. The monosialoganglioside GM_1 from BB was chromatographed twice to ensure reproducibility of the results.

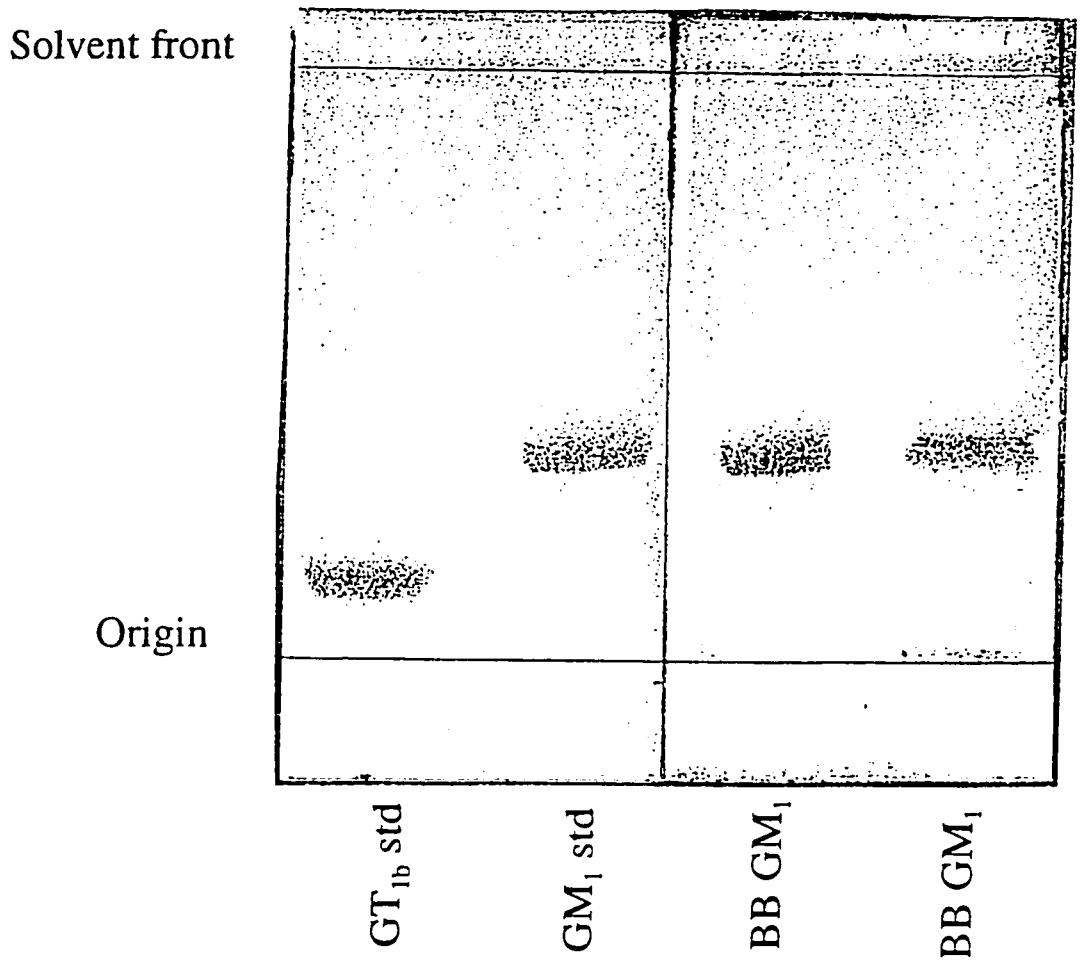
Solvent front
Origin
GT_{1b} std
GM_1 std
BB GM_1
BB GM_1

Table IV

R_f Values of Bovine Brain Gangliosides Separated by TLC using the Solvent System $CHCl_3$:CH_3OH:$CaCl_2$ (60:40:9, v/v) and those of Gangliosides Separated by Ledeen & Yu, 1982.

Glycosphingolipid	R_f*	R_f* (from Ledeen & Yu, 1982) [1]
GM_4	-	0.90
GM_3	0.82	0.83
GM_2	0.64	0.62
GM_1	0.49	0.49
GD_3	-	0.38
GD_{1a}	0.30	0.31
GT_{1a}	-	0.25
GD_2	-	0.21
GD_{1b}	0.16	0.15
GT_{1b}	0.10	0.095
GQ_{1b}	-	0.0057

* R_f = distance migrated by lipid band/distance migrated by solvent front.
[1] Reference contains picture of their chromatogram. R_f values are based on my calculations.

Figure 3.3 Negative ion FAB mass spectra of the monosialoganglioside GM_1 from bovine brain, obtained directly after thin layer chromatography with the solvent system $CHCl_3$:CH_3OH:0.20 % $CaCl_2$ (60:40:9, v/v) and staining by the resorcinol-HCl and α-naphthol reagents. This bar graph plot was obtained from the Ottawa-Carleton Universities Mass Spectrometry Center.

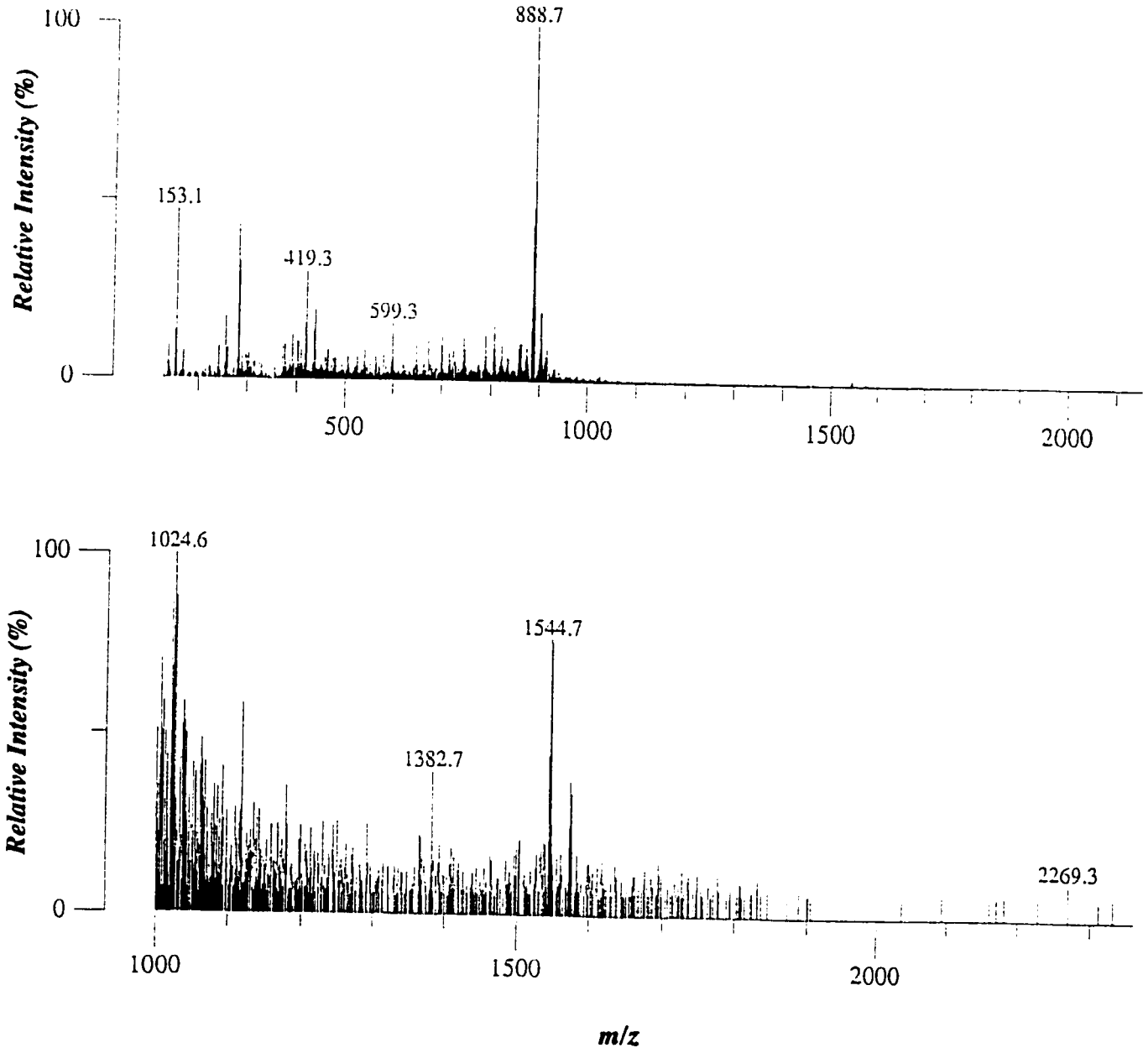
100
888.7
Relative Intensity (%)
153.1
419.3
599.3
0
500
1000
1500
2000
100
1024.6
1544.7
Relative Intensity (%)
1382.7
2269.3
0
1000
1500
2000
m/z

The fatty acid composition of GM_1 was determined by mass spectrometry as can be seen in Table V and it was heavily dominated by stearic acid, $C_{18:0}$, with the rest being a mixture of myristic $C_{14:0}$, pentadecanoic $C_{15:0}$, palmitic $C_{16:0}$, heptadecanoic $C_{17:0}$, oleic $C_{18:1}$, nonadecanoic $C_{19:0}$, arachidic $C_{20:0}$, and arachidonic $C_{20:4}$ acids. The glycolipid's sphingoid base chain length was 18 carbon atoms.

3.2 GM_1 Micellar Suspensions

Gangliosides are membrane glycosphingolipids containing a hydrophilic oligosaccharide portion glycosidically linked to a hydrophobic ceramide, which anchors the ganglioside molecule in the membrane. Several classes of gangliosides are differentiated by the number and position of attachment of one or more sialic acid residues. The presence of the latter confers a negative charge on the oligosaccharide portion of the molecule, which engenders a strong interaction with cations of biological significance, like calcium (Ca^{2+}).

The amide I stretching mode ranges fom 1590-1660 cm^{-1} (Kates, 1986). Figure 3.4 shows the infrared spectra of GM_1 micellar suspensions without Ca^{2+} (panel A, solid line) and with 10 mM $CaCl_2$ (panel A, dashed line) in this frequency range. The Fourier deconvolution of the same region, using a resolution enhancement factor of 1.5, reveals the individual component bands that comprised the broad bands in the original spectra. The deconvolved spectrum of GM_1, in the absence of the divalent cation Ca^{2+} (Figure 3.4, panel B, solid line), reveals three components in this absorption mode: a high frequency component at ca. 1645 cm^{-1}, a low frequency component at ca. 1625 cm^{-1} and a shoulder at 1605 cm^{-1}.

Table V

Major Fatty Acid Molecular Species of the Monosialoganglioside GM_1 as Deduced from the Fast Atom Bombardment Mass Spectra

		Monosialoganglioside GM_1	
Fatty Acid	**m/z**	**Relative Intensity (%)***	**Fatty Acid %** ¶
$C_{14:0}$	227	2	1
$C_{14:1}$	225	3	2
$C_{15:0}$	241	10	6
$C_{15:1}$	239	3	2
$C_{16:0}$	255	18	12
$C_{16:1}$	253	4	3
$C_{17:0}$	269	1	0.6
$C_{18:0}$	***283***	***54***	***35***
$C_{18:1}$	***281***	***32***	***21***
$C_{18:2}$	279	8	5
$C_{19:0}$	297	7	5
$C_{20:0}$	311	5	3
$C_{20:4}$	303	7	5

* The relative intensities (%) of the ion fragments of GM_1, corresponding to the major fatty acids species of the ceramide backbone, were provided along with the bar graph plot from the Ottawa-Carleton Universities Mass Spectrometry Center.

¶ The fatty acid % = $\dfrac{\text{relative intensity (re) of fatty acid}}{\sum \text{re of each fatty acid}}$

Figure 3.4 Amide I C=O stretching region of the infrared spectrum of a GM_1 micellar solution in ^2H_2O buffer, at p^{2}H 7.5, without Ca^{2+} (solid line) or with 10 mM $CaCl_2$ (dashed line), before (**A**) and after (**B**) deconvolution with a bandwidth of 18 and a breakpoint of 1.5 in the Fourier domain. The spectra were autoscaled.

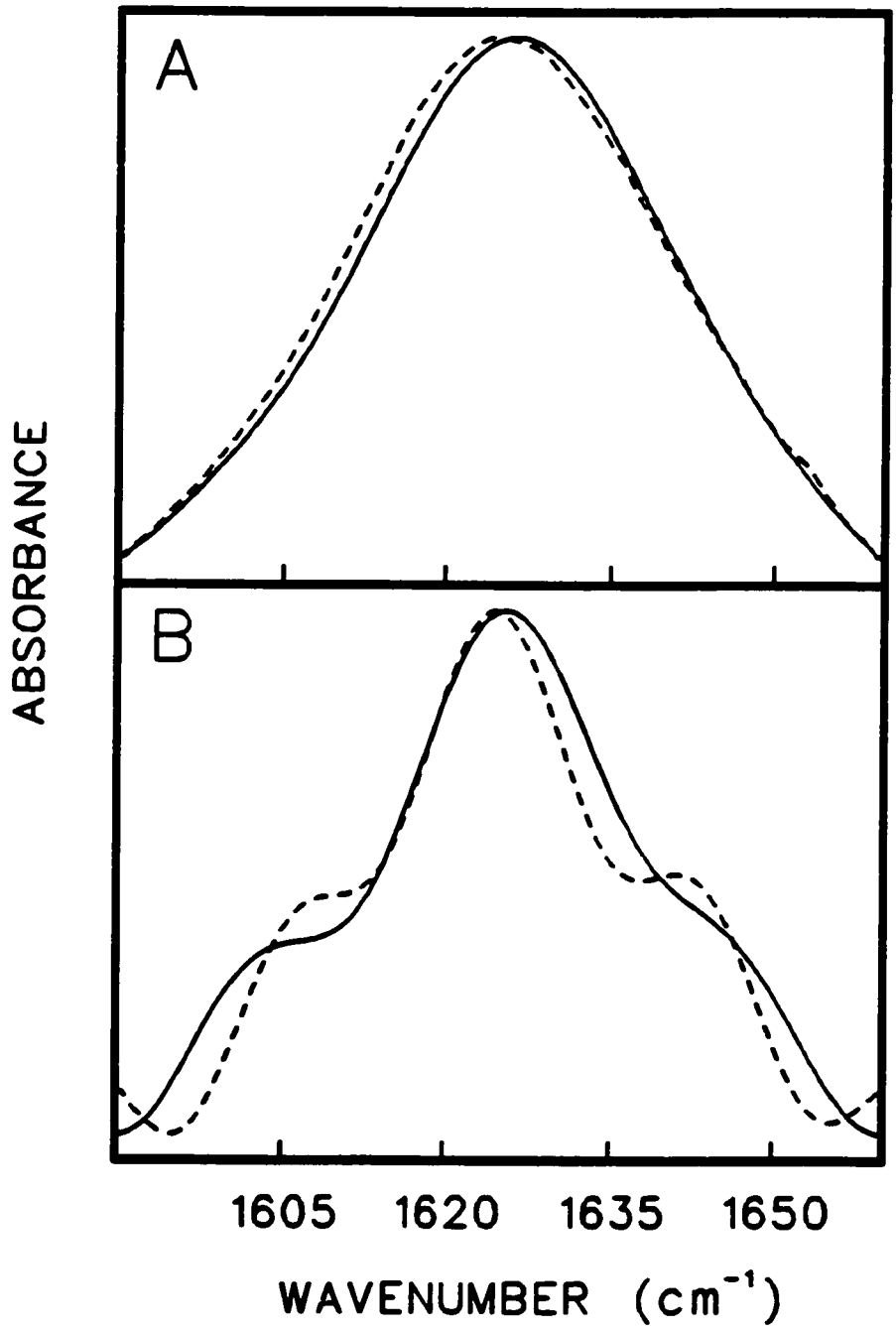
A
B
ABSORBANCE
1605
1620
1635
1650
WAVENUMBER (cm⁻¹)

After the addition of Ca^{2+} (Figure 3.4, panel B, dashed line), the high frequency component of the amide I C=O stretching mode increased in intensity and shifted slightly in frequency from 1645 to 1640 cm^{-1}; the low frequency component increased slightly in frequency from 1625 to 1620 cm^{-1} and the shoulder at 1605 cm^{-1} shifted to 1610 cm^{-1} and increased in intensity. We will show and explain below that the latter is too low in frequency to be attributed to the amide I band and that it is clearly due to the unprotonated carboxyl group (CO_2^-) of the sialic acid moiety of the monosialoganglioside GM_1. The third order Fourier transform derivative spectra of the amide I region (results not shown) were obtained with a power of 3 and a breakpoint of 0.2 and confirmed the presence of three component bands at 1645 cm^{-1}, 1625 cm^{-1} and 1605 cm^{-1} in the absence of Ca^{2+} ions and these bands were centered at 1640 cm^{-1}, 1620 cm^{-1} and 1610 cm^{-1} in the presence of the divalent cation.

3.3 $DMPC_{d54}$ Multilamellar Dispersions

The C=O stretching mode absorbs as a broad band in the frequency range 1690-1760 cm^{-1}. The ester carbonyl stretching band in aqueous suspension is presented in Figure 3.5. The original spectrum consists of an asymmetric band (panel A) and two components can be observed after resolution enhancement using Fourier self deconvolution (panel B). The frequencies of these bands were obtained with the aid of the third order Fourier derivation with a power of 3 and a breakpoint of 0.2. In the absence of Ca^{2+} (panel B, solid line), the high frequency component at 1745 cm^{-1} pertains to carbonyl groups that are not hydrogen bonded, and the peak at 1725 cm^{-1} corresponds to hydrogen bonded carbonyl groups (Wong and Mantsch, 1988; Blume *et al.*, 1988). After the addition of Ca^{2+} (panel B, dashed line),

Figure 3.5 Carbonyl stretching region of the infrared spectrum of a dispersion of $DMPC_{d54}$ in ^2H_2O buffer, at p^{2}H 7.5, without Ca^{2+} (solid line) or with 10 mM $CaCl_2$ (dashed line), before (**A**) and after (**B**) deconvolution with a bandwidth of 17 breakpoint of 1.5 in the Fourier domain. The spectra were autoscaled.

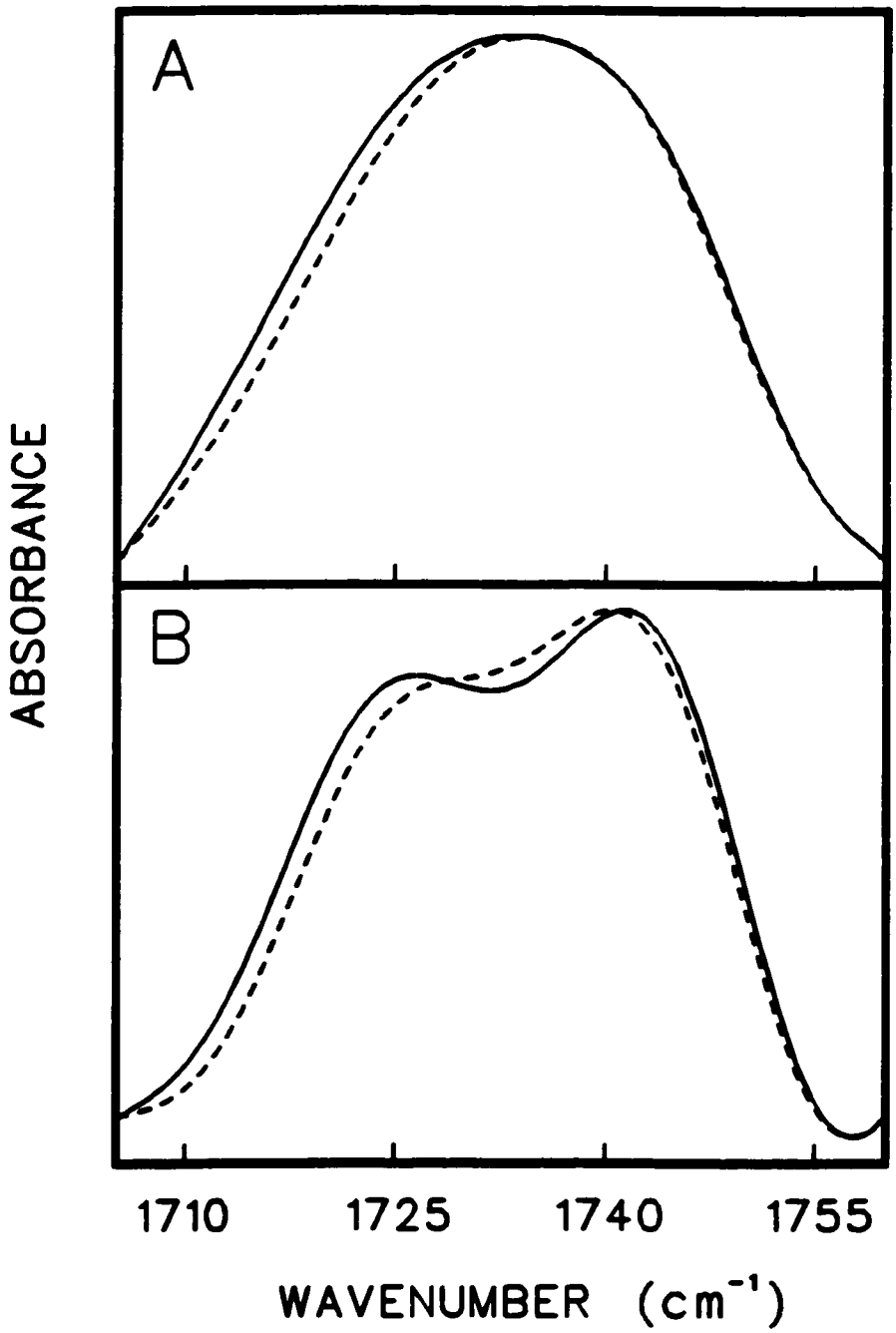
A
B
ABSORBANCE
1710
1725
1740
1755
WAVENUMBER (cm⁻¹)

the high frequency component at 1745 cm^{-1} shifts to 1742 cm^{-1}, and the low frequency component decreases in intensity and shifts in frequency from 1725 cm^{-1} to 1730 cm^{-1}. Ca^{2+} binding reduces the penetration of D_2O to the bilayer interface region and is consistent with a tightening of the lipidic network.

3.4 The Interfacial Region of $DMPC_{d54}/GM_1$ Liposomal Dispersions (Amide I and Ester C=O Groups)

The amide I C=O stretching mode (1590-1660 cm^{-1}) and the ester carbonyl stretching mode (1690-1760 cm^{-1}) are examined to assess the degree of hydrogen bonding at the interfacial region of bilayers (Kates, 1986). Figure 3.6 shows the infrared spectra of GM_1 micellar suspensions (panel A, solid line) and $DMPC_{d54}/GM_1$ mixed bilayers with a molar ratio of 4:0.66 (panel A, dashed line) in this frequency range. The deconvolved spectrum of GM_1 (panel B, solid line), with a resolution enhancement factor of 1.5, reveals three overlapping component bands: a high frequency component at ca. 1640 cm^{-1}, a low frequency component at ca. 1625 cm^{-1}, and a shoulder at 1605 cm^{-1}. The frequencies of these bands were obtained with the aid of Fourier derivation with a power of 3 and a breakpoint of 0.2. The deconvolved spectrum of the mixed liposomal bilayers (panel B, dashed line) reveals three components in the amide I C=O absorption mode: a high frequency component at ca. 1645 cm^{-1}, a low frequency component at ca. 1630 cm^{-1}, and a shoulder at 1610 cm^{-1}. All components of the amide I band, in the mixed $DMPC_{d54}/GM_1$ liposomal bilayers, slightly shifted to higher frequencies as compared to GM_1 micellar suspensions.

Figure 3.6 Amide I C=O stretching region of the infrared spectrum of a GM_1 micellar solution (solid line) and a $DMPC_{d54}/GM_1$ dispersion with a molar ratio of 4:0.66 (dashed line) in ^2H_2O buffer, at p^{2}H 7.5, before (**A**) and after (**B**) deconvolution with a bandwidth of 18 and a breakpoint of 1.5 in the Fourier domain. The spectra were autoscaled.

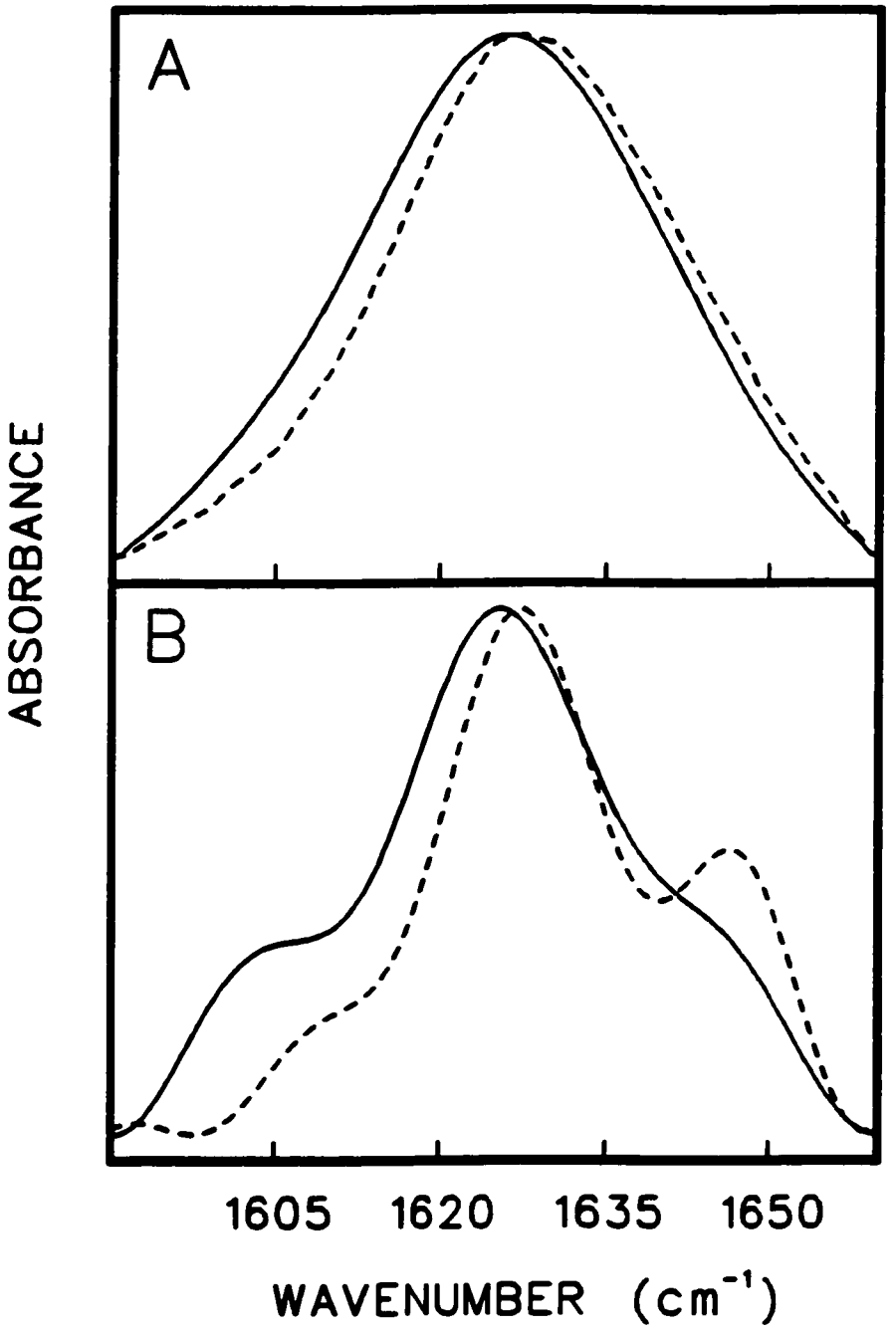
A
B
ABSORBANCE
1605
1620
1635
1650
WAVENUMBER (cm^{-1})

The ester carbonyl (C=O) stretching mode absorbs as a broad band in the frequency range 1690-1760 cm^{-1}. In Figure 3.7, the ester C=O band arising from the perdeuterated $DMPC_{d54}$ phospholipid in the mixed liposomal bilayers (panel A, dashed line) shifted to a higher frequency, 1740 cm^{-1}, as compared to 1732 cm^{-1} for the $DMPC_{d54}$ multilamellar dispersions (panel A, solid line).

The deconvolved spectrum of the $DMPC_{d54}$ (Figure 3.7, panel B, solid line) shows two component bands: a low frequency component at 1725 cm^{-1}, and high frequency component at 1745 cm^{-1}, pertaining to the C=O bonds that are involved and to the ones that are not involved in hydrogen bonding, respectively. The Fourier deconvolution of the mixed $DMPC_{d54}/GM_1$ liposomes reveals two overlapping bands at 1725 and 1745 cm^{-1}, with a marked decrease of the intensity of the low frequency component (panel B, dashed line). The frequencies of these bands were obtained with the aid of the third order Fourier derivation with a power of 3 and a breakpoint of 0.2. This decrease in the intensity of the 1725 cm^{-1} component band is translated as a decrease in the population of hydrogen bonded carbonyl groups (Wong & Mantsch, 1988; Blume *et al.*, 1988) and is due to a mutual shielding of the proton donating and accepting groups by GM_1 and $DMPC_{d54}$ molecules.

The presence of Ca^{2+} ions in the milieu led to a shift of the frequencies of the amide I band (Figure 3.8, panel A) from 1625 cm^{-1} to 1620 cm^{-1}, and of the ester C=O vibration band (Figure 3.8, panel B) from 1740 cm^{-1} to 1730 cm^{-1}. This shift to lower frequencies indicates an increase in the formation of intra- and inter-molecular hydrogen bonds at the bilayer interfacial zone of the mixed $DMPC_{d54}/GM_1$ liposomal bilayers.

Figure 3.7 Carbonyl stretching region of the infrared spectrum of a dispersion of $DMPC_{d54}$ (solid line) and $DMPC_{d54}/GM_1$ with a molar ratio of 4:0.66 (dashed line) in ^2H_2O buffer, at p^{2}H 7.5, before (**A**) and after (**B**) deconvolution with a bandwidth of 17 and a breakpoint of 1.5 in the Fourier domain. The spectra were autoscaled.

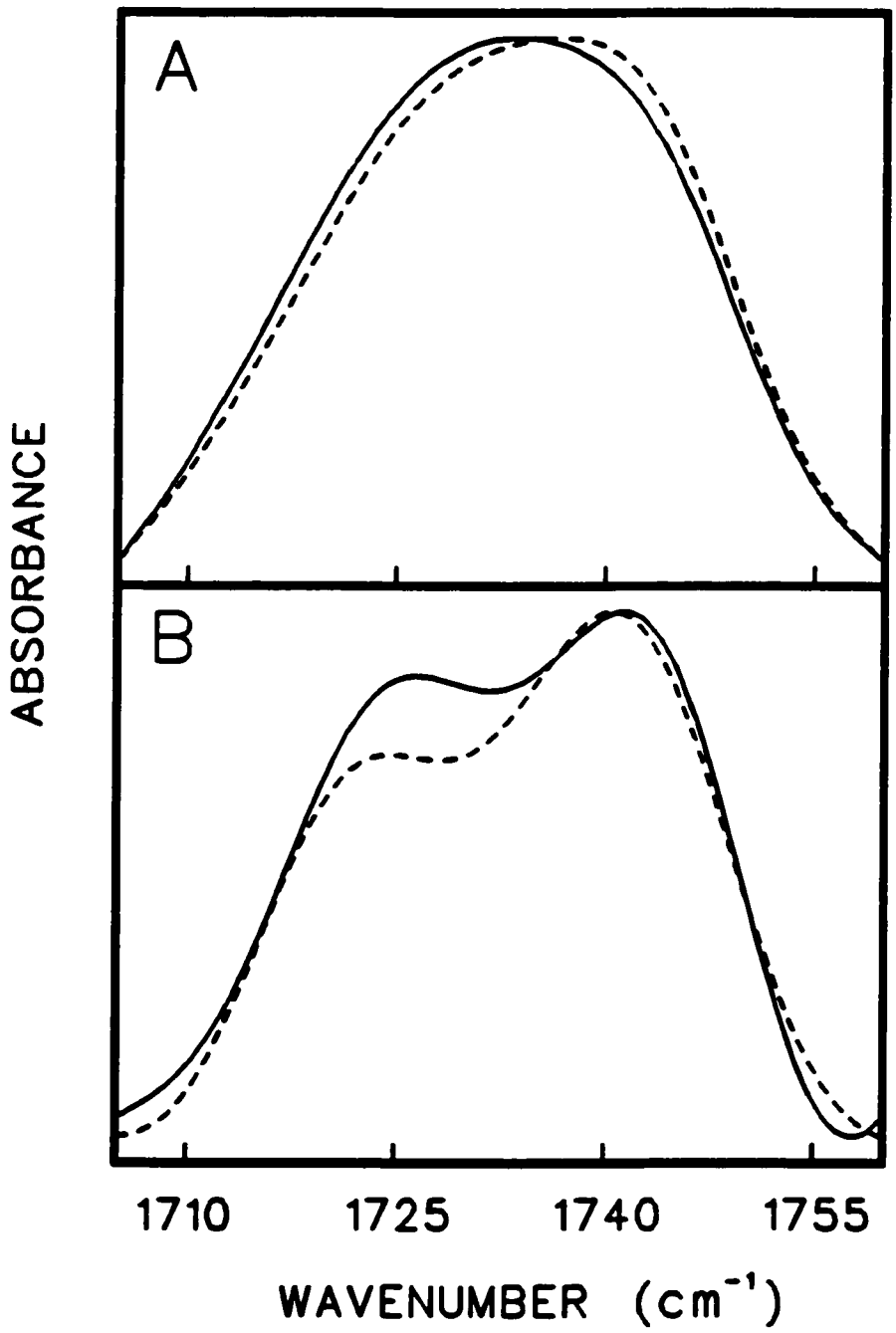
A
B
ABSORBANCE
1710
1725
1740
1755
WAVENUMBER (cm⁻¹)

Figure 3.8 Amide I C=O (**A**) and ester carbonyl (**B**) stretching regions of the infrared spectrum of a $DMPC_{d54}/GM_1$ dispersion with a molar ratio of 4:0.66 in ^2H_2O buffer, at p^{2}H 7.5, without Ca^{2+} (solid line) or with 10 mM $CaCl_2$ (dashed line). The spectra were autoscaled.

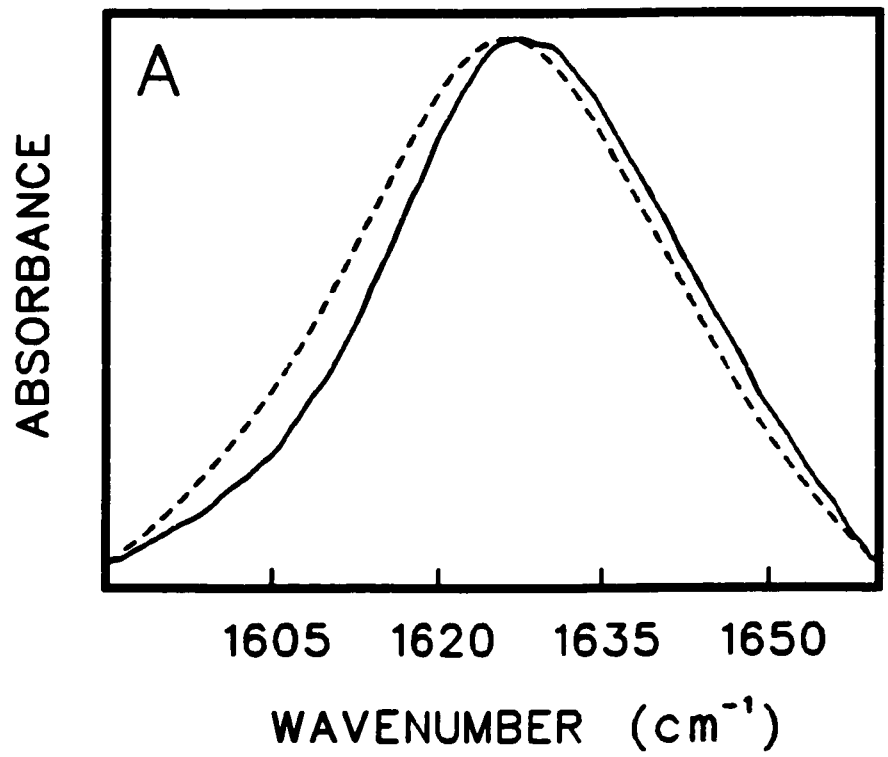
A
ABSORBANCE
1605
1620
1635
1650
WAVENUMBER (cm⁻¹)

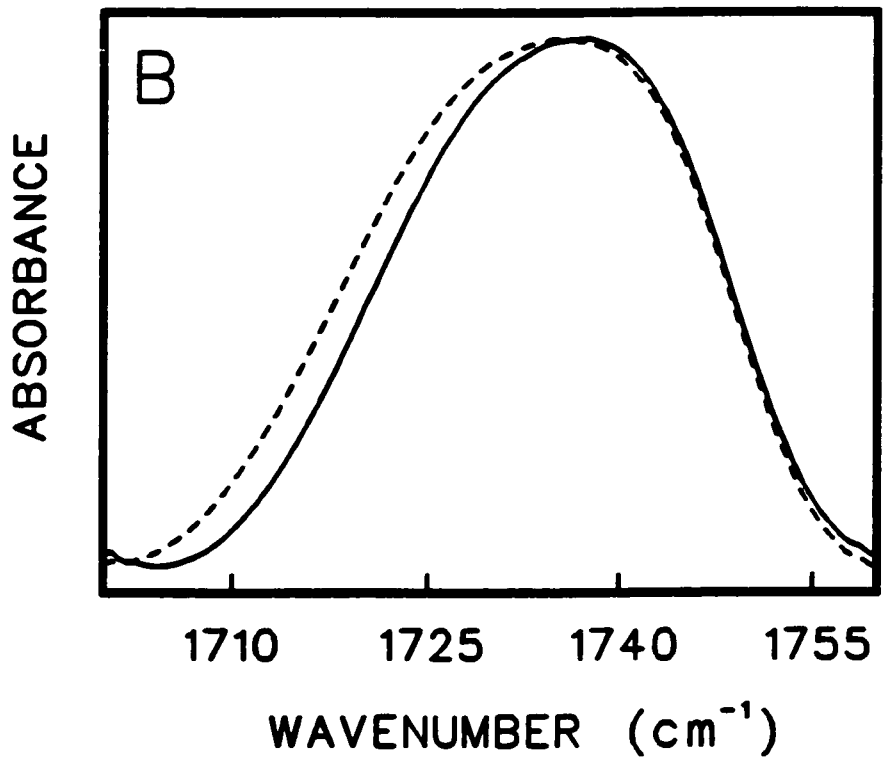
B
ABSORBANCE
1710
1725
1740
1755
WAVENUMBER (cm⁻¹)

3.5 Interaction of Ca^{2+} with the Carboxylate Moiety of GM_1 and the Phosphate Moiety of $DMPC_{d54}$

To verify Ca^{2+} binding to the sialic acid moiety of GM_1 and/or the phosphate moiety of perdeuterated $DMPC_{d54}$, the antisymmetric carboxylate and phosphate absorption modes were analysed. Due to overlapping C-OH stretching bands from the sugar headgroup, the phosphate symmetrical stretching mode (1040-1080 cm^{-1}) could not be used for analysis.

In the GM_1 micellar suspensions (Figure 3.9) as well as in the mixed $DMPC_{d54}/GM_1$ bilayers (Figure 3.10), the asymmetric absorption band of the CO_2^- vibration (1560 cm^{-1}) shows a significant change in its bandshape and its relative intensity when Ca^{2+} is added. In the absence of Ca^{2+} ions and after resolution enhancement using Fourier deconvolution, a single band is observed in Figure 3.9 for the asymmetric carboxylate stretching region of GM_1 micellar suspensions (panel B, solid line). When Ca^{2+} ions are added to the milieu (panel B, dashed line), two bands at 1560 cm^{-1} and 1580 cm^{-1} are revealed in the deconvolved spectrum of GM_1 micelles dispersed in deuterated water (D_2O).

In the mixed $DMPC_{d54}/GM_1$ bilayers (Figure 3.10), one CO_2^- band is observed in the absence of Ca^{2+} ions (panel B, solid line), and two bands at 1560 cm^{-1} and 1580 cm^{-1} are observed in the presence of the divalent cation (panel B, dashed line).

The phosphate asymmetric stretching mode absorbs in the frequency range of 1155-1305 cm^{-1}. This band was studied in the absence of D_2O to avoid interferences from its bending mode in the 1200 cm^{-1} region. The spectra are shown in Figure 3.11. The lipidic dispersion of perdeuterated $DMPC_{d54}$ (panel A, solid line) and the mixed $DMPC_{d54}/GM_1$ bilayers (panel B, solid line) yielded a broad band comprising several overlapping bands with

Figure 3.9 Carboxylate asymmetric and amide I C=O stretching region of the infrared spectrum of a GM_1 micellar solution in ^2H_2O buffer, at p^{2}H 7.5, without Ca^{2+} (solid line) or with 10 mM $CaCl_2$ (dashed line), before (**A**) and after (**B**) deconvolution with a bandwidth of 17 and a breakpoint of 1.5 in the Fourier domain. The spectra were autoscaled.

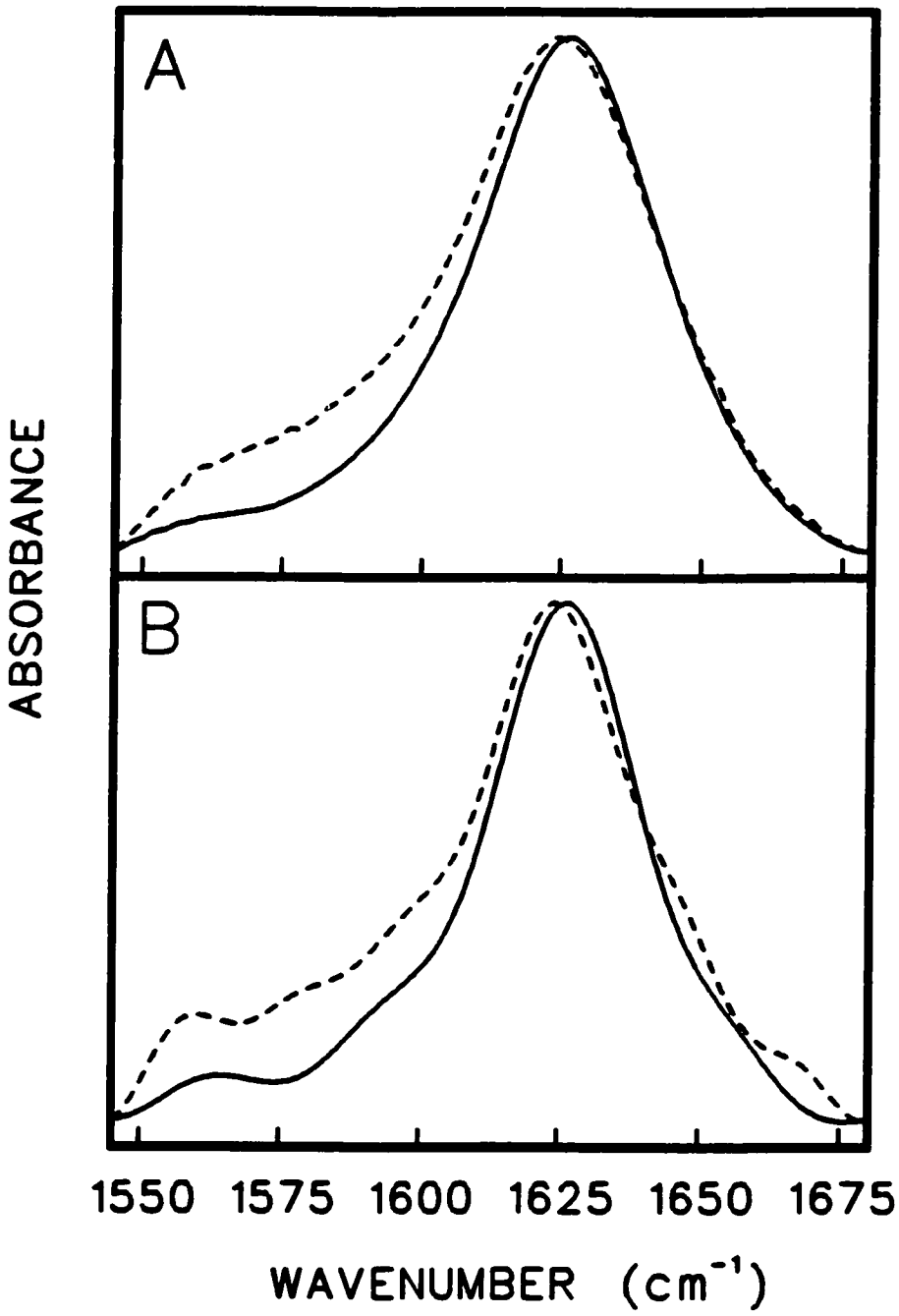
A
B
ABSORBANCE
1550 1575 1600 1625 1650 1675
WAVENUMBER (cm⁻¹)

Figure 3.10 Carboxylate asymmetric and Amide I C=O stretching region of the infrared spectrum of a dispersion of $DMPC_{d54}/GM_1$ with a molar ratio of 4:0.66 in ^2H_2O buffer, at p^{2}H 7.5, without Ca^{2+} (solid line) or with 10 mM $CaCl_2$ (dashed line), before (**A**) and after (**B**) deconvolution with a bandwidth of 17 and a breakpoint of 1.5 in the Fourier domain. The spectra were autoscaled.

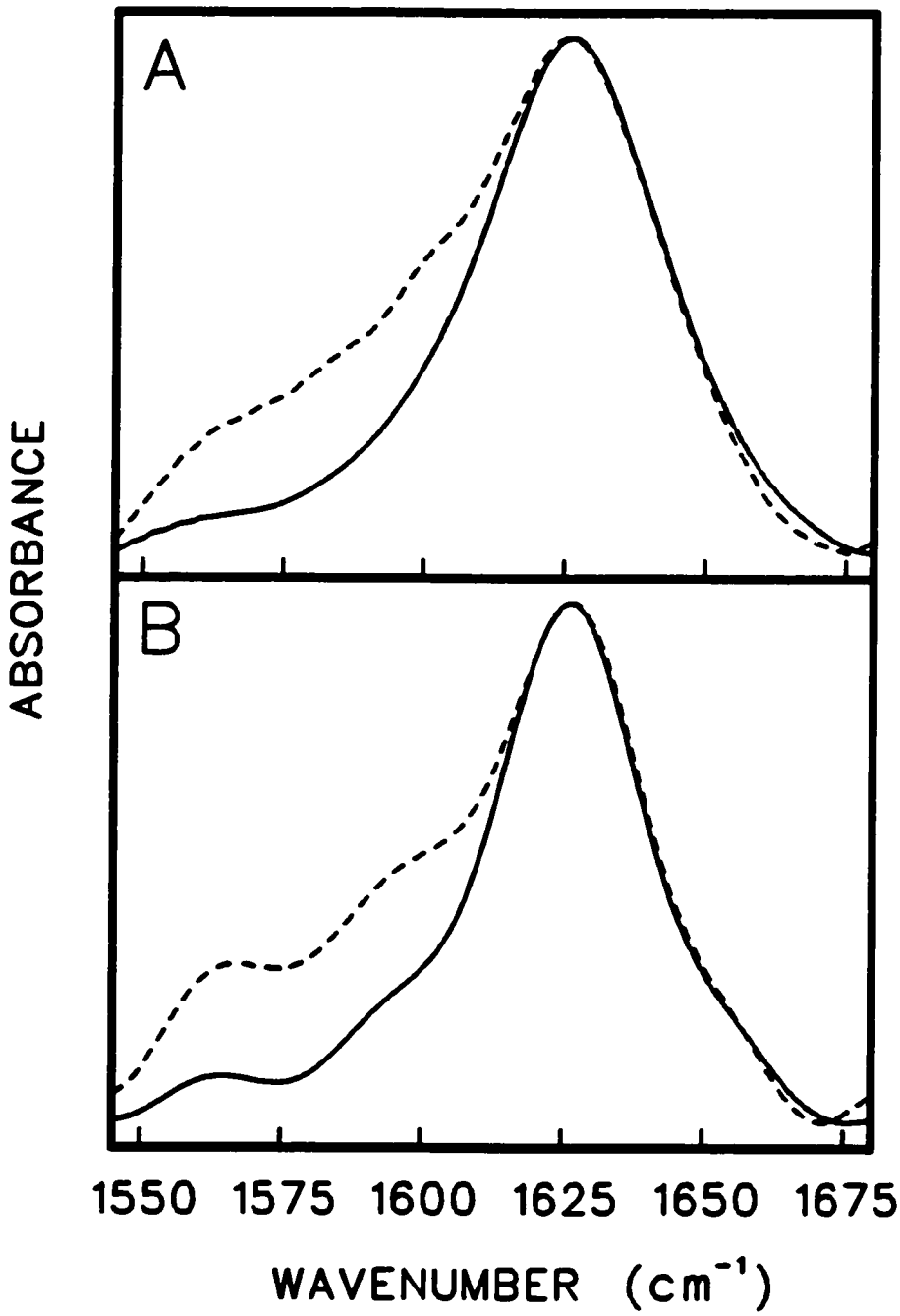
A
B
ABSORBANCE
1550 1575 1600 1625 1650 1675
WAVENUMBER (cm⁻¹)

Figure 3.11 Phosphate asymmetric stretching region of the infrared spectrum of a dispersion of $DMPC_{d54}$ (panel **A**) and $DMPC_{d54}/GM_1$ with a molar ratio of 4:0.66 (panel **B**) in ^2H_2O buffer, at p^{2}H 7.5, without Ca^{2+} (solid line) or with 10 mM $CaCl_2$ (dashed line). The spectra were autoscaled.

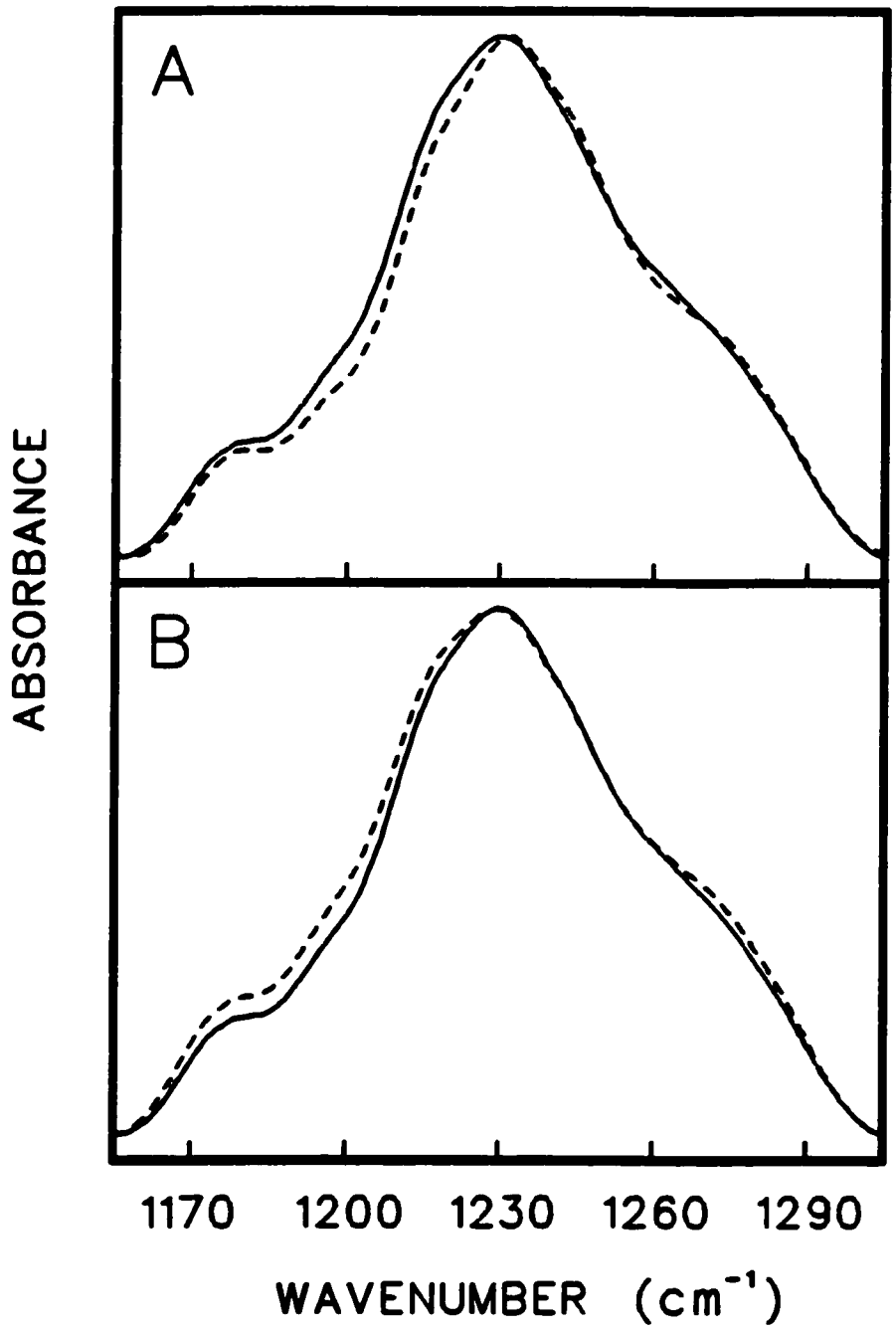
A
B
ABSORBANCE
1170
1200
1230
1260
1290
WAVENUMBER (cm⁻¹)

a maximum at 1230 cm^{-1}. The addition of Ca^{2+} to the phospholipid (panel A, dashed line) or the mixed liposomal bilayers (panel B, dashed line) had a very little effect on that band.

The FTIR experiments of the interaction of Ca^{2+} ions with GM_1, $DMPC_{d54}$ and $DMPC_{d54}/GM_1$ mixed bilayers were repeated 4 times to ensure reproducibility of results. This clearly indicates that GM_1 micelles are able to bind Ca^{2+} ions (Figure 3.9) and it proves that in the mixed liposomal bilayers the binding affinity of Ca^{2+} to the negatively charged sialic acid group of GM_1 is higher than to the phosphate group of $DMPC_{d54}$, as judged by FTIR spectroscopy.

3.6 Thermotropic Studies on Pure Monosialoganglioside GM_1 and Pure $DMPC_{d54}$

The thermotropic profile of GM_1/Ca^{2+} micellar suspensions as a function of temperature exhibits no sign of a cooperative phase transition in the temperature range of 5 to 60 °C (Figure 3.12, panel A, full circles). There is a gradual increase in the frequency of the methylene (CH_2) stretching vibration with increasing temperature, but no phase transition, although concentrations were as high as 110 mg/ml, well beyond critical micelle concentration.

The frequency of the C-D symmetric stretching mode can be used to probe membrane fluidity of $DMPC_{d54}$ multilamellar bilayers. In perdeuterated acyl chains, bands around 2195 and 2090 cm^{-1} are due to the CD_2 antisymmetric and symmetric stretching vibrations, respectively. The use of deuterated acyl chains provides a useful means of circumventing problems associated with hampering of the CH_2 asymmetric (2929 cm^{-1}) and symmetric (2850 cm^{-1}) stretching vibrations by GM_1, which becomes of crucial importance

Figure 3.12 Temperature dependence of the symmetric C-H (panel **A**) and C-D (panel **B**) stretching vibrations of the methylene groups of GM_1 and $DMPC_{d54}$, respectively, before (circles) and after (squares) the addition of Ca^{2+}. **A.** Thermotropic behaviour of the monosialoganglioside GM_1 micellar suspensions in ^2H_2O buffer, at p^{2}H 7.5, without Ca^{2+} (full circles, n=4) or with 10 mM $CaCl_2$ (full squares, n=4). **B.** Temperature profile of the $DMPC_{d54}$ dispersions in ^2H_2O buffer, at p^{2}H 7.5, without Ca^{2+} (open circles, n=4) or with 10 mM $CaCl_2$ (open squares, n=4). The frequencies of the symmetric C-H (panel **A**) and C-D (panel **B**) stretching vibrations were obtained after Fourier derivation of the original FTIR spectra with a power of 3 and a breakpoint of 0.3.

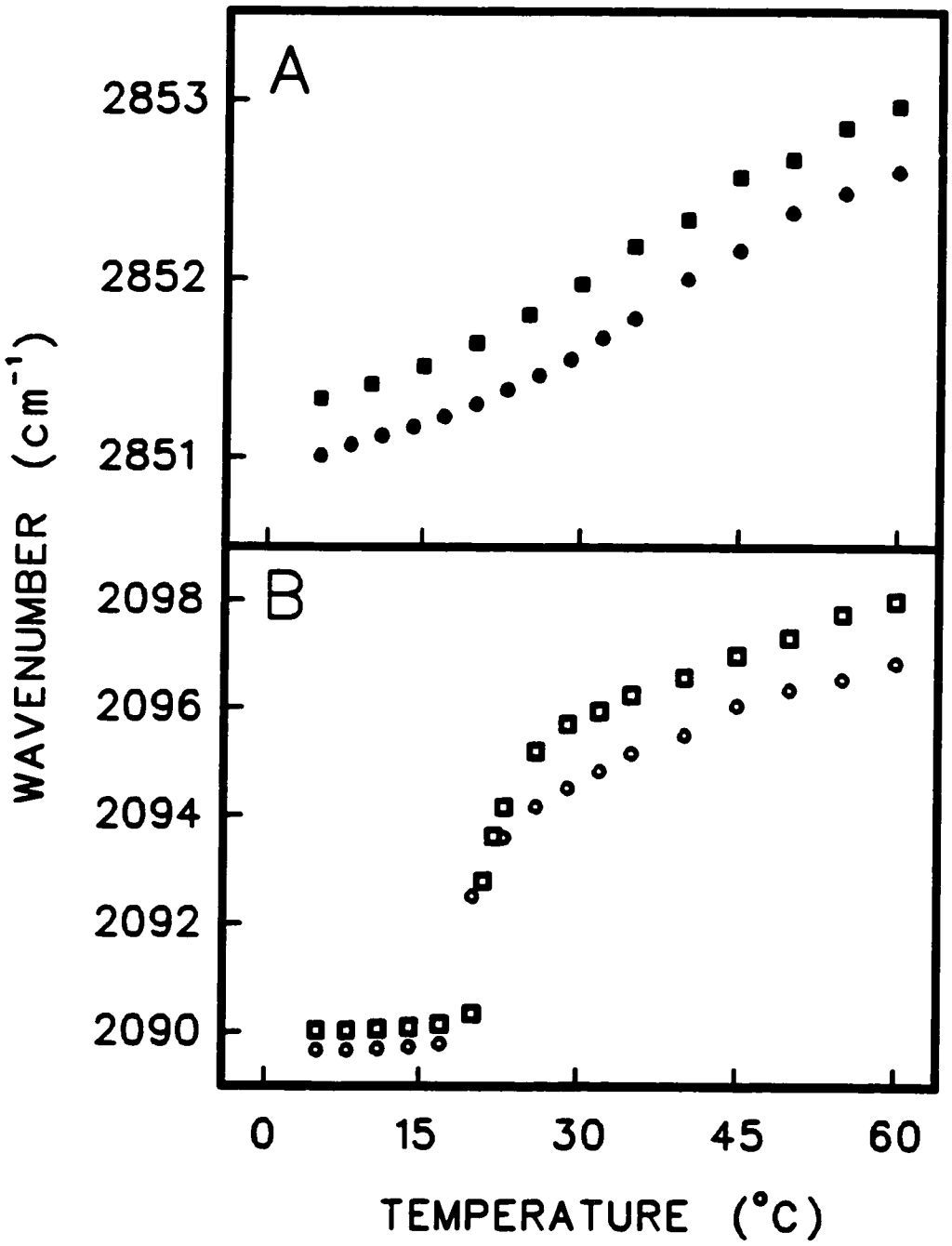
A
B
2853
2852
2851
2098
2096
2094
2092
2090
WAVENUMBER (cm⁻¹)
0
15
30
45
60
TEMPERATURE (°C)

when studying the influence of the glycolipid on $DMPC_{d54}$ liposomal bilayers. It can be seen on Figure 3.12 (panel B, open squares) that the frequency of the symmetric C-D stretching vibration increases gradually upon raising the temperature from 5 to 60 °C. At the gel-to-fluid transition, the frequency of that vibration mode changes dramatically, with a transition temperature (T_m) of 21 °C for the $DMPC_{d54}/Ca^{2+}$ model systems.

In the absence of the divalent cation Ca^{2+}, the order-disorder transition temperature of perdeuterated $DMPC_{d54}$ bilayers is lower and centered at 19 °C (Figure 3.12, panel B, open circles).

3.7 Measurements on Mixed $DMPC_{d54}/GM_1$ Multilamellar Dispersions

The effect of the monosialoganglioside GM_1 on the temperature-induced transition behaviour of 1,2-dimyristoyl-L-α-phosphotidylcholine with fully deuterated acyl chains ($DMPC_{d54}$) was monitored by FTIR spectroscopy. In perdeuterated acyl chains, bands around 2195 and 2090 cm^{-1} are due to the CD_2 antisymmetric and symmetric stretching vibrations, respectively. The use of perdeuterated acyl chains circumvents problems associated with interferences from the CH_2 asymmetric (2929 cm^{-1}) and symmetric (2850 cm^{-1}) stretching vibrations by the hydrocarbon chains of GM_1. The influence of GM_1 on the phase behaviour of $DMPC_{d54}$ can be monitored by following the frequency the CD_2 symmetric stretching vibrational band at ca. 2090 cm^{-1} as a function of temperature. Infrared observations were made on the following mol fractions of GM_1 in $DMPC_{d54}$: 0.12, 0.15, 0.19, 0.26, 0.34, 0.41, and 0.58. Table VI summarizes the order-disorder transition temperatures of the various $DMPC_{d54}/GM_1$ model membranes used in this spectroscopic investigation.

Table VI

Gel to Liquid-Crystalline Transition Temperature of Dispersions of Perdeuterated $DMPC_{d54}$ and $DMPC_{d54}$:GM_1 Mixtures.

$DMPC_{d54}$:GM_1 molar ratio	GM_1 mole fraction	Transition Temperature (±1 °C)	
		$DMPC_{d54}$	GM_1
1:0	-	21	-
0:1	-	-	No transition
10:0.66	0.12	22	22
8:0.66	0.15	23	23
6:0.66	0.19	25	25
4:0.66	0.26	25	25
2.64:0.66	0.34	26	26
2:0.66	0.41	28	28
1:0.66	0.58	28	28

The transition temperatures were obtained from the CD_2 ($DMPC_{d54}$) and CH_2 (GM_1) symmetric stretching vibrations in the infrared spectra. The GM_1 micellar solutions as well as the $DMPC_{d54}$ and $DMPC_{d54}$:GM_1 dispersions were prepared in 10 mM $CaCl_2$ buffer in D_2O, at p^2H 7.5.

The monosialoganglioside GM_1 perturbs vesicles as indicated by the increase in the gel/liquid crystalline phase transition temperature (Table VI). While in pure $DMPC_{d54}/Ca^{2+}$ vesicles the usual single transition is observed at ca. 21 °C (Figure 3.12, panel B, open circles), and in pure GM_1 micellar suspensions no phase transition is observed, the $DMPC_{d54}$ liposomal bilayers containing GM_1 ganglioside exhibit one transition, depending on the GM_1 content, between 22 and 28 °C.

Transition curves of various $DMPC_{d54}/GM_1$ liposomal mixtures are presented in Figures 3.13, 3.14 and 3.15. The thermotropic profile of the hydrocarbon chains of the glycosphingolipid and of the perdeuterated acyl chains of the synthetic phospholipid were similar, and the gel/liquid crystalline transition temperatures were identical for both the C-H (2850 cm^{-1}) and C-D (2090 cm^{-1}) symmetric stretching vibrations. The maxima of these bands shifted to higher wavenumbers when the bilayer passed into the liquid-crystalline phase.

At low monosialoganglioside GM_1 concentrations (Figure 3.13), the order-disorder T_m for $DMPC_{d54}/GM_1$ liposomal bilayers were 22 °C for a mol ratio of 10:0.66 and 23 °C for dispersions with a mol ratio of 8:0.66. At moderate glycolipid concentration (Figure 3.14), the gel/liquid-crystalline phase transition for $DMPC_{d54}/GM_1$ multilamellar dispersions was centered at 25 °C for both 6:0.66 and 4:0.66 and the T_m shifted to 26 °C for a mol ratio of 2.64:0.66. At high ganglioside concentration (Figure 3.15), the T_m continued to increase for the $DMPC_{d54}/GM_1$ dispersions with a molar ratio of 2:0.66 and 1:0.66 and it was centered at ca. 28 °C.

Figure 3.13 Temperature dependence of the symmetric C-H (panel **A**) and C-D (panel **B**) stretching vibrations of the methylene groups of GM_1 and $DMPC_{d54}$, respectively. **A.** Temperature profile of the monosialoganglioside GM_1 (full circles, n=4), and the $DMPC_{d54}/GM_1$ 10:0.66 (full squares, n=4), and 8:0.66 (full downward triangles, n=3) mixtures. **B.** Temperature profile of the $DMPC_{d54}$ (open circles, n=4), and the $DMPC_{d54}/GM_1$ 10:0.66 (open squares, n=4), and 8:0.66 (open triangles, n=3) mixtures. All the samples were prepared in 10 mM $CaCl_2$ buffer in ^2H_2O, at p^{2}H 7.5. The frequencies of the symmetric C-H (panel **A**) and C-D (panel **B**) stretching vibrations were obtained after Fourier derivation of the original FTIR spectra with a power of 3 and a breakpoint of 0.3.

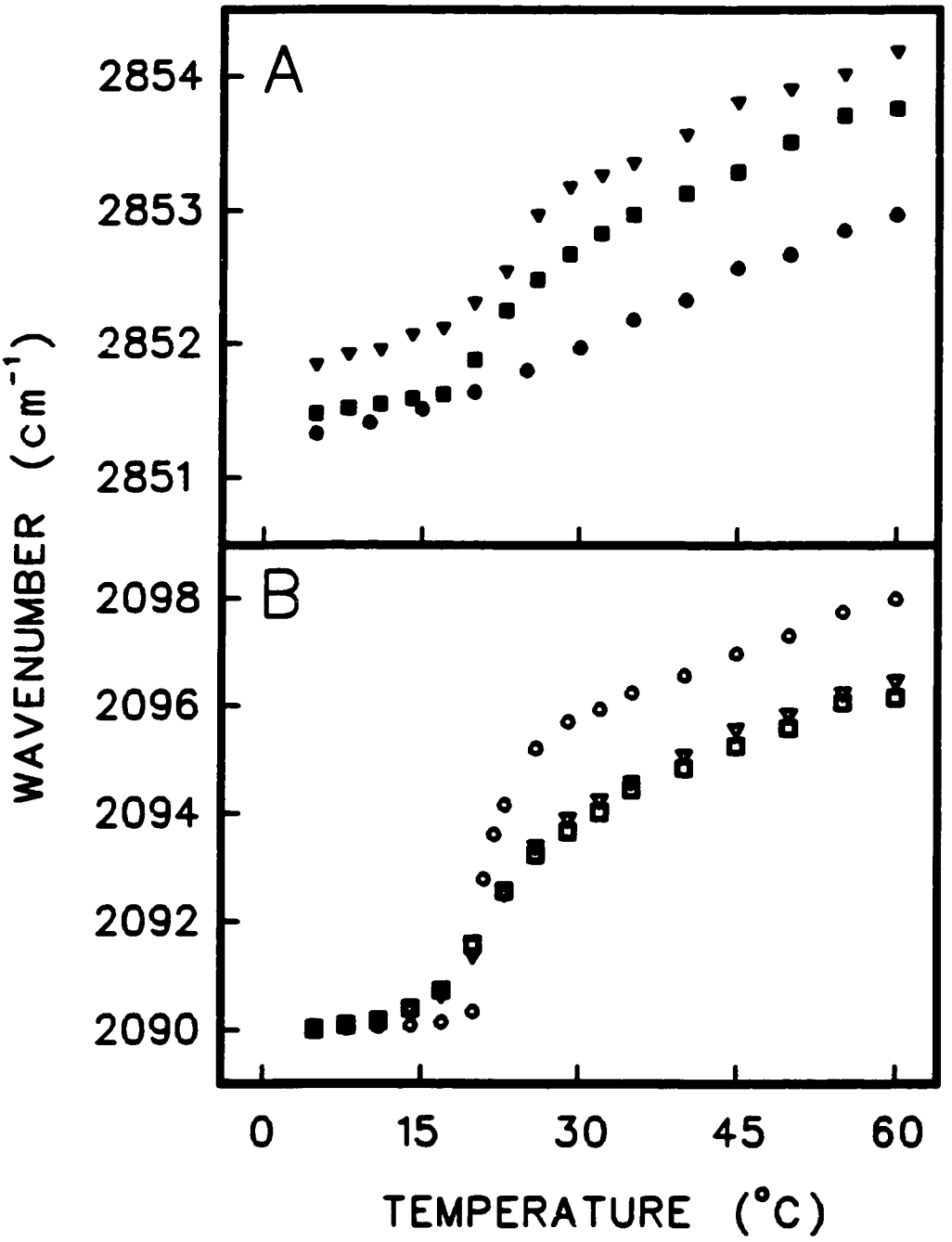
A
B
2854
2853
2852
2851
2098
2096
2094
2092
2090
WAVENUMBER (cm^{-1})
0
15
30
45
60
TEMPERATURE (°C)

Figure 3.14 Temperature dependence of the symmetric C-H (panel **A**) and C-D (panel **B**) stretching vibrations of the methylene groups of GM_1 and $DMPC_{d54}$, respectively. **A.** Temperature profile of the monosialoganglioside GM_1 (full circles, n=4), and the $DMPC_{d54}/GM_1$ 6:0.66 (full squares, n=3), 4:0.66 (full downward triangles, n=3), and 2.64:0.66 (full upward triangles, n=3) mixtures. **B.** Temperature profile of the $DMPC_{d54}$ (open circles, n=4), and the $DMPC_{d54}/GM_1$ 6:0.66 (open squares, n=3), 4:0.66 (open downward triangles, n=3), and 2.64:0.66 (open upward triangles, n=3) mixtures. All the samples were prepared in 10 mM $CaCl_2$ buffer in ^2H_2O, at p^{2}H 7.5. The frequencies of the symmetric C-H (panel **A**) and C-D (panel **B**) stretching vibrations were obtained after Fourier derivation of the original FTIR spectra with a power of 3 and a breakpoint of 0.3.

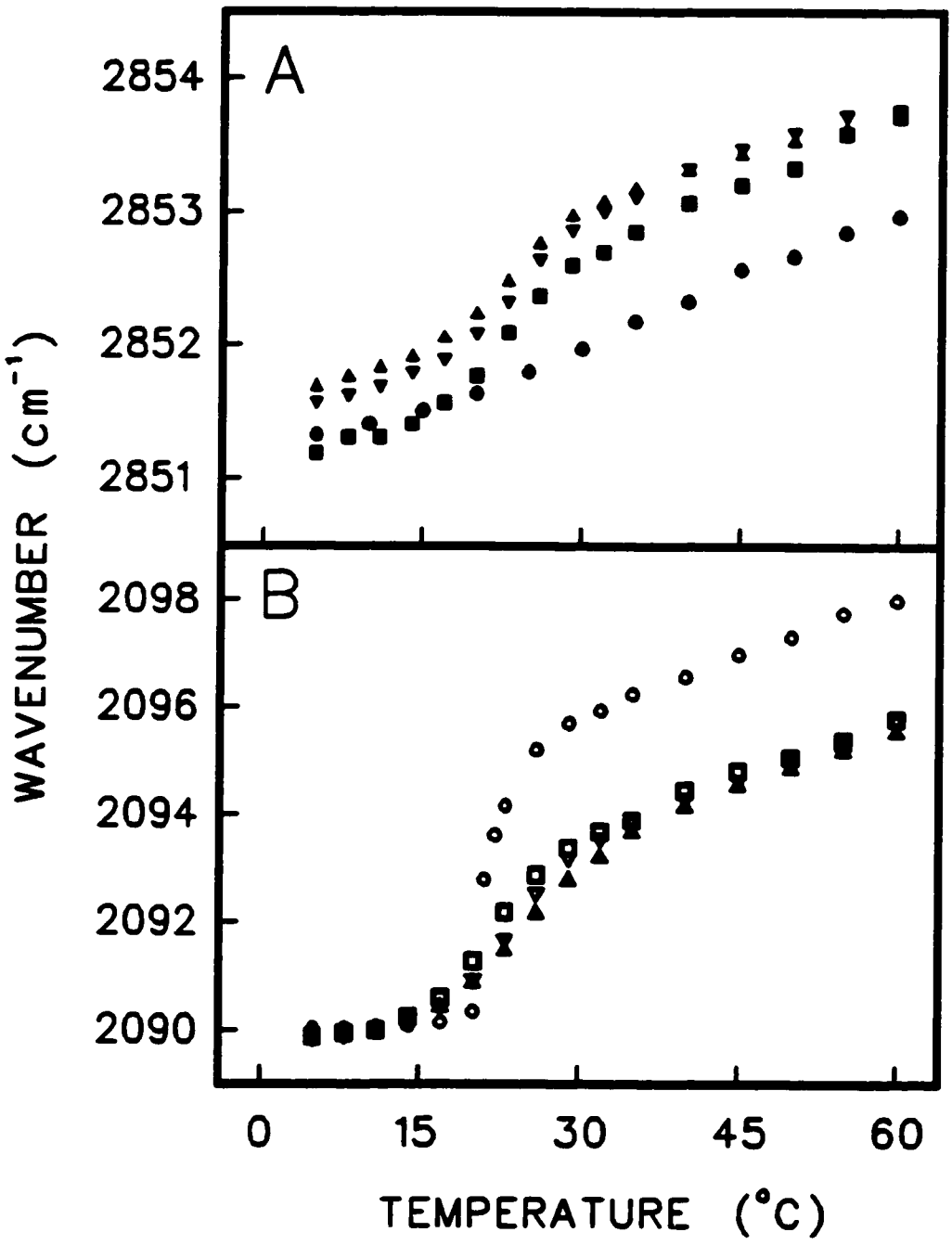
A
B
2854
2853
2852
2851
2098
2096
2094
2092
2090
WAVENUMBER (cm⁻¹)
0
15
30
45
60
TEMPERATURE (°C)

Figure 3.15 Temperature dependence of the symmetric C-H (panel **A**) and C-D (panel **B**) stretching vibrations of the methylene groups of GM_1 and $DMPC_{d54}$, respectively. **A.** Temperature profile of the monosialoganglioside GM_1 (full circles, n=4), and the $DMPC_{d54}/GM_1$ 2:0.66 (full squares, n=4), and 1:0.66 (full downward triangles, n=2) mixtures. **B.** Temperature profile of the $DMPC_{d54}$ (open circles, n=4), and the $DMPC_{d54}/GM_1$ 2:0.66 (open squares, n=4), and 1:0.66 (open downward triangles, n=2) mixtures. All the samples were prepared in 10 mM $CaCl_2$ buffer in ^2H_2O, at p^{2}H 7.5. The frequencies of the symmetric C-H (panel **A**) and C-D (panel **B**) stretching vibrations were obtained after Fourier derivation of the original FTIR spectra with a power of 3 and a breakpoint of 0.3.

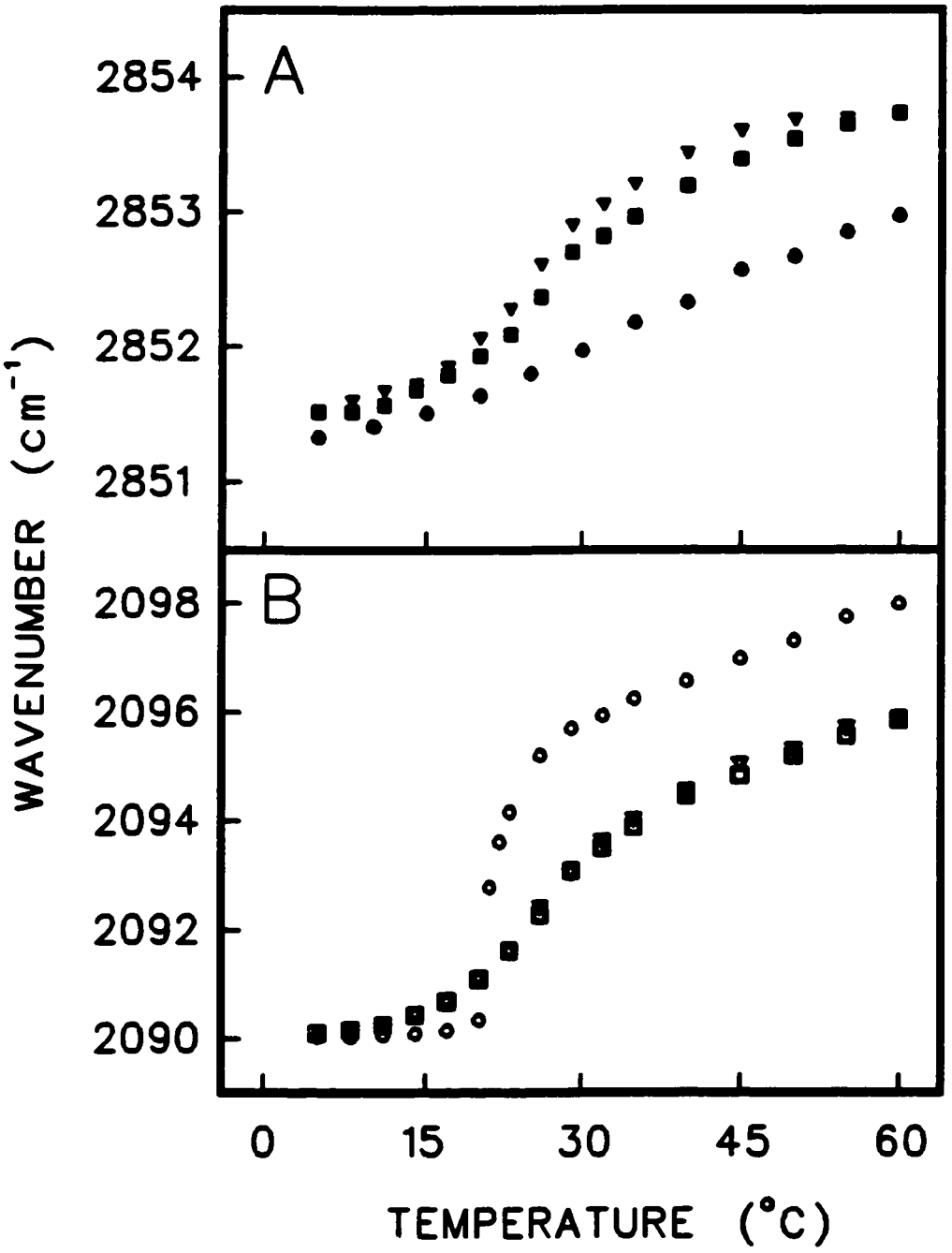
A
B
2854
2853
2852
2851
2098
2096
2094
2092
2090
WAVENUMBER (cm⁻¹)
0
15
30
45
60
TEMPERATURE (°C)

In the absence of the divalent cation Ca^{2+} (Figure 3.16), the C-H (panel A, full circles) and C-D (panel B, open circles) symmetric stretching vibrations of the mixed $DMPC_{d54}/GM_1$ liposomal bilayers (GM_1 x_g = 0.26) exhibit an order-disorder transition temperature of 24 °C, as compared to 25 °C in the presence of Ca^{2+}. The frequencies of both vibrational modes are lowered in the presence of Ca^{2+}.

In Figure 3.17, the $DMPC_{d54}/GM_1$ mixed model membranes with a molar ratio of 4:0.66, or GM_1 molar fraction of 0.26, exhibit a frequency shift of the ester carbonyl stretching band (1700-1760 cm^{-1}) from 1740 cm^{-1} in the gel phase (panel A, solid line) to 1730 cm^{-1}, in the liquid-crystalline phase (panel A, dashed line), upon increasing the temperature from 5 to 60 °C. This shift in the frequency of the ester C=O band to lower values is caused by an increased penetration of the heavy water molecules into the interfacial region of the bilayer in the liquid-crystalline phase (Cameron & Mantsch, 1978). In the gel phase, the frequency of the ester C=O stretching vibration mode is centered at ca. 1740 cm^{-1} due to a partial dehydration of the $DMPC_{d54}$ and GM_1 headgroups by Ca^{2+}.

The Fourier deconvolution of this band with a bandwidth of 17 and a resolution enhancement factor of 1.5 reveals two overlapping component bands: a high and a low frequency components centered at ca. 1740 cm^{-1} and 1725 cm^{-1}, respectively, at 5 °C (panel B, solid line). The high frequency component band shifted to 1743 cm^{-1} and the low frequency component shifted to 1728 cm^{-1} at 60 °C (panel B, dashed line). The 1725 cm^{-1} component band, corresponding to the ester C=O functional groups that are involved in hydrogen bonding (Wong & Mantsch, 1988; Blume *et al.*, 1988), is of low intensity in the

Figure 3.16 Temperature dependence of the symmetric C-H (panel **A**) and C-D (panel **B**) stretching vibrations of the methylene groups of GM_1 and $DMPC_{d54}$, respectively, before and after the addition of Ca^{2+}. **A.** Temperature profile of a dispersion of $DMPC_{d54}/GM_1$ at a molar ratio of 4:0.66 in ^2H_2O buffer, at p^2H 7.5, without Ca^{2+} (full circles, n=4) or with 10 mM $CaCl_2$ (full squares, n=4). **B.** Temperature profile of a dispersion of $DMPC_{d54}/GM_1$ at a molar ratio of 4:0.66 in ^2H_2O buffer, at p^2H 7.5, without Ca^{2+} (open circles, n=4) or with 10 mM $CaCl_2$ (open squares, n=4). The frequencies of the symmetric C-H (panel **A**) and C-D (panel **B**) stretching vibrations were obtained after Fourier derivation of the original FTIR spectra with a power of 3 and a breakpoint of 0.3.

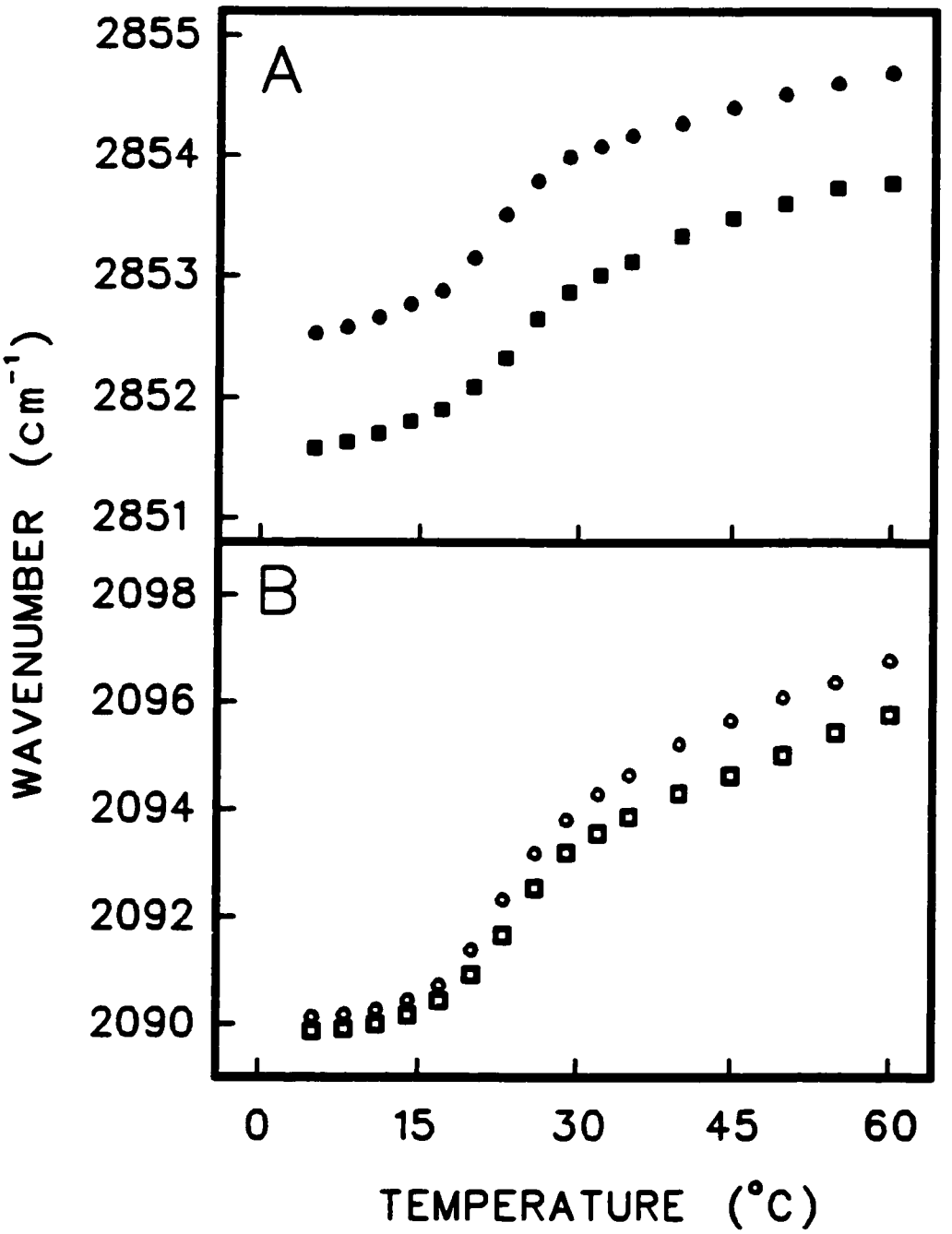
2855
2854
2853
2852
2851
A
2098
2096
2094
2092
2090
B
WAVENUMBER (cm⁻¹)
0
15
30
45
60
TEMPERATURE (°C)

Figure 3.17 Carbonyl stretching region of the infrared spectrum of a dispersion of $DMPC_{d54}/GM_1$ with a molar ratio of 4:0.66 in 10 mM $CaCl_2$ buffer in ^2H_2O, at p^{2}H 7.5, at 5 °C (solid line) and 60 °C (dashed line), before (**A**) and after (**B**) deconvolution with a bandwidth of 17 and a breakpoint of 1.5 in the Fourier domain. The spectra were autoscaled.

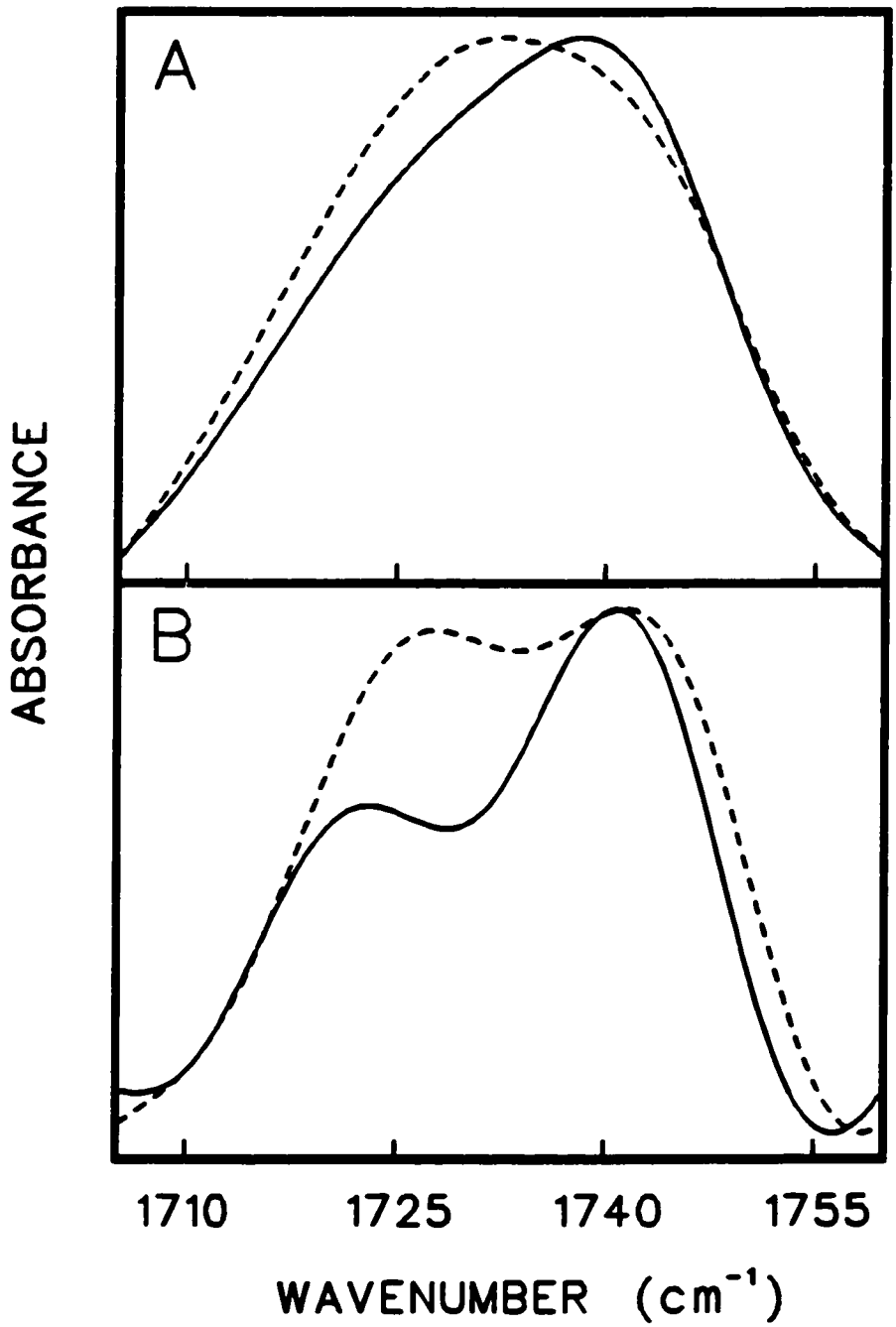
A
B
ABSORBANCE
1710
1725
1740
1755
WAVENUMBER (cm⁻¹)

gel phase and its relative intensity increases at 60 °C, in the liquid-crystalline phase, due to an increase in the population of hydrogen bonded carbonyl groups. The frequencies of the original and deconvolved bands were obtained with the aid of the third order Fourier transform derivation with a power of 3 and a breakpoint of 0.2.

CHAPTER FOUR

DISCUSSION

4.1 Characterization of GM_1 Ganglioside

The original method of Folch and colleagues (1957) for the extraction of total lipids and isolation of gangliosides, as applied to brain and other tissues, is still widely used. The procedure is based on the ability of gangliosides to partition from the chloroform:methanol phase in which they are extracted into the upper water enriched phase, leaving behind the bulk of other lipids. Many researchers have introduced various modifications to this method to improve yields and the resolution of the individual ganglioside molecular species. A modification of the classical Folch procedure has been introduced by Svennerholm and Fredman (1980). The procedure involved the extraction of human tissue lipids with chloroform-methanol-water. The crude gangliosides isolated were freed from low molecular weight contaminants by dialysis against distilled water and it was reported by the authors that the recovery of gangliosides was 3-10% higher for cerebral grey matter and 10-15% higher for cerebral white matter. The crude preparation contained sulfatides and various phospholipid contaminants. The procedure described below is the modification introduced by us to the procedure described and adopted by Fredman and colleagues (1980) to separate gangliosides quantitatively into mono di and trisialoganglioside fractions.

The anion exchange resin DEAE-sepharose was found to have a higher binding capacity, to show less unspecific adsorption and to give a better separation than did other anion exchange resins (Iwamori & Nagai, 1978; Fredman *et al.*, 1980). DEAE-sepharose

was employed to separate bovine brain gangliosides first, along with other acidic lipids, from the much larger quantity of neutral and zwitterionic lipids that do not bind the resin (e.g., cholesterol, lecithin, ethanolamine phosphoglycerides, cerebrosides, and other neutral glycolipids). The gangliosides were eluted with a discontinuous gradient of a salt solution in methanol. To avoid any changes brought to the ganglioside chemical structure upon storage, evaporation or base treatment, potassium acetate was utilized for the elution of gangliosides from the resin (Iwamori & Nagai, 1978; Fredman *et al.*, 1980; Ledeen & Yu, 1982). To ensure the complete removal of the other acidic lipids and any acidic low molecular weight contaminants (e.g., free fatty acids, sulfatides, serine and inositol phosphoglycerides) that accompany the gangliosides, a subsequent step of base treatment was introduced into the procedure. However, a final silicic acid column chromatography step is still required to remove the contaminating acidic lipids not O-deacylated by base and to ensure also the removal of small amounts of protein that may have survived the preceding treatment.

Thin layer chromatography of the crude ganglioside extract (Figure 3.1) revealed that this fraction comprised of the following gangliosides: GM_3, GM_2, GM_1, GD_{1a}, GD_{1b} and GT_{1b}, with the monosialoganglioside GM_1 and the disialogangliosides GD_{1a} and GD_{1b} being the major species. The final purity of GM_1 was greater than 99 % as judged by TLC.

In the negative ion FAB mass spectra of underivatized bovine brain GM_1 (Figure 3.3), the ion observed at m/z 1544 was assigned as the molecular ion $(M-H)^-$. Ions due to several fragments which were cleaved at the glycosidic linkages from the non reducing terminal were detected in the spectra. The fragment ion at m/z 1382 was obtained after cleavage of the

galactose residue from GM_1. The cleavage of the N-acetylgalactosamine residue generated the ion fragment at m/z 1179. The fragment ion at m/z 888 was generated after the sialic acid moiety was cleaved and the one at m/z 282 corresponded to the stearic acid portion of GM_1. Several other fragments were also obtained due to cleavage of chemical bonds, rearrangements and migration of chemical groups and secondary fragmentation of fragment ions (Kates, 1986). The negative ion FAB mass spectra also revealed the fragment ions pertaining to the fatty acids of the ceramide moiety of GM_1. The ion fragment corresponding to stearic acid comprised more than 35 % of the total fatty acids. The long chain base consisted mainly of sphingosine $C_{18:1}$. The results reported here about the chemical composition of the ceramide moiety of the glycolipid are in agreement with those reported in the literature (Svennerholm, 1963; Namoi *et al.*, 1976; Iwamori & Nagai, 1978; Sillerud *et al.*, 1978; Ando & Yu, 1979; Hinz *et al.*, 1981; Kadowaki *et al.*, 1984; Kojima *et al.*, 1988; Maggio *et al.*, 1988; Sonnino *et al.*, 1994; Palestini *et al.*, 1995, and references therein).

4.2 GM_1 Micellar Suspensions

Gangliosides are ceramide based glycosphingolipids which possess one to five *N*-acetylneuraminic acids (NeuAc). The ceramide moiety consists of a sphingosine base whose amino function is amide linked to a fatty acid (Figure 1.1). For proteins and polypeptides, the amide I and II bands can be used to determine the secondary structure of the protein or the peptide (Müller & Blume, 1993, and references therein). For glycolipids, the amide I vibrational mode is used to assess inter and intramolecular hydrogen bond formation at the

bilayer surface (Attar *et al.*, 1998). Infrared spectra of gangliosides show very complicated patterns due to the presence of three amide groups and a carboxylate group in the molecule. In the hydrophilic oligosaccharide headgroup region, the *N*-acetylgalactosamine and the *N*-acetylneuraminic acid units each contain an amide group. The presence of the carboxylate group of the sialic acid moiety complicates the situation because the deprotonated form (COO^-) absorbs in the frequency region of the amide I vibrational band (Müller & Blume, 1993; Müller *et al.*, 1996). The third amide group arises form the ceramide backbone.

The monosialoganglioside GM_1 is in a micellar state in an aqueous medium because of the large, well hydrated headgroup (Gammack, 1963; Yohe & Rosenberg, 1972; Sonnino *et al.*, 1994). In Figure 3.4, only one amide I band at ca. 1625 cm^{-1} appears in the infrared spectrum of GM_1 micellar suspensions dispersed in heavy water (1590–1660 cm^{-1}). Upon deconvolution of the original spectrum (panel B), it becomes evident that this absorption band is the sum of several overlapping bands. In the absence of Ca^{2+} ions the deconvolved spectrum of GM_1 in the amide I region reveals three constituent bands: a 1645 cm^{-1} peak, 1625 cm^{-1} peak, and a third one at 1605 cm^{-1}. The 1645 cm^{-1} and 1625 cm^{-1} components correspond to the amide groups that did not undergo hydrogen bonding and the ones that did, respectively (Wong & Mantsch, 1988). Müller and Blume (1993) have shown that the 1610 cm^{-1} component band is too low in frequency to be assigned to an amide I band. They have led a series of protonation/ deprotonation experiments on GM_1 and *N*-acetylneuraminc acid (NeuAc) samples dispersed in D_2O, and they have assigned the shoulder at ca. 1610 cm^{-1}, in the amide I C=O spectral region, to the COO^- group of the sialic acid moiety of GM_1.

The addition of Ca^{2+} (Figure 3.4, panel B, dashed line) to GM_1 micellar dispersions shifted the high frequency component from 1645 cm^{-1} to 1640 cm^{-1}, the 1625 cm^{-1} component shifted slightly to 1620 cm^{-1} and the shoulder at 1605 cm^{-1} shifted to 1610 cm^{-1} and increased in intensity. This increase in the relative intensity of the CO_2^- band might be brought upon by an increased exposure of the carboxylate group at the bilayer interface due to complexation with Ca^{2+} ions. The slight shift of the amide I C=O band to lower frequencies indicates an increase in the population of hydrogen bonded amide groups (Wong & Mantsch, 1988). Ca^{2+} forms a bridge between two neighbouring GM_1 molecules and, by doing so, it brings the hydrogen donating and accepting groups closer and, thus, increases the probability of hydrogen bonding at the bilayer interface. Our results are in agreement with those of Hayashi *et al.* (1984) which showed a significant interaction between ganglioside micelles and Ca^{2+} ions.

4.3 $DMPC_{d54}$ Multilamellar Dispersions

In aqueous dispersions, phospholipids spontaneously aggregate to form bilayers. In this study, perdeuterated $DMPC_{d54}$ liposomal bilayers are used to gain insight into the structure and function of complex biological membranes.

The ester C=O stretching mode of $DMPC_{d54}$ absorbs as a broad band in the frequency range 1690-1760 cm^{-1}. The ester carbonyl stretching band in aqueous suspension is presented in Figure 3.5. Fourier self deconvolution (panel B) was used with a bandwidth of 17 and a resolution enhancement factor of 1.5 to resolve the component bands comprised within the asymmetric ester C=O band (panel B). The high frequency component at 1745

cm^{-1} pertains to carbonyl groups that are not hydrogen bonded and the peak at 1725 cm^{-1} corresponds to hydrogen bonded carbonyl groups (panel B, solid line) (Wong & Mantsch, 1988; Blume *et al.*, 1988).

The addition of Ca^{2+} (Figure 3.5, panel B, dashed line) to $DMPC_{d54}$ liposomes caused a shift of the high frequency component from 1745 cm^{-1} to 1742 cm^{-1} and the low frequency component decreased in intensity and shifted slightly in frequency from 1725 to 1730 cm^{-1}. It has been postulated and proven that the binding of Ca^{2+} reduces the penetration of D_2O to the bilayer interfacial zone and is consistent with a tightening of the intermolecular packing of the lipidic network (Lee & Grant, 1980; Bertoli *et al.*, 1981; Ganesan, 1982; Probst et al., 1984; Müller & Blume, 1993). One would think that this increased intermolecular cohesion resulting from Ca^{2+} binding should increase the probability of hydrogen bonding. However, our results show that the Ca^{2+} ions had very little effect on the ester C=O group at the bilayer interface and, thus, it is not clear whether the divalent cation favors the formation of hydrogen bonds between neighbouring $DMPC_{d54}$ molecules. Our spectroscopic findings about the influence of Ca^{2+} on the hydration of the ester C=O group of $DMPC_{d54}$ are in agreement with those of Müller *et al.* (1996). This group did not observe a dehydration at the level of the ester carbonyl group due to the Ca^{2+} accumulation on the bilayer surface.

4.4 The Interfacial Region of $DMPC_{d54}/GM_1$ Model Membranes (Amide I and Ester C=O Groups)

The amide I stretching mode (1590-1660 cm^{-1}) and the ester carbonyl stretching mode (1690-1760 cm^{-1}) are examined to assess the degree of hydrogen bonding at the interfacial

region of bilayers. It was previously shown by Wong and Mantsch (1988) that as the frequency of these two vibrational modes decreases, the degree of hydrogen bonding increases due to the elongation of the C=O bonds.

In Figures 3.6 and 3.7, the amide I C=O band of GM_1 and the ester C=O band of perdeuterated $DMPC_{d54}$ are shifted slightly to higher frequencies in the mixed $DMPC_{d54}/GM_1$ liposomal bilayers, as compared to GM_1 micellar suspensions and $DMPC_{d54}$ liposomal bilayers. In Figure 3.6, the amide I C=O band arising from GM_1 in the mixed liposomes (panel A, dashed line) shifted slightly to a higher frequency, 1630 cm^{-1}, as compared to 1625 cm^{-1} for the GM_1 micellar suspensions (panel A, solid line). Similarly, in Figure 3.7, the ester C=O band arising from $DMPC_{d54}$ in the mixed liposomal bilayers (panel A, dashed line) shifted to a higher frequency, 1740 cm^{-1}, as compared to 1732 cm^{-1} for the $DMPC_{d54}$ multilamellar dispersions (panel A, solid line). This shift to higher frequencies for the amide I and ester C=O vibrational modes indicates that the mixed $DMPC_{d54}/GM_1$ multilamellar dispersions display an increased double bond character (Wong & Mantsch, 1988; Blume *et al.*, 1988), which likely results from mutual shielding and subsequent reduction of hydrogen bonding at the polar interfacial region.

Upon deconvolution of the original spectra, three components were revealed for the amide I absorption band of GM_1 in the micellar form (Figure 3.6 panel B, solid line): a 1640 cm^{-1} peak, a 1625 cm^{-1} peak, and 1605 cm^{-1} peak in the infrared spectral region 1590-1660 cm^{-1}. In the mixed $DMPC_{d54}/GM_1$ liposomal bilayer systems (Figure 3.6, panel B, dashed line), all components of the amide I band slightly shifted to higher frequencies as compared to GM_1 micellar suspensions: 1645 cm^{-1}, 1630 cm^{-1} and 1610 cm^{-1}.

Wong and Mantsch (1988) have shown that the frequency of the amide C=O stretching band decreases as it becomes more and more involved in hydrogen bonding at the polar interfacial region of bilayers. Therefore, the component bands at 1625 cm^{-1}, GM_1 micelles, and 1630 cm^{-1}, $DMPC_{d54}/GM_1$ bilayers, respectively, were assigned to the amide groups that are involved in hydrogen bonding, and the high frequency constituent bands at 1645 cm^{-1}, GM_1 micellar suspensions, and 1640 cm^{-1}, $DMPC_{d54}/GM_1$ dispersions, respectively, were assigned to the ones that are less involved in hydrogen bonding at the interface of membranes. The 1605 cm^{-1} component was assigned to the unprotonated carboxyl group of the sialic acid of GM_1 (Müller & Blume, 1993).

The Fourier deconvolved spectra of both $DMPC_{d54}$ and the mixed $DMPC_{d54}/GM_1$ bilayers revealed low and high frequency components in the infrared spectral region 1700-1760 cm^{-1}, reflecting contributions from the *sn*-2 and *sn*-1 C=O groups, respectively (Figure 3.7, panel B). The low and the high frequency components correspond to the C=O bonds that are heavily involved and to the ones that are less involved in hydrogen bonding, respectively (Blume *et al.*,1988; Wong & Mantsch, 1988).

It was previously reported by Wong and Mantsch (1988) that the broadness of the original spectra of the ester carbonyl group of 1,2-diacylphospholipids was attributable to both *sn*-1 chain and *sn*-2 chain absorption, which are not equivalent, and the authors concluded that the *sn*-2 ester carbonyl group is more exposed to the aqueous medium and participates to a greater extent in hydrogen bonding as compared to *sn*-1 C=O.

Blume *et al.* (1988) have conducted a series of spectroscopic studies in which the *sn*-1 and *sn*-2 chain C=O carbons of various phospholipids (e.g., DMPC) were substituted in

a selective manner with ^{13}C isotope. They have suggested that the splitting of the C=O vibrational band is caused by hydrogen bonding to both *sn*-1 and *sn*-2 ester carbonyl and that both C=O groups can contribute to the high and low frequency component bands. They concluded that the high frequency component arose from free and mono hydrogen bonded carbonyl groups, whereas the low frequency component pertained to higher orders of hydrogen bonding of carbonyl groups. The latter interpretation, however, is questionable because of the synthetic procedure used and adopted by this group for the ^{13}C isotope labelling. Complete labelling at either the *sn*-1 or *sn*-2 carbonyl group was not feasible/possible by their procedure. They have reported a 90% enriched ^{13}C label and have failed/neglected to check the purity of the lysophospholipid starting material.

The conflicting arguments presented by Wong and Mantsch (1988) and Blume *et al.* (1988) do not affect our conclusion that this shift to higher frequencies for the amide I and ester C=O vibrational modes indicates that the mixed $DMPC_{d54}/GM_1$ multilamellar dispersions display a reduced probability of hydrogen bonding at the bilayers interfacial region.

The effect of Ca^{2+} ions on the hydrogen bonding at the interfacial region was also assessed by FTIR. The binding of Ca^{2+} at the interfacial region of the mixed $DMPC_{d54}/GM_1$ multilamellar dispersions would be expected to affect not only the hydrogen bonding at the interface, but also to affect the dynamics of the hydrocarbon chains. The addition of Ca^{2+} ions to a dispersion of $DMPC_{d54}/GM_1$ with a mol ratio of 4:0.66 (mol/mol) has lead to a shift of the frequencies of the amide I band (Figure 3.8, panel A) from 1625 cm^{-1} to 1620 cm^{-1}, and of the ester C=O vibration band (Figure 3.8, panel B) from 1740 cm^{-1} to 1730 cm^{-1}. This

shift to lower frequencies indicates an increase in the formation of intra and intermolecular hydrogen bonds at the bilayer interfacial zone of the mixed $DMPC_{d54}/GM_1$ liposomal bilayers (Wong & Mantsch, 1988; Blume *et al.*, 1988) due to a tightening of the lipidic network following neutralization by Ca^{2+} ions.

4.5 Ca^{2+} Preferentially Binds to the Carboxylate Moiety of GM_1 Rather Than to the Phosphate Moiety of $DMPC_{d54}$ in the Mixed Liposomal Bilayers

The negatively charged gangliosides have the potential to bind cations on the cell surface and this binding may be of importance in cell physiology. Ca^{2+} can bind the sialic acid residue of GM_1 as well as the phosphate group of $DMPC_{d54}$. In the region 1500-1800 cm^{-1}, the infrared spectrum of GM_1 micellar suspensions (Figure 3.9, panel A) and $DMPC_{d54}/GM_1$ liposomal bilayers with a mol ratio of 4:0.66 (Figure 3.10, panel A) reveals two major absorption bands: the amide I C =O stretching vibration band at 1625 cm^{-1} and the carboxylate asymmetric stretching vibration band at 1560 cm^{-1} in the absence of Ca^{2+}. In the presence of the divalent cation, the amide I band shifted to 1620 cm^{-1} and the carboxylate band remained at ca. 1560 cm^{-1} but changed significantly in its bandshape and intensity. Upon deconvolution of the original spectrum, it becomes evident that each of these absorption bands is the sum of several overlapping bands. In the absence of Ca^{2+} ions, a single band is observed at ca. 1560 cm^{-1} for the asymmetric carboxylate stretching band of GM_1 micellar suspensions (Figure 3.9, panel B, solid line) and $DMPC_{d54}/GM_1$ liposomal bilayers (Figure 3.10, panel B, solid line) dispersed in deuterated water. The two C -O bonds are equivalent and intermediate in strength between a single and a double bond. In the

presence of 10 mM $CaCl_2$, two new peaks appear on top of that band at 1560 cm^{-1} for the GM_1 micellar suspensions (Figure 3.8, panel B, dashed line) and the $DMPC_{d54}/GM_1$ liposomal bilayers (Figure 3.10, panel B, dashed line). As reported by Deacon and Phillips (1980), the frequencies of the asymmetric stretching vibration of the carboxylate groups interacting with divalent metal cations vary according to the type of coordination: a downward shift indicates a bidentate coordination, a unidentate coordination gives an upward shift and there is no significant change for bridging coordinations between one divalent cation and two oxygen atoms from distinct carboxylate groups. The bands at ca. 1560 cm^{-1} and ca. 1580 cm^{-1} can therefore be attributed to carboxylate groups interacting with Ca^{2+} ions in the bidentate and unidentate coordinations, respectively.

In the mixed $DMPC_{d54}/GM_1$ bilayers (Figure 3.10) the asymmetric absorption band of the CO_2^- vibration at ca. 1560 cm^{-1} showed a dramatic change in its bandshape and relative intensity when Ca^{2+} is added. On the other hand, the asymmetric phosphate vibrational band of $DMPC_{d54}$ (Figure 3.11, panel A) and $DMPC_{d54}/GM_1$ mixed multilamellar dispersions (Figure 3.11, panel B) reveals no measurable change when the divalent cation is added.

Our results clearly indicate that the affinity of Ca^{2+} toward the negatively charged sialic acid moiety of GM_1 is greater than its affinity toward the phosphate moiety of $DMPC_{d54}$ and are supported by the findings of McDaniel and McLaughlin (1985), which showed that Ca^{2+} bound weakly to the phosphate moiety of PC multilamellar vesicles with an intrinsic association constant of < 100 M^{-1}. Therefore, based on the fact that, upon Ca^{2+} binding, the asymmetric carboxylate vibrational band of the glycosphingolipid underwent dramatic changes and due to the lack of measurable spectral changes in the phosphate absorption mode

of the perdeuterated phospholipid, we have concluded that the divalent cation preferentially binds to GM_1 even in the mixed $DMPC_{d54}/GM_1$ liposomal bilayers.

The ceramide moiety of GM_1 comprises fatty acids with acyl chains longer than the perdeuterated myristoyl chain of $DMPC_{d54}$, therefore, its insertion into the hydrophobic core of a bilayer of shorter chain symmetric phospholipids affects the packing of the perdeuterated acyl chains. Dahlen and Pascher (1979) have suggested that the sphingosine chain of glycosphingolipids penetrates into the bilayer by only 14 carbons . Boggs and Koshy (1994) have demonstrated that, in the liquid-crystalline phase of all the PC derivatives, the acyl chain of the glycosphingolipid cerebroside sulfate (CBS) containing C_{18}, C_{24}, and C_{26} fatty acid spin labels is not interdigitated. This has led them to conclude that the fatty acid chain of the CBS terminated at the PC bilayer center and remained relatively extended, thus forcing the carbohydrate headgroup farther above the bilayer surface and allowing it to be recognized by various carbohydrate binding ligands and proteins. Both GM_1 ganglioside and $DMPC_{d54}$ can bind divalent cations such as Ca^{2+}. Whether the binding affinity of Ca^{2+} towards GM_1 is greater than $DMPC_{d54}$ is still debatable and findings in this area have not been conclusive. Our results clearly show that the divalent cation preferentially binds to the sialic acid moiety of GM_1 in the mixed $DMPC_{d54}/GM_1$ model systems. Based on the interpretations of Boggs and Koshy (1994) and Dahlen and Pascher (1979), we have drawn the conclusion that the ceramide moiety of GM_1 inserted into the $DMPC_{d54}$ bilayer and terminated at the bilayer center, with its carbohydrate headgroup projecting out of the bilayer surface to allow a better binding to Ca^{2+} ions, as compared to $DMPC_{d54}$.

To our knowledge, we are the first group to provide spectroscopic evidence of a significant interaction of Ca^{2+} with GM_1 and our results clearly show that the sialic acid moiety of GM_1 binds Ca^{2+} with a greater affinity than the phosphate moiety of $DMPC_{d54}$, leading us to conclude that the glycolipid may be involved in processes in nerve endings that require the divalent cation such as cell fusion and neurotransmitter movement (Boggs, 1986; Kalueff, 1996; Tsuji *et al.*, 1996).

Recent FTIR-ATR spectroscopic evidence by Müller *et al.* (1993, 1996) indicated that Ca^{2+} bound weakly to GM_1 and this binding did not significantly affect the CO_2^- vibrational band of the glycolipid in the mixed DMPC/GM_1 bilayers (5:1, mol/mol). However, this group did not check the purity and the fatty acid composition of their GM_1.

It is our strong belief that the surface location and the conformation of the headgroup region of gangliosides govern their ability to interact with ions and carbohydrate binding ligands. The unique surface position of the headgroup region of GM_1 is determined by the fatty acid chains of the ceramide backbone of the glycolipid. The contradictory results presented by Müller and colleagues (1993, 1996) and other research groups may be caused by different fatty acid chain lengths, by the different degree of saturation of the GM_1 acyl chains and by the conformation of the oligosaccharide moiety, which would ultimately affect the surface location of the glycolipid and its interaction with various ligands, specifically Ca^{2+} ions.

In the mixed $DMPC_{d54}$/GM_1 liposomal bilayers and in the absence of Ca^{2+} ions, the degree of hydrogen bonding was reduced as compared to GM_1 micellar suspensions and $DMPC_{d54}$ bilayers. This can be explained by the fact that the mutual shielding of hydrogen

donating and accepting groups have affected the hydrogen bonding properties of the glycolipid and the phospholipid. On the other hand, the complexation of Ca^{2+} ions with GM_1 in the mixed bilayers increased the probability of hydrogen bonding. A reduction of the effect of negatively charged sialic acids by interaction with Ca^{2+} affects the surface potential and the orientation of the sialic acid residue at the interfacial zone, which would ultimately affect molecular packing of the acyl chains in the bilayer. These modifications in the headgroup region of GM_1 affect hydration at the interface, leading to increased hydrophobic chain interactions and intermolecular cohesion, which brings the oligosaccharide moiety of GM_1 and the headgroup of $DMPC_{d54}$ closer and, thus, strengthens the hydrogen bonding network.

4.6 Physical State of the Lipid Mixture and Thermotropic Behavior of GM_1 Micellar Suspensions and Multilamellar Dispersions of $DMPC_{d54}$ and Mixed $DMPC_{d54}/GM_1$

The physical state of the lipidic bilayers depends on the temperature. In the gel state, the acyl chains are packed tightly, get locked in the all trans conformation and have less energy to rotate about the C-C bonds, which results in a reduction of their mobility and a maximization of their van der Waals interactions. In the fluid state, the lipid hydrocarbon chains are highly disordered. The frequencies of the temperature dependent methylene symmetric (C-H) stretching band of GM_1 (ca. 2850 cm^{-1}) and C-D symmetric stretching mode (ca. 2090 cm^{-1}) of $DMPC_{d54}$ give information about the fluidity or the phase state of the membrane. The maxima of these absorption bands typically shifts by about 2-3 cm^{-1} to

higher values at the phase transition temperature due to an increase of disorder or mobility of the fatty acid chains (Müller & Blume, 1993).

The ganglioside GM_1 is an amphiphilic molecule which forms aqueous micelles (Gammack, 1963; Yohe & Rosenberg, 1972). The fatty acid composition of the ceramide backbone of bovine brain GM_1, used throughout this study, was not homogeneous. It is a mixture of many fatty acids that differ in the hydrocarbon chain length, with stearic acid being the major species (Svennerholm, 1963; Namoi *et al.*, 1976; Nagai & Iwamori, 1978; Sillerud *et al.*, 1978, 1979; Ando & Yu, 1979; Hinz *et al.*, 1981; Kadowaki *et al.*, 1984; Kojima *et al.*, 1988; Maggio *et al.*, 1988; Sonnino *et al.*, 1994; Palestini *et al.*, 1995, and references therein). This acyl chain heterogeneity abolishes cooperativity in the gel to liquid-crystalline transition: the fluidity of the hydrophobic core increases gradually with temperature from 5 to 60 °C, but no thermal phase transition of the GM_1 micelles dispersed in heavy water was observed (Figure 3.12, panel A, full circles), although concentrations were as high as 110 mg/ml, well beyond critical micelle concentration (0.02 g/ml). These results are in agreement with the absence of transition in pure unsonicated suspensions of GM_1 (4 mg/ml) reported by Sillerud *et al.* (1979) and in pure sonicated suspensions of GM_1 and GD_{1a} (15 mg/ml) reported by Hinz *et al.* (1981).

Hirai and Takizawa (1998) reported that the elevation of temperature induced a significant shrinkage of the hydrophilic region of the ganglioside micellar suspensions. The authors have found clear evidence that the ganglioside molecules can reversibly occlude or extrude a large amount of water, like a water cavity, in the physiological temperature range of 6 to 60 °C. They have concluded that the ganglioside induced changes of the local

hydrophobicity of the cell surface, in response to variations in temperature, might modulate various surface events such as cell/cell interaction and cell/surface-protein interaction. Their results were in agreement with those reported by Masserini and Freire (1986), Masserini *et al.* (1989) and Hirai *et al.* (1996).

Contrasted to GM_1 are phospholipids, such as $DMPC_{d54}$ used for this study, which form multilamellar bilayers in aqueous dispersions. The gel/liquid-crystalline phase transition temperature of $DMPC_{d54}$ liposomal bilayers was centered at 19 °C without Ca^{2+} (Figure 3.12, panel B, open circles) and at 21 °C with 10 mM $CaCl_2$ (Figure 3.12, panel B, open squares), suggesting that the divalent cation had an ordering effect on the hydrocarbon region of the perdeuterated bilayer.

The addition of Ca^{2+} to the GM_1 micellar suspensions (Figure 3.12, panel A, full squares) and the $DMPC_{d54}$ liposomal bilayers (Figure 3.12, panel A, open squares) resulted in a shift of the symmetric CH_2 and CD_2 stretching vibration bands of the glycolipid and the phospholipid, respectively, to higher frequencies due to an increase in gauche conformers. The temperature induced transition behavior of multilamellar dispersions of perdeuterated $DMPC_{d54}$ containing bovine brain GM_1 was monitored by FTIR spectroscopy as a function of the ganglioside molar fraction. Infrared observations were made on the following mol fractions of GM_1 in $DMPC_{d54}$: 0.12, 0.15, 0.19, 0.26, 0.34, 0.41 and 0.58. The influence of GM_1 on the phase behavior of $DMPC_{d54}$ was monitored by following the frequency the CD_2 symmetric stretching vibrational band at ca. 2090 cm^{-1} as a function of temperature.

The transition curves of various $DMPC_{d54}/GM_1$ mixtures are presented in Figures 3.13, 3.14 and 3.15. The addition of GM_1 to the phospholipid vesicles perturbs the lipid

bilayer and leads to increased gel/liquid-crystalline phase transition temperatures with increasing ganglioside content (Table VI). While in pure $DMPC_{d54}/Ca^{2+}$ vesicles the usual single transition is observed at ca. 21 °C, $DMPC_{d54}$ vesicles containing GM_1 and the divalent cation Ca^{2+} exhibit a single, cooperative transition between ca. 22 and 28 °C, depending on the GM_1 content. The presence of a single and cooperative transition is consistent with a homogeneous mixing of GM_1 and $DMPC_{d54}$ within the bilayers, without lateral phase separation. The thermotropic profile of the hydrocarbon chains of GM_1 and $DMPC_{d54}$ were identical (± 0.3), with a gel/liquid-crystalline transition temperature occurring at a higher temperature than in pure $DMPC_{d54}$ dispersions for both the methylene C-H (2850 cm^{-1}) and C-D (2090 cm^{-1}) symmetric stretching vibrations.

At low monosialoganglioside GM_1 concentrations and for GM_1 molar fractions of 0.12 and 0.15 (Figure 3.13), the order-disorder T_m for $DMPC_{d54}/GM_1$ liposomal bilayers were 22 and 23 °C, respectively. At moderate glycolipid concentration (Figure 3.14), the gel/liquid crystalline phase transition for the mixed model membranes was 25 °C for GM_1 molar fractions of 0.19 and 0.26, and the T_m was 26 °C for a GM_1 molar fraction of 0.34. At high ganglioside concentration (Figure 3.15), the T_m continued to increase for the $DMPC_{d54}/GM_1$ dispersions with GM_1 molar fractions of 0.41 and 0.58, and it was centered at ca. 28 °C. Therefore, the glycolipid stabilized the $DMPC_{d54}$ bilayers at all concentrations.

The addition of GM_1 to $DMPC_{d54}$ bilayers increased the transition temperature, with the acyl chains becoming more ordered or motionally restricted. As increasing amounts of GM_1 were added to $DMPC_{d54}$ to mimic physiological conditions associated with the accumulation of gangliosides, the ordering effect on the hydrocarbon region became more

pronounced, with a concomitant decrease in the amplitude and the cooperativity of the phase transition.

The effect of Ca^{2+} ions on the thermotropic behavior of the mixed $DMPC_{d54}/GM_1$ (GM_1 $x_g = 0.26$) liposomal bilayers is shown in Figure 3.16. The order-disorder T_m of GM_1 (panel A, full circles) and of $DMPC_{d54}$ (panel B, open circles) is 24 °C in the absence of Ca^{2+}. The ordering effect of GM_1 on $DMPC_{d54}$ model membranes is enhanced by the presence of Ca^{2+} ions in the milieu. The divalent cation shifted the transition temperature to 25 °C, suggesting a reduction of the mobility of the hydrocarbon chains of the glycolipid and of the perdeuterated phospholipid. The $\nu_s CH_2$ of GM_1 (panel A, full squares) and the $\nu_s CD_2$ of $DMPC_{d54}$ (panel B, open squares) in the mixed $DMPC_{d54}/GM_1/Ca^{2+}$ dispersions are lowered, indicating that the mixed liposomes contained less gauche conformers and that the acyl chains were packed tightly in the hydrophobic core of the PC bilayer.

In the case of phospholipids, the rearrangement of the acyl chains in the hydrophobic core of the bilayer is associated with a transition from the gel to the liquid-crystalline state (Lichtenberg & Schmidt, 1981). The thermal phase transition undergone by GM_1 in the mixed $DMPC_{d54}/GM_1$ liposomal bilayers in the temperature range between 5 and 60 °C could be attributed to a rearrangement of the hydrocarbon chains from one disordered state to another, possibly more disordered state (Curatolo *et al.*, 1977). However, Lee and colleagues (1980), Probst and Rahmann (1980), Baret *et al.* (1982) and Gershfeld (1982) have demonstrated that the thermal transitions of gangliosides compared to those of phospholipids are much more influenced by rearrangement of the large polar headgroups.

They have explained that these phase transitions were possibly due to a second order liquid-expanded (more disordered) to liquid-condensed (less disordered) transition.

Our results clearly showed that GM_1 was incorporated and molecularly dispersed in the mixed $DMPC_{d54}/GM_1$ bilayers, without lateral phase segregation, and that the ordering effect of the glycolipid on the hydrocarbon region of the $DMPC_{d54}$ matrix was enhanced by Ca^{2+} ions. These findings are in agreement with those of Sillerud *et al.* (1979), Felgner *et al.* (1981), Hinz *et al.* (1981), Uchida *et al.* (1981), Müller and Blume (1993) and Müller *et al.* (1996).

4.7 Significance of the Research Findings

The interactions that GM_1 can establish with the synthetic $DMPC_{d54}$ will provide a better understanding in molecular terms of the ability of the glycolipid to induce changes in membrane permeability and stability. The charge, size, and overall conformation of the ganglioside oligosaccharide headgroup region influence the surface electrical potential, the phase state and the molecular organization of the model $DMPC_{d54}$ bilayers in which they are incorporated.

GM_1 is present on the outer leaflet of the plasma membrane and it is plausible that this glycolipid, along with other negatively charged lipids comprised in the interfacial region of the bilayer, may serve as an anionic site to trap Ca^{2+} and other cations of biological significance. Since membrane ganglioside content is typically low, these molecules may reasonably be expected to be randomly distributed in the bilayer plane, notably because they are anionic and should repulse each other.

Briefly summarizing, our spectroscopic findings showed that the monosialoganglioside GM_1 micellar suspensions did not exhibit any sign of thermal phase transition in the temperature range from 5 to 60 °C. The interaction between GM_1 and our model $DMPC_{d54}$ revealed that the glycolipid and the perdeuterated phospholipid formed a homogeneous mixture, with the absence of lateral phase segregation. The GM_1 molecules were capable of undergoing phase transition in a lipid bilayer environment and it was reported that this thermal phase transition is influenced by rearrangement of the large polar headgroups of the glycolipid (Probst & Rahmann, 1980; Baret *et al.*, 1982; Gershfeld, 1982). The assessment of the C=O stretching vibrations at the interfacial zone revealed that hydrogen bonding was disrupted, in the absence of Ca^{2+} ions, which likely resulted from mutual shielding of the hydrogen bonding partners. These induced modifications by GM_1 might affect the fluidity of the lipid bilayer and the interactions of membrane lipids with proteins, altering their behavior and consequently their dynamic functions (Boggs, 1986).

Our spectroscopic results led us to suggest the following simplistic model for the implication of GM_1 in synaptic transmission and in Ca^{2+} homeostasis at the presynaptic membrane. The negatively charged sialic acid residues of GM_1 bind Ca^{2+} (Jacques *et al.*, 1977, 1980; Sillerud *et al.*, 1978) and the synaptic membrane is tightened or rigidified. This is consolidated by our results which showed a significant interaction between *Ca^{2+} ions and GM_1*, an increased orderness of the acyl chains of $DMPC_{d54}$ model membranes and a strengthened hydrogen bonding network in the presence of the divalent cation (Sharom & Grant, 1977,1978; Seimiya *et al.*, 1978a, b; Uchida *et al.*, 1981; Bach *et al.*, 1982). The stabilizing effect of Ca^{2+} on the mixed $DMPC_{d54}/GM_1$ liposomes is most likely attributed to

intermolecular bridging effects of Ca^{2+} (Sharom & Grant, 1978; Tettamanti *et al.*, 1980) as shown for phospholipids (Träuble, 1977; Lee & Grant, 1980; Bertoli *et al.*, 1981; Ganesan *et al.*, 1982). When an action potential arrives at the synapse, Ca^{2+} is displaced from the gangliosides and the hydrogen bonding network is disrupted, thus increasing the fluidity of the cluster area and inducing increased permeability for the divalent cation. The ion concentration or voltage dependent influx of calcium fulfills the task of a primary messenger for the internalization of the electrically encoded information. The entry of calcium to the intracellular space could be easily facilitated via ganglioside modulated ion channels. The transmitter is released and Ca^{2+} is pumped out of the neuroplasm by means of ganglioside modulated membrane proteins. The divalent cation then rebinds to gangliosides, which induces a retightening of the membrane for a new transmission cycle (Bach & Sela, 1980; Maggio *et al.*, 1980; Baret *et al.*, 1982; Gershfeld *et al.*, 1982; Rahmann, 1983; Probst *et al.*, 1984; Rahmann *et al.*, 1994, 1998; Sonnino *et al.*, 1994; Kalueff, 1996).

In summary, GM_1 exhibited two properties suggesting possible mechanisms for its involvement in receptor modulation and general cell physiology. Firstly, our spectroscopic findings showed that *GM_1 bound Ca^{2+} ions*, without a shadow of a doubt, and GM_1/Ca^{2+} interactions were more pronounced than those of $DMPC_{d54}/Ca^{2+}$. Secondly, the glycolipid can act as a receptor for extracellular signals, transmit or amplify these signals to other membrane components and take part in dynamic membrane functions (e.g., synaptic transmission, translocation of the cholera toxin, etc.) by undergoing phase transition, by causing protein conformational changes within the bilayer via hydrogen bonding and by acting as a water cavity (Masserini & Freire, 1986; Masserini *et al.*, 1989; Hirai *et al.*, 1996;

Hirai & Takizawa, 1998) to modulate the local hydrophobicity of cell surfaces and events such as cell/cell and cell/surface protein interactions.

REFERENCES

Abrahamsson, S., Dahlen, B., Lofgren, H., Pascher, J. and Sandell, S. (1977) Structure of Biological Membranes. In: *The Structure of Biological Membranes* (Abrahamsson, S. and Pascher, J., Eds.). Plenum Press, New York, pp. 1-23.

Ando, S. and Yu, R.K. (1979) Isolation and Characterization of two Isomers of Brain Tetrasialogangliosides. *J. Biol. Chem.*, **254**, 12224-12229.

Attar, M., Wong, P.T.T., Kates, M., Carrier, D., Jaklis, P. and Tanphaichitr, N. (1998) Interaction Between Sulfogalactosylceramide and Dimyristoylphosphatidylcholine Increases the Orientational Fluctuation of Their Lipid Hydrocarbon Chains. *Chem. Phys. Lipids.*, **94**, 227-238.

Bach, D. and Sela, B.A. (1980) A Differential Scanning Calorimeter Study of the Interactions of Gangliosides with Peanut Lectin, Serotonin and Daunomycin. *Biochimica et Biophysica Acta*, **506**, 186-191.

Bach, D., Miller, J.R. and Sela, B.A. (1982) Calorimetric Studies on Various Gangliosides and Ganglioside-Lipid Interactions. *Biochimica et Biophysica Acta*, **686**, 233-239.

Baret, J.F., Bois, A.G., Dupin, J.J. and Firpo, J.L. (1982) The Liquid-Expanded and the Liquid-Condensed Phases in Amphiphile Monolayers are Separated by a Second-Order Phase Transition. *J. Colloid Interface Sci.*, **86**, 370-376.

Beitinger, H., Probst, W., Möbius, D. and Rahmann, H. (1987) Influence of Ca^{2+} and Temperature on the Interaction of Gangliosides with Valinomycin in Mixed Monolayers at the Air/Water Interface. *Journal of Biochemistry*, **102**, 963-966.

Bertoli, E., Masserini, M., Sonnino, S., Ghidoni, R., Cestaro, B. and Tettamanti, G. (1981) Electron Paramagnetic Resonance Studies on the Fluidity and Surface Dynamics of Egg Phosphatidylcholine Vesicles Containing Gangliosides. *Biochimica et Biophysica Acta*, **647**, 196-202.

Blume, A., Hübner, W. and Messner, G. (1988) Fourier Transform Infrared Spectroscopy of $^{13}C{=}O$ Labeled Phospholipids Hydrogen Bonding to Carbonyl Groups. *Biochemistry*, **27**, 8239-8249.

Boggs, J.M. (1986) Effect of Lipid Structural Modifications on Their Intermolecular Hydrogen Bonding Interactions and Membrane Functions. *Biochem. Cell Biol.*, **64**, 50-57.

Boggs, J.M. and Koshy, K.M. (1994) Do the Long Fatty Acid Chains of Sphingolipids Interdigitate Across the Center of a Bilayer of Shorter Chain Symmetric Phospholipids? *Biochimica et Biophysica Acta*, **1189**, 233-241.

Brady, R.O. and Fishman, P.H. (1979) Biotransducers of Membrane Mediated Information. *Adv. Enzymol.*, **50**, 303-324.

Cameron, D.G. and Mantsch, H.H. (1978) The Phase Transition of 1,2-Dipalmitoyl-*sn*-Glycero-3-Phosphocholine by Fourier Transform Infrared Difference Spectroscopy. *Biochem. Biophys. Res. Commun.*, **83**, 886-892.

Cameron, D.G. and Moffatt, D.J. (1987) A Generalized Approach to Derivative Spectroscopy. *Appl. Spectrosc.*, **41**, 539-544.

Cheresh, D.A., Pytela, R., Pierschbacher, M.D., Klier, F.G., Ruoslahti, E. and Reisfeld, R.A. (1987) An Arg-Gly-Asp Directed Adhesion Receptor on Human Melanoma Cells Exists in a Calcium-dependent Functional Complex with the Disialoganglioside GD_2. *J. Cell Biol.*, **105**, 1163-1173.

Choma, C.T. and Wong, P.T.T. (1992) The Structure of Anhydrous and Hydrated Dimyristoylphosphatidylglycerol: a Pressure Tuning Infrared Spectroscopic Study. *Chem. Phys. Lipids*, **61**, 131-137.

Clancy, J., Tait-Kamardt, A., Petitpas, J., Manousos, M., McGuirk, P.R., Subashi, T., Watts, P. and Wondrack, L. (1994) Assays to Detect and Characterize Human Immunodeficiency Virus Type I (HIV-I) Receptor Antagonists, Compounds that Inhibit Binding of the HIV-I Surface Glycoprotein, gp120, to the CD_4 Receptor on Human T-lymphocytes. *Antimicrobial Agents and Chemotherapy*, **38**, 2008-2013.

Colthup, N.B., Daly, L.H. and Wiberley, S.E. (1990) *Introduction to Infrared and Raman Spectroscopy*, 3rd Edition. Academic Press, Inc., New York, pp. 1-83.

Cross, A.D. (1964) *An Introduction to Practical Infrared Spectroscopy*, 2nd Edition. Butterworths, London, pp. 1-19.

Cuello, A.C. (1990) Glycosphingolipids that Can Regulate Nerve Growth and Repair. *Adv. Pharmacol.*, **21**, *1-50.*

Curatolo, W., Small, D.M. and Shipley, G.G. (1977) Phase Behaviour and Structural Characteristics of Hydrated Bovine Brain Gangliosides. *Biochimica et Biophysica Acta*, **468**, 11-20.

Czarniecki, M.F. and Thornton, E.R. (1977) Carbon-13 Nuclear Magnetic Resonance Spin-Lattice Relaxation in the N-Acetylneuraminic Acids. Probes for Internal Dynamics and Conformational Analysis. *J. Am. Chem. Soc.*, **99**, 8273-8278.

Dahlen, B. and Pascher, I. (1979) Molecular Arrangements in Sphingolipids - Thermotropic Phase Behavior of Tetracosanoylphytosphingosine. *Chem. Phys. Lipids*, **24**, 119-133.

Deacon, G.B. and Phillips, R.J. (1980) Relationships Between the C-O Stretching Frequencies of Carboxylato Complexes and the Type of Carboxylate Coordination. *Coord. Chem. Rev.*, **33**, 227-250.

Delmelle, M., Dufrane, S.P., Brasseur, R. and Ruysschaert, J.M. (1980) Clustering of Gangliosides in Phospholipid Bilayers. *FEBS Lett.*, **121**, 11-14.

Dixon, S., Stewart, D., Grinstein, S. and Spiegel, S. (1987) Transmembrane Signalling by the B Subunit of Cholera Toxin: Increased Cytoplasmic Free Calcium in Rat Lymphocytes. *J. Cell Biol.*, **105**, 1153-1161.

Felgner, P.L., Freire, E., Barenholz, Y. and Thompson, T.E. (1981) Asymmetric Incorporation of Trisialoganglioside into Dipalmitoylphosphatidylcholine Vesicles. *Biochemistry*, **20**, 2168-2172.

Felgner, P.L., Thompson, T.E., Barenholz, Y. and Lichtenberg, D. (1983) Kinetics of Transfer of Gangliosides from their Micelles to Dipalmitoylphosphatidylcholine Vesicles. *Biochemistry*, **22**, 1670-1674.

Fishman, P.H. (1982) Role of Membrane Gangliosides in the Binding and Action of Bacterial Toxins. *J. Membr. Biol.*, **69**, 85-97.

Folch J., Ascoli I., Lees M., Meath J.A. and LeBaron F.N. (1951) Preparation of Lipid Extract from Brain Tissue. *J. Biol. Chem.*, **191**, 833-841.

Folch J., Lees M. and Sloane-Stanley, G.H. (1957) A Simple Method for the Isolation and Purification of Total Lipids from Animal Tissues. *J. Biol. Chem.*, **226**, 497-509.

Fredman, P., Nilsson O., Tayot, J.L. and Svennerholm, L. (1980) Separation of Gangliosides on a New Type of Anion-Exchange Resin. *Biochimica et Biophysica Acta*, **618**, 42-52.

Fueshko, S.M. and Schengrund, C.L. (1990) Murine Neuroblastoma Cells Express Ganglioside Binding Sites on Their Cell Surface. *J. Neurochem.*, **54**, 1791-197.

Fürst, W. and Sandhoff, K. (1992) Activator Proteins and Topology of Lysosomal Sphingolipid Catabolism. *Biochimica et Biophysica Acta*, **1126**, 1-16.

Gammack, D.B. (1963) Physicochemical Properties of Ox-Brain Gangliosides. *Biochemical Journal*, **88**, 373-383.

Ganesan, M.G., Schwinke, D.L. and Weiner, N. (1982) Effect of Ca^{2+} on Thermotropic Properties of Saturated Phosphatidylcholine Liposomes. *Biochimica et Biophysica Acta*, **686**, 245-248.

Garcia, J.V. and Miller, A.D. (1991) Serine Phosphorylation-Independent Down-Regulation of Cell-Surface CD_4 by nef. *Nature*, **350**, 508-511.

Gazzotti, G., Sonnino, S. and Ghidoni, R. (1985) Normal-Phase High-Performance Liquid Chromatographic Separation of Non-Derivatized Ganglioside Mixtures. *Journal of Chromatography*, **348**, 371-378.

Gershfeld, N.L. (1982) The Liquid-Condensed/Liquid-Expanded Transition in Lipid Films: A Critical Analysis of the Film Balance Experiment. *J. Colloid Interface Sci.*, **85**, 28-40

Griffiths, P.R. and Pariente, G.L. (1986) Introduction to Spectral Deconvolution. *Trends in Analytical Chemistry*, **5**, 209-215.

Hakomori, S. (1996) Sphingolipid-Dependent Protein Kinases. *Adv. Pharmacol.*, **36**, 155-171.

Hakomori, S. and Siddiqui B. (1974) Isolation and Characterization of Glycosphingolipid from Animal Cells and their Membranes. *Methods Enzymol.*, **32**, 345-367.

Harris, P.L. and Thornton, E.R. (1978) Carbon-13 and Proton Nuclear Magnetic Resonance Studies of Gangliosides. *J. Am. Chem. Soc.*, **100**, 6738-6745.

Harris, D.C. (1987) *Quantitative Chemical Analysis*, 2nd Edition. W.H. Freeman and Co., New York, pp. 495-643.

Hayashi, K., Mühleisen, M., Probst, W. and Rahmann, H. (1984) Binding of Ca^{2+} to Phosphoinositols, Phosphatidylserines and Gangliosides. *Chem. Phys. Lipids*, **34**, 317-322.

Higashi, H. and Yamagata, T. (1992) Mechanism for Ganglioside Mediated Modulation of Calmodulin-Dependent Enzyme. *J. Biol. Chem.*, **267**, 9839-9843.

Higashi, H., Omori, A. and Yamagata, T. (1992) Calmodulin, A Ganglioside Binding Protein. *J. Biol. Chem.*, **267**, 9831-9838.

Hilbush, B.S. and Levine, S.M. (1992) Modulation of a Ca^{2+} Signalling Pathway by GM_1 Ganglioside in PC12 Cells. *J. Biol. Chem.*, **267**, 24789-24795.

Hill, M.W. and Lester, R. (1972) Mixtures of Gangliosides and Phosphatidylcholine in Aqueous Dispersions. *Biochimica et Biophysica Acta*, **282**, 18-30.

Hinz, H.J., Körner, O. and Nicolau, (1981) Influence of Ganglioside GM_1 and GD_{1a} on Structural and Thermotropic Properties of Sonicated Small 1,2-Dipalmitoyl-L-α-Phosphatidylcholine Vesicles. *Biochimica et Biophysica Acta*, **643**, 557-571.

Hirai, M. and Takizawa, T. (1998) Intensive Extrusion and Occlusion of Water in Ganglioside Micelles with Thermal Reversibility. *Biophysical Journal*, **74**, 3010-3014.

Hirai, M., Takizawa, T., Yabuki, S., Nakata, Y. and Hayashi, K. (1996) Thermotropic Phase Behaviour and Stability of Monosialoganglioside Micelles in Aqueous Solution. *Biophysical Journal*, **70**, 1761-1768.

Holmgren, J., Mansson, J.E. and Svennerholm, L. (1974) Tissue Receptor for Cholera Enterotoxin: Structural Requirements of GM_1 Ganglioside in Toxin Binding and Inactivation. *Med. Biol.*, **52**, 224-233.

Igarashi, Y., Nojiri, H., Hanai, N. and Hakomori, S. (1989) Gangliosides that Modulate Membrane Protein Function. *Methods Enzymol.*, **179**, 521-541.

Iwamori, M. and Nagai, Y. (1978) A New Chromatographic Approach to the Resolution of Individual Gangliosides. Ganglioside Mapping. *Biochimica et Biophysica Acta*, **528**, 257-267.

Jacques, L.W., Brown, E.B., Barret, J.M., Brey, W.S. and Weltner, W. (1977) Sialic Acid. A Calcium Binding Carbohydrate. *J. Biol. Chem.*, **252**, 4533-4539.

Jacques, L.W., Riesco, B.F. and Weltner, W. (1980) NMR Spectroscopy and Calcium Binding of Sialic Acids: N-Glycolyl-Neuraminic Acid and Periodate-Oxidized N-Acetyl Neuraminic Acid. *Carbohydrate Res.*, **83**, 21-32.

Kadowaki, H., Evans, J.E. and McCluer, R.H. (1984) Separation of Brain Monosialoganglioside Molecular Species by High-Performance Liquid Chromatography. *J. Lipid Res.*, **25**, 1132-1139.

Kalueff, A.V. (1996) Signal Properties of Brain Gangliosides. *Ukrainskii Biokhimicheski Zhurnal*, **68**, 15-19.

Kates, M. (1986) Techniques of Lipidology. In: *Biochemistry and Molecular Biology* (Work, T.S. and Work, E., Eds.). Elsevier, Amsterdam, pp. 100-278.

Kauppinen, J.K., Moffatt, D.J., Mantsch, H.H. and Cameron, D.G. (1981) A Method for Resolving Intrinsically Overlapped Bands. *Appl. Spectrosc.*, **35**, 271-276.

Kawaguchi, T., Nakakuma, T., Kagimoto, T., Shirono, K., Horikawa, K., Hidaka, M., Iwamori, M., Nagai, Y. and Takatsuki, K. (1989) Characteristic Mode of Action of Gangliosides in Selective Modulation of CD_4 on Human T-lymphocytes. *Biochem. Biophys. Res. Commun.*, **158**, 1050-1059.

Kojima, H., Hanada-Yoshikawa, K., Katagiri, A. and Tamai, Y. (1988) Thermotropic Behavior and Electron Microscopic Structures of Mixtures of Gangliosides and Dipalmitoylphosphatidylcholine. *Journal of Biochemistry*, **103**, 126-131.

Koerner, T.A.W., Prestegard, J.H., Demou, P.C. and Yu, R.K. (1983) High Resolution Proton NMR of Gangliosides. 1. Use of Homonuclear Two-Dimensional Spin-Echo J-Correlated Spectroscopy for Determination of Residue Composition and Anomeric Configurations. *Biochemistry*, **22**, 2676-2687.

Krifuks, O., Bergelson, L.D. and Schlesinger, M. (1998) The Down Modulation of CD_4 Induced by the GM_1 Ganglioside is Regulated by Phosphatases and Kinases: Evidence from Enzyme Inhibitors and Anti-CD45 Antibodies. *Cellular Immunology*, **187**, 45-51.

Krishan, K. (1984) *Fourier Transform Infrared Spectroscopy*, 2nd Edition. D. Reidel Publishing Company, New York, pp. 139-158.

Ledeen, R.W. (1989) Biosynthesis, Metabolism and Biological Effects of Gangliosides. In: *Neurobiology of Glycoconjugates* (Margolis, R.U. and Margolis, R.K., Eds.). Plenum Press, New York, pp. 43-83.

Ledeen, R.W. and Yu, R.K. (1982) Gangliosides: Structure, Isolation and Analysis. *Methods Enzymol.*, **83**, 139-191.

Ledeen, R.W., Yu, R.K. and Eng, L.F. (1973) Gangliosides of Human Myelin: Sialosylgalactosyl-Ceramide (G7) as a Major Component. *J. Neurochem.*, **21**, 829-835.

Ledeen, R.W., Wu, G., Lu, Z.H, Kozireski Chuback, D. and Fang, Y. (1998) The Role of GM_1 and Other Gangliosides in Neuronal Differentiation. *Annals of the New York Academy of Sciences*, **845**, 161-175.

Lee, P.M. and Grant, C.W.M. (1980) Ganglioside Headgroup Disorder as a Sequel to Lectin Binding. *Biochem. Biophys. Res. Commun.*, **95**, 1299-1305.

Lee, P.M., Ketis, N.V., Barber, K.R. and Grant, C.W.M. (1980) Ganglioside Headgroup Dynamics. *Biochimica et Biophysica Acta*, **601**, 302-314.

Leon, A, Facci, L., Toffano, G., Sonnino, S. and Tettamanti, G. (1981) Activation of (Na^+,K^+)-ATPase by Nanomolar Concentrations of GM_1 Ganglioside. *J. Neurochem.*, **37**, 350-357.

Lester, R., Hill M.W. and Bangham, A.D. (1972) Molecular Mechanism of Tay-Sachs Disease. *Nature*, **236**, 32-33.

Lichtenberg, D. and Schmidt, C.F. (1981) Molecular Packing and Stability in the Gel Phase of Curved Phosphatidylcholine Vesicles. *Lipids*, **16**, 555-557.

Maggio, B., Cumar, F.A. and Caputto, R. (1980) Configuration and Interactions of the Polar Headgroup in Gangliosides. *Biochemical Journal*, **189**, 435-440

Maggio, B., Albert, J. and Yu, R.K. (1988) Thermodynamic-Geometric Correlations for the Morphology of Self-Assembled Structures of Glycosphingolipids and Their Mixtures with Dipalmitoylphosphatidylcholine. *Biochimica et Biophysica Acta*, **945**, 145-160.

Masserini, M. and Freire, E. (1986) Thermotropic Characterization of Phosphatidylcholine Vesicles Containing Ganglioside GM_1 with Homogeneous Ceramide Length. *Biochemistry*, **25**, 1043-1049.

Masserini, M., Giuliani, A., Venerando, B., Fiorilli, A., D'Aniello, A., and Tettamanti, G. (1985) α-Fucosidase-Ganglioside Interactions. Action of α-L-Fucosidase from the Hepatopancreas of *Octopus Vulgaris* on a Fucose Containing Ganglioside (Fuc-GM_1). *Biochemical Journal*, **229**, 595-603.

Masserini, M., Palestini, P., Venerando, B., Fiorilli, A., Acquotti, D. and Tettamanti, G. (1988) Interactions of Proteins with Ganglioside Enriched Microdomains on the Membrane; the Lateral Phase Separation of Molecular Species of GD_{1a} Ganglioside Having Homogeneous Long Chain Base Composition is Recognized by Vibrio-Cholera Sialidase. *Biochemistry*, **27**, 7973-7978.

Masserini, M., Palestini, P. and Freire, E. (1989) Influence of Glycolipid Oligosaccharide and Long Chain Base Composition on the Thermotropic Properties of Dipalmitoylphosphatidylcholine Large Unilamellar Vesicles Containing Gangliosides. *Biochemistry*, **28**, 5029-5034.

McDaniel, R. and McLaughlin, S. (1985) The Interaction of Ca^{2+} with Gangliosides in Bilayer Membranes. *Biochimica et Biophysica Acta*, **819**, 153-160.

McDaniel, R.V. and McIntosh, T.J. (1986) X-Ray Diffraction Studies of the Cholera Toxin Receptor, GM_1. *Biophysical Journal*, **49**, 97-96.

McDaniel, R.V., McLaughlin, A., Winiski, A.P., Eisenberg, M. and McLaughlin, S. (1984) Bilayer Membranes Containing the Ganglioside GM_1: Models for Electrostatic Potentials Adjacent to Biological Membranes. *Biochemistry*, **23**, 4618-1624.

Moffatt, D.J., Kauppinen, J.K., Cameron, D.G., Mantsch, H.H. and Jones, R.N. (1986) Computer Programs for Infrared Spectrophotometry. *N.R.C.C. Bulletin*, **18**, 23-29.

Müller, E. and Blume, A. (1993) FTIR Spectroscopic Analysis of the Amide and Acid Bands of Ganglioside GM_1, in Pure Form and in Mixtures with DMPC. *Biochimica et Biophysica Acta*, **1146**, 45-51.

Müller, E., Giehl, A., Schwarzmann, G., Sandhoff, C. and Blume, A. (1996) Oriented 1,2-Dimyristoyl-*sn*-Glycero-3-Phosphorylcholine/Ganglioside Membranes: A Fourier Transform Infrared Attenuated Total Reflection Spectroscopic Study. Band Assignments; Orientational, Hydrational, and Phase Behavior; and Effects of Ca^{2+} Binding. *Biophysical Journal*, **71**, 1400-1421.

Mushayakarara, E.C., Wong, P.T.T. and Mantsch, H.H. (1986) The Effect of Pressure on the Hydrogen Bonding Between Carbonyl and Hydroxyl Moieties in 1,2-Dipalmitoylglycerol: a Fourier Transform Infrared Spectroscopy Study. *Biochimica et Biophysica Acta*, **857**, 259-264.

Myers, M., Wortman, C. and Freire, E. (1984) Modulation of Neuraminidase Activity by the Physical State of Phospholipid Bilayers Containing Ganglioside GD_{1a} and GT_{1b}. *Biochemistry*, **23**, 1442-1448.

Nagai, Y. (1995) Functional Roles of Gangliosides in Bio-Signalling. *Behav. Brain Res.*, **66**, 99-104.

Nagata, Y., Ando, M., Iwata, H, Hara, A. and Taketomi, T. (1987) Effect of Exogenous Gangliosides on Amino Acid Uptake and (Na^+,K^+)-ATPase Activity in Superior Cervical and Nadose Ganglia of Rats. *J. Neurochem.*, **49**, 201-207.

Namoi, T., Ando, S. and Magai, Y. (1976) High Resolution Preparative Chromatographic System for Gangliosides Using DEAE-Sephadex and New Porous Silica, Iatrobeads. *Biochimica et Biophysica Acta*, **441**, 488-497.

Pascher, I. (1976) Molecular Arrangements in Sphingolipids. Conformation and Hydrogen Bonding of Ceramide and Their Implication on Membrane Stability and Permeability. *Biochimica et Biophysica Acta*, **455**, 433-451.

Pascher, I., Lundmark, M., Nyholm, P.G. and Sundell, S. (1992) Crystal Structures of Membrane Lipids. *Biochimica et Biophysica Acta*, **1113**, 339-373.

Palestini, P., Masserini, M., Fiorilli, A., Calappi, E. and Tettamanti, G. (1991) Evidence of Non Random Distribution of GD_{1a} Ganglioside in Rabbit Brain Microsomal Membranes. *J. Neurochem.*, **57**, 748-753.

Palestini, P., Allietta, M., Sonnino, S., Tettamanti, G., Thompson, T.E. and Tillack, T.W. (1995) Gel Phase Preference of Ganglioside GM_1 at Low Concentration in Two Component, Two Phase Phosphatidylcholine Bilayers Depends Upon the Ceramide Moiety. *Biochimica et Biophysica Acta*, **1235**, 221-230.

Probst, W. and Rahmann, H. (1980) Influence of Temperature Changes on the Ability of Gangliosides to Complex with Ca^{2+}. *J. Therm. Biol.*, **5**, 243-247.

Probst, W., Möbius, D. and Rahmann, H. (1984) Modulatory Effects of Different Temperatures and Ca^{2+} Concentrations on Gangliosides and Phospholipids in Monolayers at Air/Water Interfaces and Their Possible Functional Role. *Cellular and Molecular Neurobiology*, **4**, 157-176.

Quinet, C.C., McGuiness, T.L. and Greengard, P. (1984) Immunocytochemical Localization of Calcium/Calmodulin-Dependent Protein Kinase II in Rat Brain. *Proc. Natl. Acad. Sci. U.S.A.*, **81**, 5604-5608.

Rahmann, H. (1983) Functional Implication of Gangliosides in Synaptic Transmission. *Neurochem. Int.*, **5**, 539-547.

Rahmann, H. (1992) Calcium-Ganglioside Interactions and Modulation of Neuronal Functions. In: *Current Aspects of the Neurosciences* (Osborne, N.N., Ed.). MacMillan Press, London, pp. 87-125.

Rahmann, H., Rösner, H., Körtje, K.H., Beitinger, H. and Seybold, V. (1994) Ca^{2+}-Ganglioside-Interaction in Neuronal Differentiation and Development. *Prog. Brain Res.*, **101**,127-145.

Rahmann, H., Jonas, U., Kappel, T. and Hildebbrandt, H. (1998) Differential Involvement of Gangliosides versus Phospholipids in the Process of Temperature Adaptation in Vertebrates. *Annals of the New York Academy of Sciences*, **845**, 73-91.

Reed, R.A., Mattai, J. and Graham Shipley, G. (1987) Interaction of Cholera Toxin with Ganglioside GM_1 Receptors in Supported Lipid Monolayers. *Biochemistry*, **26**, 824-832.

Repke, H., Barber, E., Ulbright, S., Buchner, K., Hucho, F., Kopp, R., Scholz, H., Rudd, C.E. and Haseltine, W. (1992) Ganglioside-Induced CD_4 Endocytosis Occurs Independent of Serine Phosphorylation and is Accompanied by Dissociation of $p56^{lck}$. *Journal of Immunology*, **149**, 2585-2591.

Saggioro, D., Sorio C., Calderazzo, F., Callegaro, L., Panozzo, M., Berton, G. and Chieco-Bianchi, L. (1993) Mechanism of Action of the Monosialoganglioside GM_1 as a Modulator of CD_4 Expression. Evidence that GM_1-CD_4 Interaction Triggers Dissociation of $p56^{lck}$ from CD_4 and CD_4 Internalization and Degradation. *J. Biol. Chem.*, **268**, 1368-1375.

Schifferer, F., Beitinger, H., Rahmann, H. and Möbius, D. (1988) Effect of Calcium and Temperature on the Interaction of Gangliosides with Valinomycin Monolayers: A Comparison of Glycosphingolipids (GT_{1b}, Sulphatides) and Phosphatidylcholine. *FEBS Lett.*, **233**, 963-966.

Schifferer, F., Cordroch, W., Beitinger, H., Möbius, D. and Rahmann, H. (1991) Evidence for the Presence of a Specific Ganglioside GM_1/Valinomycin Complex in Mixed Monolayers. *Journal of Biochemistry*, **109**, 622-626.

Seimiya, T., Ashida, M., Muramutsu, T., Hara, I. and Hayashi, M. (1978a) Temperature Dependent Ionic Structure of Phospholipid Monolayers. *Chem. Phys. Lipids*, **22**, 221-226.

Seimiya, T., Ashida, M., Hayashi M., Muramutsu, T. and Hara, I. (1978b) Hydrogen Bond Among the Ionic Groups of Ampholitic Phospholipid. *Chem. Phys. Lipids*, **21**, 69-76.

Seybold, V., Rösner, H., Greis, C., Beck, E. and Rahmann, H. (1989) Possible Involvement of Polysialogangliosides in Nerve Sprouting and Cell Contact Formation: An Ultracytochemical *in vitro* Study. *J. Neurochem.*, **52**, 1958-1961.

Seyfried, T.N. and Yu, R.K. (1985) Ganglioside GD_3: Structure, Cellular Distribution and Possible Function. *Molecular and Cellular Biochemistry*, **68**, 3-10.

Sharom, F.J. and Grant, C.W.M. (1977) A Ganglioside Spin Label: Ganglioside Headgroup Interactions. *Biochem. Biophys. Res. Commun.*, **74**, 1039-1045.

Sharom, F.J. and Grant, C.W.M. (1978) A Model for Ganglioside Behavior in Cell Membranes. *Biochimica et Biophysica Acta*, **507**, 280-293.

Sillerud, L.O., Prestegard, J.H., Yu R.K., Schafer, D.E. and Königsberg, W.H. (1978) Assignment of ^{13}C Nuclear Magnetic Resonance Spectrum of Aqueous Ganglioside GM_1 Micelles. *Biochemistry*, **17**, 2619-2628.

Sillerud, L.O., Schafer, D.E., Yu R.K. and Königsberg, W.H. (1979) Calorimetric Properties of Mixtures of Ganglioside GM_1 and DPPC. *J. Biol. Chem.*, **254**, 10876-10880.

Sillerud, L.O., Yu R.K. and Schafer, D.E. (1982) Assignment of Carbon-13 Nuclear Magnetic Resonance Spectrum of Gangliosides GM_4, GM_3, GM_2, GM_1, GD_{1a}, GD_{1b} and GT_{1b} . *Biochemistry*, **21**, 1260-1271.

Slenzka, K., Appel, R. and Rahmann, H. (1990) Influence of Exogenous Gangliosides (GM_1, GD_{1a}, GM_{1x}) on a Ca^{2+}-Activated Mg^{2+}-Dependent ATPase in Cellular and Subcellular Brain Fractions of the Djungarian Dwarf Hamster (*Phodopus Sungorus*). *Neurochem. Int.*, **17**, 609-614.

Sonnino, S., Chigorno, V., Valsecchi, M., Pitto, M. and Tettamanti, G. (1992) Specific Ganglioside-Cell Protein Interactions: A Study Performed with GM_1 Ganglioside Derivative Containing Photoactive Azide and Rat Cerebellar Granule Cells in Culture. *Neurochem. Int.*, **20**, 315-321.

Sonnino, S., Cantù, L., Corti, M., Acquotti, D. and Venerando, B. (1994) Aggregative Properties of Gangliosides in Solution. *Chem. Phys. Lipids*, **71**, 21-45.

Sorio, C., Saggiorio, D., Chieco-Bianchi, L. and Berton, G. (1993) The Monosialo-ganglioside GM_1 Induces Internalisation and Degradation of the CD_4 Antigen in U937 Cells: Evidence for a Novel Mechanism of CD_4 Down-Modulation in a $p56^{lck}$ Negative Cell Line, which is Independent of Protein Kinase C Activation. *Biochem. Biophys. Res. Commun.*, **158**, 1105-1110.

Spiegel, S. (1988) Gangliosides are Biomodulators of Cell Growth. In: *New Trends in Ganglioside Research: Neurochemical and Neuroregenerative Aspects* (Ledeen, R.W., Hogan, E.L., Tettamanti, G., Yates, A.J. and Yu, R.K., Eds.). Liviana Press/Springer Verlag, Padova/Berlin, pp. 405-421.

Spiegel, S., Handler, J.S. and Fishman, P.H. (1986) Gangliosides Modulate Sodium Transport in Cultured Toad Kidney Epithelia. *J. Biol. Chem.*, **261**, 15755-15760.

Svennerholm, L. (1957) I. Quantitative Estimation of Sialic Acids. II. A Colorimetric Resorcinol-Hydrochloric Acid Method. *Biochimica et Biophysica Acta*, **24**, 604-611.

Svennerholm, L. (1963) Chromatographic Separation of Human Brain Gangliosides. *J. Neurochem.*, **10**, 613-623.

Svennerholm, L. (1972) Gangliosides, Isolation. *Methods Carbohydr. Chem.*, **6**, 464-474.

Svennerholm, L. and Fredman, P. (1980) A Procedure for the Quantitative Isolation of Brain Gangliosides. *Biochimica et Biophysica Acta*, **617**, 97-109.

Tettamanti, G., Preti, A., Cestaro, B., Masserini, M., Sonnino, S. and Ghidoni, R. (1980) Gangliosides and Associated Enzymes at the Nerve Ending Membranes. In: *Cell Surface Glycolipids* (Sweely, C., Ed.). Am. Chem. Soc. Symp., pp. 321-343.

Thomas, P.P. and Brewer, G.J. (1990) Gangliosides and Synaptic Transmission. *Biochimica et Biophysica Acta*, **1031**, 277-289.

Thompson, T.E., Allietta, M., Brown, R.E., Johnson, M.L. and Tillack, T.W. (1985) Organization of Ganglioside GM_1 in Phosphatidylcholine Bilayers. *Biochimica et Biophysica Acta*, **817**, 229-237.

Tiemeyer, M., Yasuda, Y. and Schnaar, R.L. (1990) Ganglioside Specific Binding Protein on Rat Brain Membranes. *J. Biol. Chem.*, **264**, 1671-1681.

Tomasi, M., Roda, C., Ausiello, C., D'Agnolo, G., Venerando, B., Ghidoni, R., Sonnino, S., and Tettamanti, G. (1980) Interaction of GM_1 Ganglioside with Bovine Serum Albumin. Formation and Isolation of Multiple Complexes. *Eur. J. Biochem.*, **111**, 315-324.

Tsuji, S., Kojima, N. and Hitoshi, S. (1996) New Evidence for the Occurrence of a Glycolipid-Mediated Signal Transduction System. *Journal of Lipid Mediators and Cell Signalling*, **14**, 289-294.

Träuble, H. (1977) Membrane Electrostatics. In: *The Structure of Biological Membranes* (Abrahamsson, S. and Pascher, J., Eds.). Plenum Press, New York, pp. 509-550.

Uchida, T., Nagai, Y., Kawasaki, Y. and Wakayama, N. (1981) Fluorospectroscopic Studies of Various Gangliosides and Ganglioside-Lecithin Dispersions. Steady-State and Time Resolved Fluorescence Measurements with 1,6-Diphenyl-1,3,5-Hexatriene. *Biochemistry*, **20**, 162-169.

Urban, P.F., Harth, S., Freysz, L. and Dreyfus, H. (1979) Brain and Retinal Ganglioside Composition from Different Species Determined by TLC and HPTLC. *Adv. Experimental Med. and Biol.*, **125**, 149-157.

Varon, S., Pettmann, B. and Manthorpe, M. (1988) Extrinsic Regulations of Neuronal Maintenance and Repair. In: *New Trends in Ganglioside Research: Neurochemical and Neuroregenerative Aspects* (Ledeen, R.W., Hogan, E.L., Tettamanti, G., Yates, A.J. and Yu, R.K., Eds.). Liviana Press/Springer Verlag, Padova/Berlin, pp. 607-623.

Venerando, B., Fiorilli, A., Masserini, M., Giuliani, A. and Tettamanti, G. (1985) Interactions of Pig Brain Cytosolic Sialidase with Gangliosides. Formation of Catalytically Inactive Enzyme-Ganglioside Complexes. *Biochimica et Biophysica Acta*, **833**, 82-92.

Venerando, B., Fiorilli, A., Caimi, L. and Tettamanti, G. (1987) Interactions of Pig Brain Cytosolic Sialidase with Gangliosides. The Formation of Catalytically Inactive Enzyme-Ganglioside Complexes Requires Homogeneous Ganglioside Micelles and is a Reversible Phenomenon. *Journal of Biochemistry*, **102**, 1167-1176.

Walkley, S.U., Siegel, D.A. and Dobrebnis, K. (1995) GM_2 Ganglioside and Pyramidal Neuron Dendritogenesis. *Neurochemical Res.*, **20**, 1287-1299.

Wong, P.T.T. and Mantsch, H.H. (1988) High Pressure Infrared Spectroscopic Evidence of Water Binding Sites in 1,2-Diacylphospholipids. *Chem. Phys. Lipids*, **46**, 213-224.

Wynn, C.G. and Robson, B. (1986) Calculation of the Conformation of Glycosphingolipids. 2. GM_1 and GM_2 Gangliosides. *J. Theor. Biol.*, **123**, 221-230.

Yohe, H.C. and Rosenberg, A. (1972) Interaction of Triiodide Anion with Gangliosides in Aqueous Iodine. *Chem. Phys. Lipids*, **9**, 279-294.

Yasuda, Y., Tiemeyer, M., Blackburn, C.C. and Schnaar, R. (1988) Neuronal Recognition of Gangliosides: Evidence for a Brain Ganglioside Receptor. In: *New Trends in Ganglioside Research: Neurochemical and Neuroregenerative Aspects* (Ledeen, R.W., Hogan, E.L., Tettamanti, G., Yates, A.J. and Yu, R.K., Eds.). Liviana Press/Springer Verlag, Padova/Berlin, pp. 229-243.

Yasukawa, M., Inoue, Y., Sada E., Yakushijin, Y., Furukawa, M. and Fujita, S. (1995) CD_4 Down-Modulation by Ganglioside and Phorbol Ester Inhibits Human Herpes Virus 7 Infection. *J. General Virology*, **79**, 2381-2385.

Yates, A.J., Walters, J.D., Wood, C.L. and Johnson, J.D. (1989) Ganglioside Modulation of cyclic AMP-dependent Protein Kinase and Cyclic Nucleotide Phosphodiesterase *in vitro*. *J. Neurochem.*, **53**, 162-167.

APPENDIX ONE

THEORY OF INFRARED DISPERSION SPECTROSCOPY

A1.1 Absorption and Scattering of Electromagnetic Radiation

A1.1.1 The Nature of Electromagnetic Radiation

The movement of electrical or magnetic charges in space results in a change in the electric and magnetic field. When periodic changes in the field occur, an electromagnetic wave propagating in space is generated. A collection of such waves constitutes electromagnetic radiation. This radiation travels in vacuum with the speed $c \approx 3 \times 10^{10}$ cm/s and in other medium, its velocity is smaller than c. Each wave of electromagnetic radiation associated with the vibration of one oscillator can be characterized by specifying the value of intensity of the electrical component which varies along the way of radiation according to the expression

Equation A1

$$E = E_0 \cos(\omega t + \varphi) = E_0 \cos(2\pi\nu t + \varphi)$$

where E_0 = wave amplitude
t = time
φ = phase
ω = angular frequency
$= 2\pi\nu$
ν = frequency

The wave described by equation A1 is called a monochromatic wave. Electromagnetic radiation usually consists of many such waves. One vibration of the electromagnetic field occurs in a period T, and the wavelength of the radiation is λ.

A1.1.2 Properties of Electromagnetic Radiation

Qualitative characteristics of electromagnetic radiation include the wavelength λ, frequency ν, speed of light υ, wave period T and the radiant energy E. There is a direct relationship between the wavelength, the frequency and the speed of light in vacuum c

Equation A2 $\lambda \nu = c$

ν = frequency, in s^{-1}
λ = wavelength, in cm
c = velocity, 3×10^{10} cm/s

In vibrational spectroscopy, it is common to express frequency in units of wavenumbers $\bar{\nu}$ (cm^{-1}). The wavenumber is defined as the number of wave periods per cm, *i.e.*

Equation A3 $\bar{\nu}\ (cm^{-1}) = 1/\lambda$

The next qualitative characteristic of radiation is its polarization. The wave can be polarized linearly, circularly or elliptically. Electromagnetic radiation is a collection of waves. Natural radiation consists of unpolarized waves, but the radiation obtained, for example, from a laser is linearly polarized. Radiation can be mono- or polychromatic. Natural radiation is polychromatic, *i.e.* contains waves of different wavelengths, in contrast with the monochromatic radiation from a laser. The full spectrum of electromagnetic radiation (Figure A1.1) is very broad and is characterized by its wavelength λ (the length of one wave), its frequency ν (the number of vibrations per unit time) and its wavenumber $\bar{\nu}$ (Colthup, 1990). The energy of a molecule consists partly of electronic energy (ultraviolet and visible region of the electromagnetic spectrum), partly of vibrational energy (infrared region) and partly of rotational energy (infrared and microwave region) (Colthup, 1990).

Figure A1.1 The electromagnetic spectrum. Reproduced from Harris (1987).

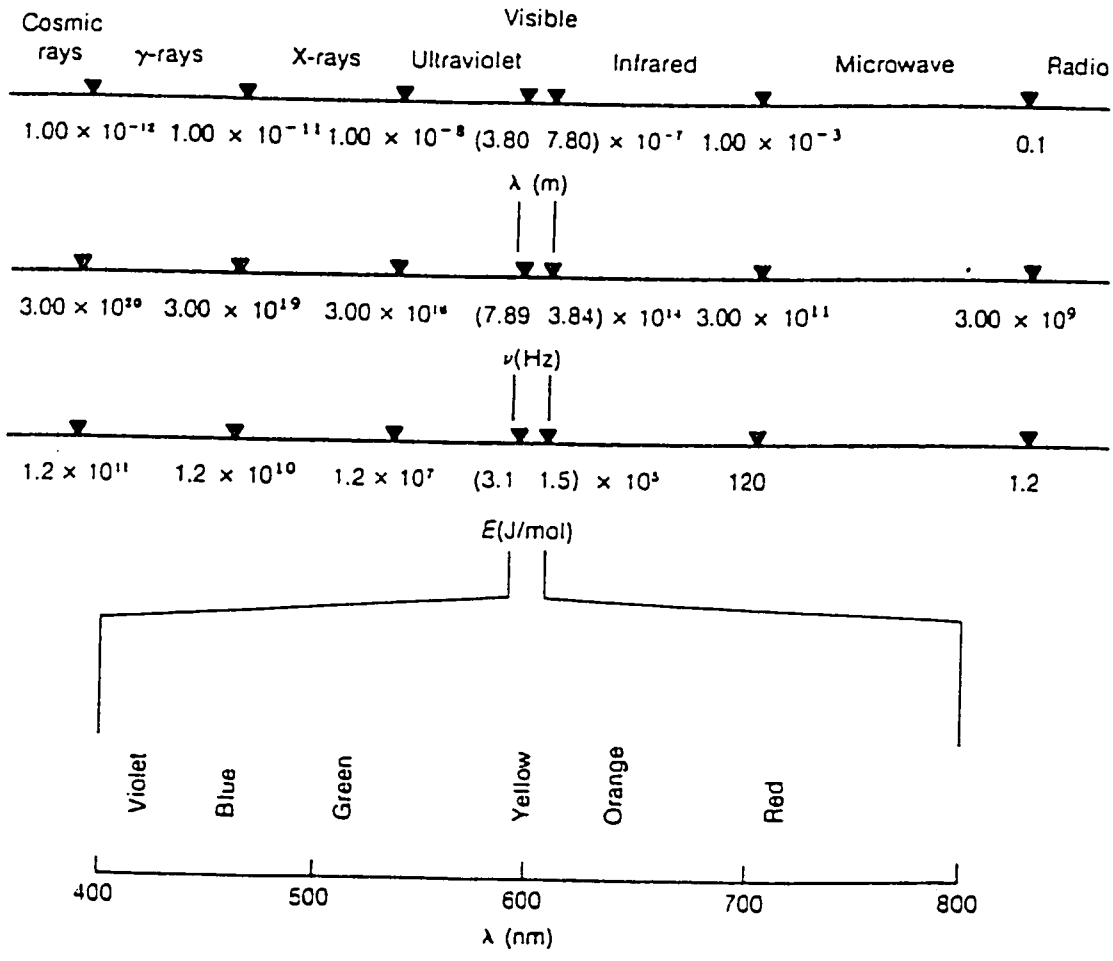
Cosmic rays
γ-rays
X-rays
Ultraviolet
Visible
Infrared
Microwave
Radio
1.00 × 10⁻¹² 1.00 × 10⁻¹¹ 1.00 × 10⁻⁸ (3.80 7.80) × 10⁻⁷ 1.00 × 10⁻³ 0.1
λ (m)
3.00 × 10²⁰ 3.00 × 10¹⁹ 3.00 × 10¹⁶ (7.89 3.84) × 10¹⁴ 3.00 × 10¹¹ 3.00 × 10⁹
ν(Hz)
1.2 × 10¹¹ 1.2 × 10¹⁰ 1.2 × 10⁷ (3.1 1.5) × 10⁵ 120 1.2
E(J/mol)
Violet
Blue
Green
Yellow
Orange
Red
400
500
600
700
800
λ (nm)

The properties of radiation discussed so far are associated with its wave nature. In many phenomena, however, radiation reveals its particle nature, *i.e.* it must be treated as a collection of discrete packets, or quanta of energy called photons (Harris, 1987). These quanta travel in the direction of propagation of the electromagnetic radiation, and the energy of one photon E is given by the Planck equation:

Equation A4 $E = h\nu = h\mathrm{V}c$ h = Planck's constant $= 6.62 \times 10^{-24}$ J/s

The Planck equation unifies the wave and particle nature of electromagnetic radiation by specifying the relationship between the energy of a photon, that is, its particle property, and the wave characteristic which is frequency (Harris, 1987).

A1.1.3 Types of Normal Modes of Vibrations

Vibrations of atoms of a molecule are closely related to the types of vibrating atoms, the forces of their interactions (described by the force constants) and the manner of their arrangement in the molecule, *i.e.* the structure of the molecule. The molecule's structure reflects its typical arrangement, characterized by certain defined symmetry properties. Classification of a given vibration depends on the symmetry of the molecule and describes the properties of the vibration. The symmetry elements of a molecule, such as axis of rotation, plane of symmetry (reflection), centre of inversion (symmetry), rotation-inversion axis are associated with the symmetry operations which define all vibrational motions (Colthup *et al.*, 1990).

There are many distinct types of bond vibrational modes: stretching, deformation, wagging and rocking vibrations (Figure A1.2). The stretching vibration is associated with a motion of atoms causing stretching and shortening of the chemical bond. For a system of three atoms, the motion can be symmetric and asymmetric in nature. A deformation mode is an in-plane movement of atoms during which the angle between bonds changes; the wagging vibration is an in-phase, out-of-plane movement of atoms, while other atoms of the molecule are in plane. In the rocking vibration, atoms swing back and forth in phase in the symmetry plane of the molecule and if during movement of the atoms the plane is twisted, the vibration is called a twisting vibration (Cross, 1964; Colthup *et al.*, 1990).

In 1931, E. Fermi discovered in the vibrational spectrum of the CO_2 molecule the effect associated with the combination of two vibrations, now called the Fermi resonance. Fermi resonance occurs when vibrations of similar frequencies are coupled, *i.e.* they mutually interact.

A1.2 FTIR Spectroscopy

A1.2.1 Fourier Analysis of Infrared Data

Infrared spectra of complex mixtures are often difficult to use for quantitative and sometimes qualitative analysis because of the effect of band overlap. The spectra of condensed phase samples can be considered to be the resultant of several (usually overlapped) bands, each of which is caused by one vibrational mode of one of the components of the mixture (Griffiths & Pariente, 1986).

Figure A1.2 Schematic representation of the different types of stretching and bending molecular vibrations for AX_2 and AX_3 groups. Reproduced from Cross (1964).

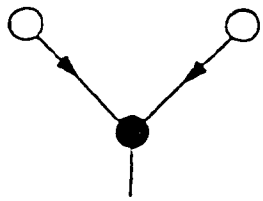

AX_2 symmetrical stretching

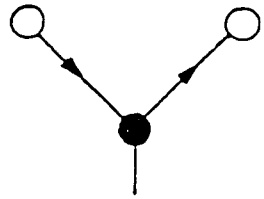

AX_2 asymmetrical stretching

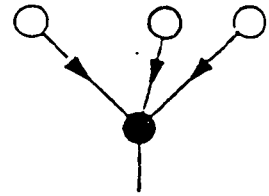

AX_3 symmetrical stretching

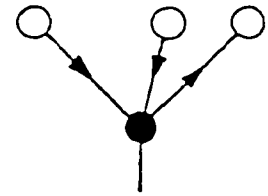

AX_3 asymmetrical stretching

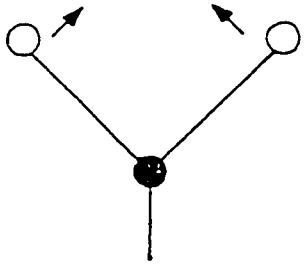

AX_2 in-plane deformation, or scissoring

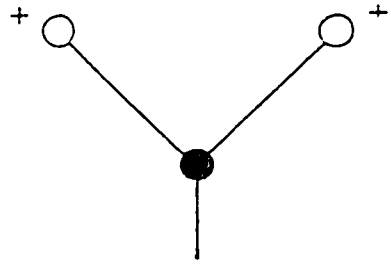

AX_2 out-of-plane deformation, or wagging

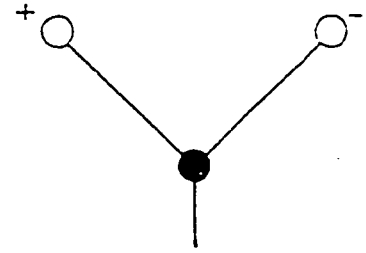

AX_2 out-of-plane deformation, or twisting

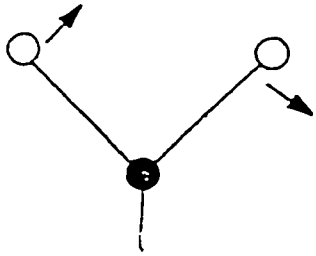

AX_2 rocking

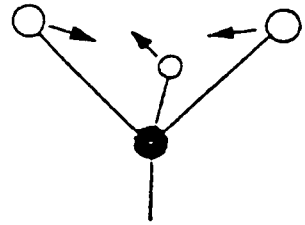

AX_3 symmetrical deformation

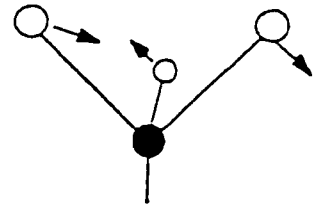

AX_3 asymmetrical deformation

The profile of each band in these infrared spectra is approximately Lorentzian. *i.e.* the absorbance of the *i*th band at wavenumber ν is given by:

Equation A4

$$A_i(\nu) = A^0_i \frac{\gamma_i^2}{\gamma_i^2 (\nu - \nu^0_i)^2}$$

where A^0_i = maximum absorbance of the band
ν^0_i = wavenumber for A^0_i
γ_i = half-width at half-height (HWHH)

Thus a spectrum with *N* bands may be approximated as:

Equation A5

$$A(\nu) = \sum_{i=1}^{N} A^0_i \frac{\gamma_i^2}{\gamma_i^2 (\nu - \nu^0_i)^2}$$

If in the spectral region between two wavenumbers, ν_1 and ν_2, the number of bands, *N*, exceeds the spectral range divided by the average full width at half-height (FWHH) of each band, *i.e.*

$$N > \frac{|\nu_1 - \nu_2|}{2 \Sigma \gamma_i}$$

not all the bands will be resolved and at least half of them will be overlapped to the point that they are unresolved (Griffiths & Pariente, 1986).

Previous approaches to enhancing the information content of infrared spectra of mixtures have included spectral subtraction, curve fitting, second derivative calculations and sometimes two of these three techniques in combination. In 1981, a technique known as Fourier self-deconvolution (FSD) was described by Kauppinen and co-workers, whereby the values of γ_i or HWHH for each band in a given spectral region can be reduced without seriously distorting the spectrum and its concepts were put into useful practice for infrared spectrometry (Griffiths & Pariente, 1986).

A1.2.2 Theory of Fourier self-deconvolution

The cosine Fourier transform (FT) of the band described by eqn. A4 is given by:

Equation A6

$$\mathcal{F}(x) = \int_0^\infty A_i(\nu) \cos 2\pi \nu x \, d\nu$$

$$= 0.5 A^0_i \gamma_i \cos(2\pi \nu^0_i x) \exp(2\pi \gamma_i x)$$

where x = spatial frequency and has the units of reciprocal wavenumbers, or cm
$0.5 A^0_i \gamma_i$ = coefficient
$\cos(2\pi \nu^0_i x)$ = cosine term
$\exp(2\pi \gamma_i x)$ = exponential decay term

The coefficient $0.5 A^0_i \gamma_i$ is directly proportional to the area of the band. The cosine term has a frequency that is dependent on ν_0, the centre wavenumber of the band. This term has exactly the same form as the corresponding wave in an interferogram, so that x may also be thought of as being equivalent to the optical retardation of a Michelson interferometer. Finally the rate of decay of this cosine wave is determined by the width of the band: the wider the band, the more rapidely its FT decays. When x = 0, both the cosine and exponential terms have a value of unity, so that the magnitude of $\mathcal{F}(0)$ is directly proportional to the area of the peak.

Kauppinen *et al.* (1981) have developed the general theory of a digital self-deconvolution method carried out in Fourier transform space. They demonstrated that an enhancement of 3 in the spectral resolution of spectra with moderate signal/noise ratios (ca. 1000) can be attained.

They described the relationship between a spectrum, $E(\upsilon)$, in the wave number domain and its interferogram, $I(x)$, by the following equations:

Equation A6 $$E(\dot{\upsilon}) = \int_{-\infty}^{\infty} I(x)\exp(i2\pi\,\dot{\upsilon}\,x)dx = \mathcal{F}\{I(x)\}$$

Equation A7 $$I(x) = \int_{-\infty}^{\infty} E(\dot{\upsilon})\exp(-i2\pi\,\dot{\upsilon}\,x)d\dot{\upsilon} = \mathcal{F}^{-1}\{E(\dot{\upsilon})\}$$

where $\mathcal{F}\{I(x)\}$ is the Fourier transform and x has units of centimeters (cm).

Any experimental spectrum, $E(\dot{\upsilon})$, can be expressed as a convolution of a lineshape function, $G(\dot{\upsilon})$, and a spectrum, $E'(\dot{\upsilon})$, that is

Equation A8 $$E(\dot{\upsilon}) = G(\dot{\upsilon}) * E'(\dot{\upsilon}) = \int_{-\infty}^{\infty} G(\dot{\upsilon}\,')E'(\dot{\upsilon} - \dot{\upsilon}\,')d\dot{\upsilon}\,',$$

where $*$ indicates the convolution operation.

In order to deconvolve $G(\dot{\upsilon})$ from $E(\dot{\upsilon})$, we take the inverse Fourier transform of both sides of equation A8, giving

Equation A9 $$I(x) = \mathcal{F}^{-1}\{G(\dot{\upsilon})\} \cdot I'(x)$$

and the interferogram corresponding to the deconvolved spectrum is given by:

Equation A10 $$I'(x) = \frac{1}{\mathcal{F}^{-1}\{G(\dot{\upsilon})\}} \cdot I'(x)$$

That is, the deconvolution operation in Fourier transform space requires a particular form of the interferogram. $E'(\dot{\upsilon})$ is then simply obtained by taking the Fourier Transform of of $I'(x)$ and the final lineshape in $E'(\dot{\upsilon})$ is dependent on the lineshape function $G(\dot{\upsilon})$. Consequently, although the instrumental resolution is infinite (the integrals in equations A6 and A7 are not limited), the resultant spectral resolution may not be maximal.

Therefore, this technique developed by Kauppinen and co-workers (1981) permits the resolution of unresolvable lines and, thus, facilitates the interpretation of data contained in heavily overlapped band contours of an infrared spectrum. FSD of an infrared absorption band is a practical approach used to extract more information from the infrared spectrum of a sample. It decreases the widths of infrared bands, thus allowing for separation and better identification of overlapping component bands. The resolution enhancement factor is defined by the ratio γ_i(HWHH of the original band)/γ_i' (HWHH of the deconvolved band) (Surewicz & Mantsch, 1988).

Another way to increase separation between overlapping bands is to obtain the nth-order derivative on the frequency domain of FT of the absorbance spectrum. Typically, the power of the derivative is kept at the default value of 3 with a smoothing breakpoint in the range of 0 to 1 (Moffatt *et al.*, 1986). By varying the breakpoint, the derivative can be subjectively optimized when noting the noise level in the resulting FT band. In contrast to FSD, Fourier derivation manipulates the frequency domain of the Fourier series rather than the absorbance domain.

While there are several advantages to FSD and Fourier derivation, there are also some pitfalls. The major problems arise form the appearance of side lobes and the disproportionate enhancement of bands originating from water vapour or random noise.

APPENDIX TWO

THEORY OF MASS SPECTROMETRY

A2.1 The Mass Spectrometer

In its simplest form, the mass spectrometer performs three essential functions. First it subjects molecules to bombardment by a stream of high energy electrons, converting some of the molecules to ions which are accelerated in an electric field. Second, the accelerated ions that have a particular mass-to-charge ratios in a magnetic or electric field. Finally, the ions that have a particular mass-to-charge ratio are detected by a device which can count the number of ions striking it. The detector's output is amplified and fed to a recorder. The trace from the recorder is a ***mass spectrum***— a graph of the number of particles detected as a function of mass-to-charge ratio. When each function is examined in detail, it becomes obvious that the mass spectrometer is actually somewhat more complex than just described. Before the ions can be formed, a stream of molecules must be introduced into the ionization chamber where the ionization takes place. A sample inlet system provides this stream of molecules (Kates, 1986).

A sample studied by mass spectrometry may be a gas, a liquid, or a solid. Enough of the sample must be converted to the vapour state (with gases, of course, the substance is already vaporized) to obtain the stream of molecules that must flow into the ionization chamber. This inlet system is only partially evacuated so that the ionization chamber itself is at lower pressure than the sample inlet system. The sample is introduced into a larger reservoir, from which the molecules of vapour can be drawn into the ionization chamber.

which is at low pressure. To ensure that a steady stream of molecules is passing into the ionization chamber, the vapour travels through a small pinhole called a molecular leak, before entering the chamber. Once the stream of sample molecules has entered the ionization chamber, a beam of high energy electrons bombards it, thus converting the molecules to ions which are then accelerated in an electric field (Kates, 1986).

In the ionization chamber, the beam of high energy electrons, having an energy of about 70 electron volts (eV), is emitted from a filament that is heated to several thousand degrees Celsius. These high energy electrons strike the stream of molecules, which has been emitted from the sample system, and ionize the molecules in the stream by removing electrons from them; the molecules are thus converted to positive ions. A repellar plate, which carries a positive electrical potential, directs the newly created ions toward a series of accelerating plates. A large potential difference applied across these accelerating plates produces a beam of rapidely travelling positive ions. One or more focusing slits direct the ions into a uniform beam. From the ionization chamber, the beam of ions passes through a short field free region and enters the mass analyser, where the ions are separated according to their mass-to-charge ratios (Kates, 1986).

The kinetic energy of an accelerated ion is equal to:

Equation A1 $\frac{1}{2}(mv^2) = eV$

m = mass of the ion
v = velocity of the ion
e = charge of the ion
V = potential difference of the ion accelerated plates

In the presence of a magnetic field, a charged particle describes a curved flight path. The equation which yields the radius of curvature of this path is:

Equation A2 $$r = \frac{mv}{eH}$$

r = radius of curvature of the path

H = strength of the magnetic field

If these two equations are combined to eliminate the velocity term, the result is:

Equation A3 $$\frac{m}{e} = \frac{H^2r^2}{2V}$$

This is the equation which governs the behaviour of an ion in the mass analyser portion of the mass spectrometer.

As can be seen from equation A3, the greater the value of *m/e*, the larger the radius of the curved path. The analyser tube of the instrument is constructed to have a fixed radius of curvature. A particle with the correct *m/e* ratio can negotiate the curved analyser tube and reach the detector. Particles with *m/e* ratios which are either too large or too small strike the sides of the analyser tube and do not reach the detector; therefore, either the accelerating voltage or the magnetic field strength is continuously varied in order that all of the ions produced in the ionization chamber can be detected. The record produced from the detector system is in the form of a plot of the numbers of ions versus the values of *m/e* (Kates, 1986).

A2.2 Fast Atom Bombardment Mass Spectrometry

Fast atom bombardment (FAB) mass spectrometry involves the transfer of kinetic energy from a beam of highly energetic atoms such as argon or xenon to a matrix such as glycerol and then to the sample. This technique has gained wide popularity and is now used in many applications for the structural analysis of complex carbohydrates. Like the other

kind of desorption ionization, it has the advantage that nonvolatile polar substances usually give intense peaks in the molecular ion region. Another advantage, especially as compared to field desorption (FD), is that a high intensity of ions from the sample can be maintained for prolonged periods of time, even with rather small amounts of sample. Fragment ions indicative of structure may be observed under appropriate conditions. The degree of fragmentation appears to be dependent upon structural parameters that are not entirely understood. Typical sample sizes for FAB are about one nmol dissolved in one μliter of matrix (Kates, 1986).